TWO PHASE FORMATION IN PHARMACEUTICAL AND FINE CHEMICALS

TAN CHIN LEE

NATIONAL UNIVERSITY OF SINGAPORE

2005

TWO PHASE FORMATION IN PHARMACEUTICAL AND FINE CHEMICALS

TAN CHIN LEE
(B. Eng (Hons.), UTM, MALAYSIA)

A THESIS SUBMITTED

FOR THE DEGREE OF MASTER OF ENGINEERING

DEPARTMENT OF CHEMICAL

AND BIOMOLECULAR ENGINEERING

NATIONAL UNIVERSITY OF SINGAPORE

2005

ACKNOWLEDGEMENTS

I wish to express my heartfelt thanks to my supervisor, Professor Reginald Tan for his continual support, guidance and commitment throughout the project. I would like to thank my co-supervisor, Dr. Keith J. Carpenter, for his generosity, patience and, invaluable advice and support. Two-year supervision of them allowed me the luxury of thinking, writing and reading in which I have been gained fruitfully both academically and in terms of character building. This project could not have been completed without their guidance and support.

I am indebted to Dr. Ann Chow for her guidance and support in carrying out the experiments in crystallization lab. Her knowledge, integrity, scholarship and friendship inspired me in my research life in ICES (Institute of Chemical and Engineering Sciences).

Colleagues of ICES provided valuable helps, assistances, criticism and suggestions. I am grateful to all, but especially to Dr. Lu Jie, Dr. Feng Shaohua, Dr. Zaher Judeh, Dr. Xu Rong, Dr. Ong Teng Teng, Dr. Fethi Kooli, Dr. Jeyagowry , Dr, Ilya Lyapkala, Dr. Krishna Gopol Dongol, Dr. Selvasothi Selvaratham, Dr. Venkateswarlu Bhamidi, Mr. Fabien Cabirol, Mr. Quah Chee Wee, Mr. Lim Seng Chong, Mr. Mohammad Khalid s/o Nizamudin, Mr. Tharumaraja Tirunavukarasu, Ms. Callie Wong and Ms. Joanne Loi. I am grateful to Xingyi, Zaiqun, Guangwen, Sendhil, Nicholas, Yen Yen, Chen Wei, Xuen Tien, Roderick, Maricar and Jeffery for providing me an environment of friendship and appreciation for scholarship that I treasure. Without them, my research life would not as fun and enjoyable as ever.

Thanks are extended to the Department of Chemical and Biomolecular Engineering, NUS (National University of Singapore) and ICES for the financial support.

My parents taught me the importance of having faith in work and working hard, thinking positively and rationally, and holding on to aims in life. It is a lesson that guides me to carry on to this day. My sisters, brothers and nieces provided me the unfailing love, enjoyment, support and understanding without which this work would not have been completed.

Chin Lee
Jan 2005

TABLE OF CONTENTS

Chapter 6 Conclusions and Recommendations for Fututre Work

SUMMARY

In this project, two phase formation or liquid-liquid phase separation during cooling crystallization of hen egg-white Lysozyme (HEWL) and the effect of that phenomenon on crystal properties were studied.

Two phase formation in Lysozyme solutions was observed as the formation of protein-rich droplets (protein-rich phase) dispersed in the matrix of continuous phase (protein-lean phase) when the solutions were cooled to lower temperature (less than 10°C; from ambient temperature). Onset of the cloudiness of Lysozyme solutions during phase separation was determined as the cloud point temperature (T_{cloud}). Sets of T_{cloud} form the cloud point curve of Lysozyme system. The cloud point temperature of Lysozyme system was studied as a function of buffer solution (acetate ion) and cooling rates. Use of acetate buffer increased the T_{cloud} of Lysozyme solutions possibly due to the increase in ionic strength between Lysozyme molecules. Rates of cooling (0.25°C/min-1.5°C/min) were found to influence the T_{cloud} which leads to a controlled pathway for crystallization.

Crystallization kinetics in Lysozyme solutions was affected by the formation of two liquid phases in which the supersaturation level in each phase is different. Micrographs show that more crystals were formed in the protein-rich phase as compared to fewer and bigger crystals obtained in the protein-lean phase, implying higher nucleation rate in that phase. Spherically-shaped Lysozyme crystals, which were formed inside the oil droplets, were obtained during phase separation. These crystals have a different morphology compared to the well-known tetragonal and orthorhombic crystals of Lysozyme. However, the spherical crystals of Lysozyme

were metastable as the crystals gradually transformed into the stable tetragonal shape once the crystallization conditions (temperature and crystallization time) were changed. In addition, XRPD studies showed that these spherical crystals are possibly one of the polymorphs of Lysozyme system.

The oil droplets formed during phase separation were found to be protein-rich regardless of the initial concentration of Lysozyme solutions. These droplets sustained a predominant size of 3-5μm determined by Focused-Beam Reflectance Measurement (FBRM) method for 2 hours. SEM images of the crystals formed in that measurement period revealed the crystals possibly formed from nucleation in oil-droplet phase. Crystals formed via two phase formation (spherically-shape or spherical transformed tetragonal crystals) were uniform in size and had a narrower crystal size distribution as compared to the crystals formed in solutions without passing through two liquid-phase region.

From the results of this study, it is proposed that crystallization via two phase formation could be applied as a means to obtain crystals with different shape and size distribution. In addition, an improved control of crystallization process can be achieved by understanding the kinetics of the crystallizing system during two phase formation.

NOMENCLATURE

A	Pre-exponential constant
AAS	Atomic absorbance spectrometer
API	Active pharmaceutical ingredient
B_2	Second virial coefficient of osmotic pressure
C	Concentration
C*	Concentration at saturation state
C.V	Coefficient of Variation, %
C_b	Salt concentration in bottom liquid layer of solutions during phase separation
C_{cri}	Critical concentration
CH_3CO^{-2}	Acetate ion
Cl^-	Chloride ion
ClO^-	Chlorate ion
CrO_4^{2-}	Chromate ion
C_t	Salt concentration in top liquid layer of solutions during phase separation
DLVO	Derjaguin-Landau-Verway-Overbeek model
FBRM	Focused-Beam Reflectance Measurement
FTIR	Fourier-Transformed Infra-Red spectrometer
HCO^{-3}	Hydrogen carbonate ion
HEWL	Hen egg white Lysozyme
HPO_4^{2-}	Hydrogen phosphate ion
IR	Infra-Red
J	Nucleation rate
k	Boltzmann constant, the gas constant per molecule (1.3802 x 10-23 JK^{-1})

K	Partition coefficient
KBr	Potassium Bromide
k_{CG}	Diffusion coefficient of crystal growth
K^+	Potassium ion
Li^+	Lithium ion
lys	Lysozyme
MCT IR	Mercury-Cadmium-Telluride IR spectrometer
Mg^{2+}	Magnesium ion
micro-DSC	Micro-Differential Scanning Calorimeter
NaCl	Sodium chloride
Na	Sodium
Na^+	Sodium ion
NH_4^+	Ammonium ion
NO^{-2}	Nitrite ion
NO_3^-	Nitrate ion
r	Radius of particles
R	Rate of crystal growth
r_c	Critical radius of particles
S	Supersaturation
SEM	Scanning Electron Microscopy
SO_4^{2-}	Sulfate ion
T	Temperature
T_{cloud}	Cloud point temperature
T_{cri}	Critical temperature
XRPD	X-Ray Powder Diffraction

ΔC	Concentration gradient
ΔG	Excess Gibbs free energy
ΔG_c	Critical excess Gibbs free energy
ΔG_s	Surface excess Gibbs free energy (+ve)
ΔG_v	Volume excess Gibbs free energy (-ve)
λ	Wavelength, nm
σ	Surface tension between crystalline solid particle and supersaturated solution
υ	Molecular volume

LIST OF FIGURES

LIST OF TABLES

CHAPTER 1

INTRODUCTION

1.1 Two Phase Formation / Liquid-Liquid Phase Separation

Active pharmaceutical ingredients (API) and fine chemical compounds are complex organic molecules which are frequently purified by crystallization from solution. The operating conditions of this process will determine if the final product (crystals) to meet the stringent specifications especially in drugs for therapeutic applications. Therefore, control on the final products (such as crystal morphology and polymorphs, crystal size distributions, purities etc.) is needed to ensure the applicability of the products and the operability of subsequent processes. However, in real systems, the crystallization kinetics can be slowed and hindered by process variables, and lead to undesirable or unexpected phenomena that create a massive impact on severe pathological conditions.

Two phase formation in pharmaceutical and fine chemical crystallization, particularly in protein crystallization, is another event occurring during crystallization which is little understood. This is a phenomenon where liquid phases are formed prior to the solid phase of crystals. Two phase formation during crystallization can be first

observed when the solution turns cloudy or opaque. The formation of oil droplets can be microscopically observed as visible droplets dispersed in the matrix of another liquid phase as shown in Figure 1.1. Crystals formed via this phenomenon may vary in size, habit and other properties which subsequently affect the performance of product separation and purification processes. Consequently, the performance of the down stream stages in an industrial process may be adversely affected. In addition, it may become an impurity in the form of an amorphous precipitate as the final product once the oil droplets solidify (http://www.cm.utexas.edu/CH210C/). Hence, the control of two phase formation or preventing it from occurring during crystallization can be the key to obtaining the desirable crystal form and properties directly. For these reasons, this project aims to study how two phase formation influences crystal formation under different crystallization conditions.

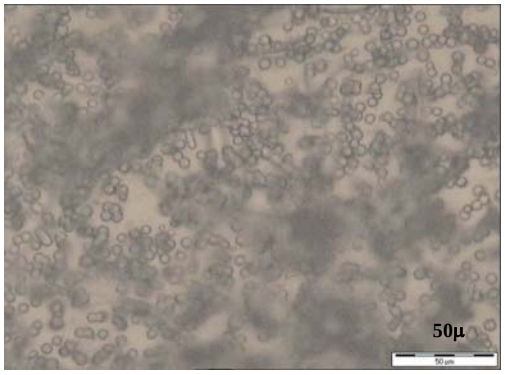

Figure 1.1 Oil droplets formed in protein solution (9wt% Lysozyme and 5.5wt% NaCl, pH 4.5). Protein-rich droplets dispersed in the matrix of continuous protein-lean phase

1.2 Objectives and Scopes of the Study

The overall objective of this study is to provide a deeper understanding of two phase formation during crystallization based on a model compound. The system chosen for this investigation is the protein hen egg-white Lysozyme (HEWL), because its

properties and crystallization behavior are fairly well documented, and yet its behavior during two phase formation has not been systematically studied.

This study will include investigating the conditions under which two phase formation is favored, crystallization behavior and kinetics of two phase formation, and the effect on crystal quality and properties. Potential applications of two phase formation will be discussed. For example, deliberate formation of a solute-rich phase in a controlled way may provide a means to develop novel crystal forms with specific formulation properties.

Specific steps to achieve the objectives are:

i. To examine the effect of process variables (cooling rates, buffer solutions, and salt effects) on two phase formation during crystallization of Lysozyme system. Various techniques will be used to monitor the onset of two phase formation. These techniques include the measurement on turbidity (using a colorimeter), enthalpy change (using micro-DSC) and concentration distribution (of two liquid phases, using UV-Vis spectrophotometer). The salt partitioning during phase separation will be examined with AAS.

ii. To characterize the Lysozyme crystals from crystallization under 'normal' conditions and via two phase formation, such as

    a. Crystal morphologies and polymorphisms examined using an optical cross-polarized light microscope, SEM and XRPD.

    b. Functional groups of Lysozyme molecules determined with different types of IR spectrometer.

c. Optical characteristics of Lysozyme crystals observed under an optical cross-polarized light microscope.

iii. To characterize the oil droplets. The identity of two phases (either in solute-rich or solute-lean phase) is examined based on Lever rule and images obtained from the polarized-light microscope. In addition, the particle size distribution of these oil droplets is determined using Focused-Beam Reflectance Measurement (FBRM).

iv. To study the effect of oil droplets on crystal properties. In this context, the particle size distribution of crystals formed via oiling-out will be determined and agglomeration is studied qualitatively with a polarized-light microscope.

1.3 Thesis Outline

A brief introduction in Chapter 1 is followed by the project background studies (Chapter 2) including the theories of crystallization events and the two phase formation (or commonly known as oiling-out phenomenon or liquid-liquid phase separation), particularly in the Lysozyme system. The characteristics and properties of Lysozyme will be explained in this chapter in order to provide further understanding when crystallization via two phase formation occurs.

The effect of process variables such as buffer solution and cooling rates on two phase formation will be discussed in Chapter 3. In addition, the role of sodium chloride, which is used as the precipitant, is examined and explained in this chapter. Chapter 4 discusses the crystal morphology and polymorphism of Lysozyme crystals under different crystallization conditions. The optical property and functional groups of Lysozyme crystals will also be discussed in Chapter 4. The characteristics of oil droplets forming in the crystallizing solutions are examined and reported in Chapter 5. The effects of two phase formation on the particle size distribution and agglomeration of Lysozyme crystals are studied and discussed in Chapter 5.

Finally, the conclusions from the results of this study will be made and the suggestions are given in Chapter 6 to provide guidelines or directions for the future study of two phase formation during crystallization.

CHAPTER 2

LITERATURE REVIEW

2.1 Theories in Crystallization Process

Crystallization from solution is a two-step process: (1) nucleation, where initial nuclei are formed; and (2) growth, where these nuclei grow to bigger size.

Figure 2.1 shows a hypothetical phase diagram. The region above the solubility curve is the undersaturated zone and the system remains in a solution or liquid phase. Below the solubility curve is the supersaturated zone where the formation of a new solid phase, either crystalline or amorphous, is possible. Supersaturation is the driving force in crystallization and crystals can nucleate and grow only if the solution is supersaturated. According to Arkenbout (1995), supersaturation can be expressed in terms of undercooling, concentration surplus, or as a relative number, but it can also be based on thermodynamics. Different definitions have been used by various authors to define supersaturation. For examples, Hollander et al. (2002) used $S = \Delta\mu/kT$ (where $\Delta\mu$ is the difference between the chemical potentials of the crystallizing component in the actual state and in the equilibrium state), and Finnie et al. (1999) used $S = \ln(C/C^*)$.

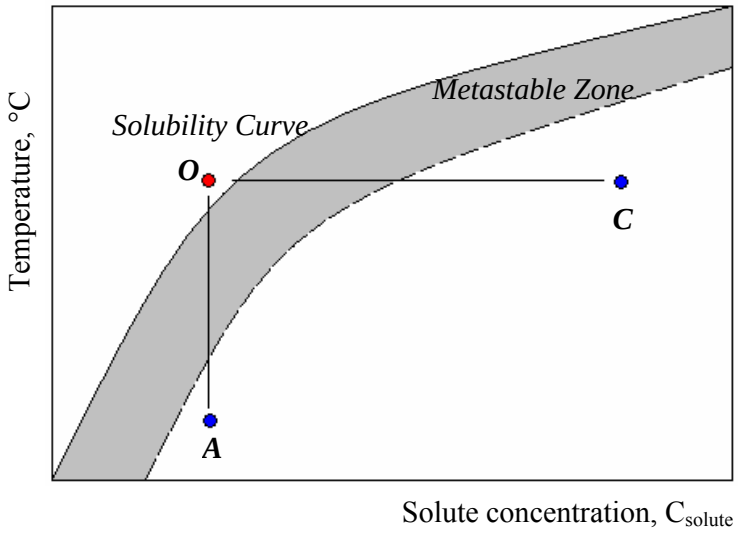

Figure 2. 1 The region between the solubility curve and the 'nucleation curve' is termed as the metastable zone. Crystallization may follow different pathways (from O to A or B) once supersaturation is achieved

The shaded region in Figure 2.1 is the metastable zone in which nucleation does not occur spontaneously but can be induced by the presence of seed crystals or impurities. An understanding on the metastable zone is of the utmost important for the design of crystallization experiments or processes as the width of this region measures the crystallize-ability of a system. A true metastable zone width is hard to determine as it can be influenced by the presence of impurities, rate of cooling, solution history, etc. Therefore, an effective metastable zone width has to be determined experimentally for each system.

Crystallization can be carried out via different pathways. For examples, in Figure 2.1, the solution can be brought into the supersaturated region from the starting conditions (indicated by point O) either by cooling (via path OA), or by solvent evaporation (via path OB). In either case, once supersaturated solution past the

metastable zone, spontaneous nucleation will occur and solute concentration will decrease until the equilibrium concentration at the prevailing condition is attained.

2.1.1 Nucleation

Nucleation can be classified into (i) primary nucleation, which comprises of homogeneous and heterogeneous nucleation, and (ii) secondary nucleation, a nucleation process induced by the presence of crystals in the supersaturated solution.

(i) Primary Nucleation

Homogeneous Nucleation

In homogeneous nucleation, only nuclei greater than a certain critical size will be stable and grow to a detectable size. Local concentration fluctuations may give rise to the formation of these nuclei via a bimolecular addition mechanism (Mullin, 2001).

The homogeneous nucleation rate, J, via the addition nucleation mechanism can be considered as a thermally activated process. Thus, it can be expressed in the form of Arrhenius equation:

$$J = A \exp \frac{-\Delta G_c}{kT} \quad , \qquad (2.1)$$

where A is the pre-exponential factor, k is the Boltzmann constant which is the gas constant per molecule (1.3802 x 10-23 JK^{-1}), and ΔG_c is the critical excess Gibbs free energy.

The overall excess free energy change for the formation of solute particles in equilibrium with the solute in solution is the sum of the surface excess free energy, ΔG_s (+ve) and the volume excess free energy, ΔG_v (-ve) as shown in Figure 2.2.

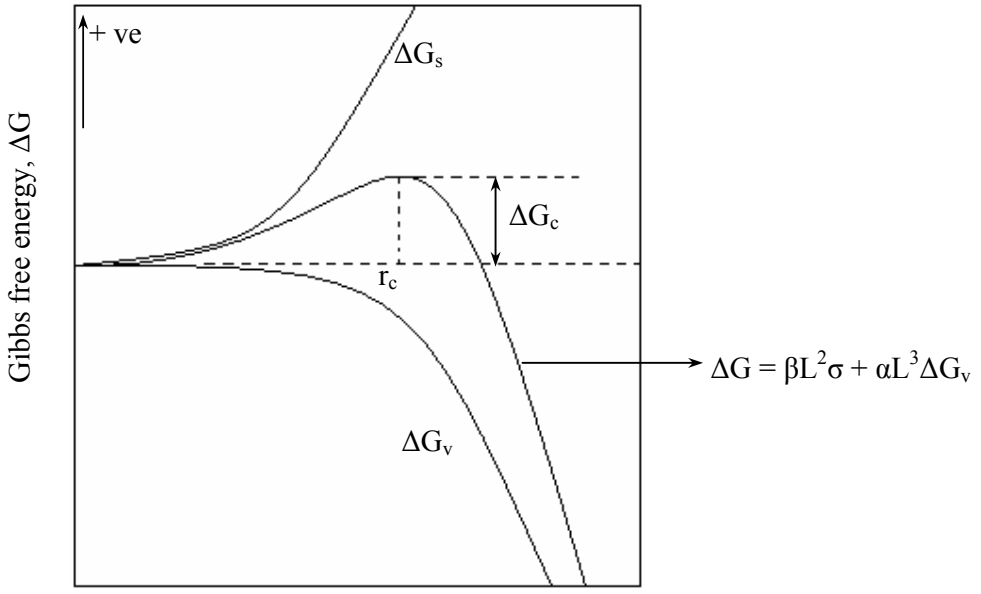

Figure 2.2 Gibbs free energy change, ΔG, of a crystallizing system during nucleation. The constant β and α correspond to the shape factors of the crystallizing particles and σ is the surface tension between the particle and bulk solution during nucleation

Therefore,

$$\Delta G_c = \Delta G_s + \Delta G_v \qquad (2.2)$$

For spherical particles, $\Delta G = 4\pi r^2\sigma + {}^4/_3\pi r^3\Delta G_v$, where σ is the surface tension between the crystalline solid particle and the supersaturated solution. Nucleation will only occur when the energy change exceeds the maximum point of the ΔG curve and this corresponds to when the solid particles exceed the critical nuclei size. At this point,

$$\frac{d(\Delta G)}{dr} = 8\pi r_c\sigma + 4\pi r_c^2\Delta G_v = 0 \qquad (2.3)$$

$$r_c = -\frac{2\sigma}{\Delta G_v} \qquad (2.4)$$

Substituting for ΔG_v (eqn. 2.4) into eqn. 2.2,

$$\Delta G_v = \frac{4\pi r_c^2\sigma}{3} \qquad (2.5)$$

Crystalline particles formed in the solution are stable only if the particle size exceeds the critical nuclei size or in other word, the nucleation process should result in the decrease in the free energy of the crystalline particles. Hence, particles with sizes

lower than the critical nuclei size is unstable and will re-dissolve due to the increase in Gibbs free energy of the system.

As mentioned in previous paragraph, supersaturation, S, determines the nucleation event in crystallization process and its relationship to the critical size of nuclei is correlated by the Gibbs-Thompson equation,

$$\ln S = \frac{2\sigma\upsilon}{kTr} \quad , \qquad (2.6)$$

where υ is the molecular volume. At the critical radius of particle,

$$\frac{2\sigma}{r_c} = \frac{kT\ln S}{\upsilon} \qquad (2.7)$$

Thus,

$$\Delta G_c = \frac{16\pi\sigma^3\upsilon^2}{3k^2T^2(\ln S)^2} \qquad (2.8)$$

and nucleation rate can be defined as

$$J = A \exp -\frac{16\pi\sigma^3\upsilon^2}{3k^3T^3(\ln S)^2} \qquad (2.9)$$

Hence, nucleation rate increases with increasing supersaturation and temperature.

Heterogeneous Nucleation

Cases of spontaneous homogeneous nucleation are rarely a common event. Impurities may be present in the solution as atmospheric dust or foreign substance in the investigating materials. These substances may act as “heteronuclei” during nucleation. In addition, these substances tend to reduce the energy barrier in nucleation by reducing the surface energy between the crystalline particles and the bulk solution. Hence, heterogeneous nucleation requires a lower driving force (lower supersaturation level) than in spontaneous nucleation (homogeneous nucleation). However, heterogeneous nucleation depends on the contact angle or wetting angle between the

deposited crystalline solid to the surface of heteronuclei (e.g. seeds, or walls of the retaining vessel etc.).

(ii) Secondary Nucleation

The presence of crystals in a supersaturated solution induces secondary nucleation. These crystals stimulate nucleation to occur at lower supersaturation than in primary nucleation (no crystals are present in the saturated solution). The occurrence of secondary nucleation may originate from the parent crystals or from the solute in the liquid phase. The understandings on the mechanisms and kinetics of secondary nucleation have yet to be developed (Myerson, 1993). However, several possible mechanisms have been proposed such as initial or dust breeding, needle-breeding, collision breeding and "polycrystalline" breeding. Nucleation in these systems occurs by forming tiny crystallites on the crystal surface or fragments. In some cases, crystal fragments serve as nucleation sites (needle breeding) and these fragments possibly aggregate to form irregular "polycrystalline" nucleation sites.

As agitation is normally applied to ensure solution homogeneity in crystallization, the shear force acting on the crystals results in the fragmentation in crystals or rounded-edge crystals depends on the speed of agitation. In either case, distorted crystals will serve as attachment sites for solute molecules in solution. However, these mechanisms may be obscured by contact nucleation, the most prominent nucleation mechanism. The nucleation occurs via this mechanism at the contact surface between crystals and walls of containers, impellers and other crystals in solution (Davey and Garside, 2000). The nucleation rate of this mechanism depends,

not only on supersaturation, but also on crystal concentration in suspension, agitation speed and other hydrodynamic factors.

2.1.2 Crystal Growth

Once nucleation occurs, the nuclei begin to grow larger through the attachment of solute molecules from supersaturated solution to crystal surface. This transport phenomenon is known as crystal growth. Thereafter, nucleation may occur simultaneously with the growth event. The final size distribution and shape of the crystals are determined by both crystal growth and nucleation.

Crystal growth is generally described as the change in dimension with time which is normally known as the linear growth rate (length per unit time). The measurement of linear growth rate is based on the growth of one of the faces of crystals. However, on a more microscopic scale, crystals are thought to grow in layers. This involves the incorporation of a molecule onto a crystal face by adsorption followed by diffusion along the surface, depending on the type of faces (Figure 2.3).

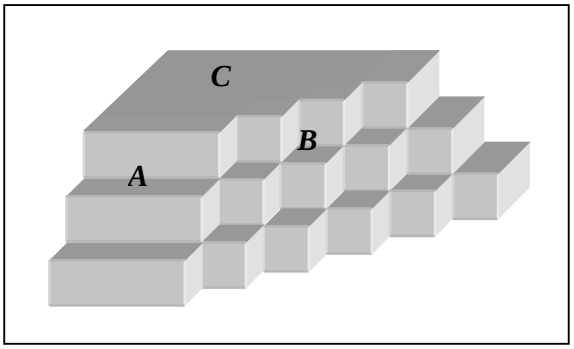

Figure 2.3 Faces of a crystal, (A) stepped faces, (B) kinked faces and (C) flat faces

The equilibrium shape of a crystal is bounded by the crystal faces with the lowest specific surface energies. From an energetic point of view, kinked sites are more favorable for an atom to be incorporated into the crystals (Davey and Garside, 2000). This is probably because the kinked sites determine the equilibrium of an infinitely large crystal with the ambient phase, and the desorption energy of this site is equal to the crystal's enthalpy of evaporation. The understandings on the favorable growth sites can be studied through the growth mechanisms. In general, the growth mechanism can be classified into (i) continual growth mechanism and (ii) layer growth.

(i) Continual Growth Mechanism

Growing surfaces or crystal faces undergo a surface roughening transition at a critical temperature known as roughening temperature, T_r, when temperature is increased and entropic factors become more dominant. Thus, faces at temperature higher than T_r become rough and favorably grow continuously. Fluxes of atoms from the bulk phase attach to these faces rigorously and the growth rate is controlled by molecular diffusion from the bulk phase. Hence, the rate of crystal growth is given by

$$R = k_{CG}\Delta C \quad , \qquad (2.10)$$

over the entire range of supersaturation and k_{CG} is the diffusion coefficient of crystal growth which is proportional to the surface roughness and varies exponentially with the activation energy.

(ii) Layer Growth Mechanism

Continual growth is more likely to occur in a kinked face. On the other hand, layer growth is the growth mechanism on the flat faces of crystals. Atoms bounded on these faces are weak unless a cluster of atoms is bounded to the surface. In such case, the

atoms must surpass an energy barrier to the formation of each crystal layer. However, the crystal faces are normally imperfect, hence providing steps for layer growth on crystal faces. The former case leads to the two-dimensional nucleation-growth mechanism while the later leads to a dislocation mechanism in layer growth of crystal face (Figure 2.4 and 2.5).

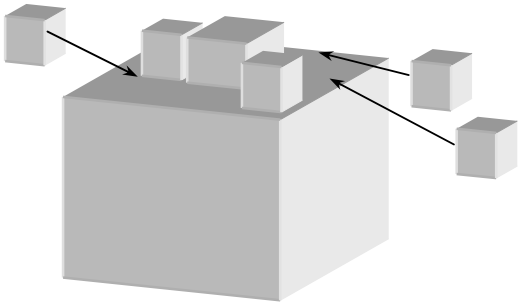

Figure 2.4 Deposition of molecules on the surface of a growing crystal which leads to the two-dimensional nucleation-growth mechanism

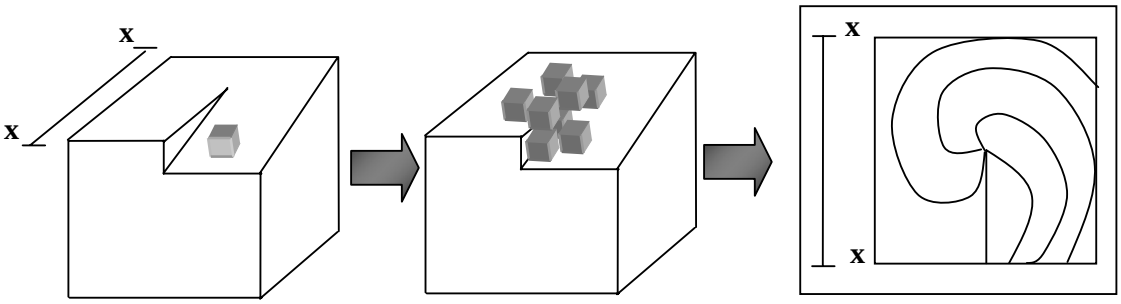

Figure 2.5 Growth on an imperfect crystal surface where deposition of molecules on these surfaces will ultimately lead to a growth spiral

2.2 Protein Lysozyme

In this project, protein Lysozyme was chosen as the model system. Protein Lysozyme (chicken-type or c-type) was first discovered by Alexander Fleming in 1921 (Jollès, 1996). It is a natural enzyme that can be isolated from chicken egg-whites (Alderton et

al, 1945). It is a relatively small enzyme that prevents bacterial infection in human body by attacking the protective walls of bacteria. Lysozyme breaks the carbohydrate chains in the bacteria cell walls by hydrolyzing the β-1,4-glycosidic linkage of N-acetylmuramic acid in peptidoglycans, and that of N-acetalglucosamine in chitin and chitodextrin. This reaction leads to cell lyses in most Gram-positive bacteria such as Micrococcus luteus, Oenococcus, Pediococcus and Lactobacillus (www.webster-online-dictionary.org). Ever since the discovery of c-type Lysozyme, other types of Lysozyme have been discovered in many animals and plants (Jollès & Jollès, 1984) with the same specificity in cleaving a β-glycosidic bond between C-1 of N-acetylmuranic acid and the C-4 of N-acetylglucosamine of the peptidoglycan.

Protein Lysozyme is also termed as muraminidases or Peptidoglycan N-acetylmuramohydrolases (EC 3.2.1.17 or CAS 12650-88-3). Hen egg-white Lysozyme (HEWL) was the first protein found to contain all the twenty amino acids (Jollès, 1996). It can be found in the tissues and organs of human body such as tears, saliva, urine, finger nails and human milk in which the Lysozyme content is about 0.2-2.6mg/ml (Grosswicz and Ariel, 1958). It is one of the enzymes which have been studied extensively with regard to its structure-function relationships. It has been widely used as a food preservative in cheeses and milk where the spoilage organism is inhibited while not interfering with the starter culture (Bester and Lombard, 1990). It is also used to inhibit malolactic fermentation and to promote microbial stabilization in wines production (www.scottlab.com/fodras.htm). Lysozyme is also used in toothpaste to lyse Streptococcus mutans in combination with fluoride, chloride and, bicarbonate and thiocynate (Goodman et al., 1981). Moreover, it serves as a model system in crystallography, enzymology and immunology, and in therapeutic applications on

human pathologies, including viral diseases, gynaecology and obstetrics, neurological diseases etc (Sava, 1996).

2.2.1 Properties of Protein Lysozyme

Lysozyme is a basic protein that consists of a single polypeptide chain of 129 amino acid residues and cross-linked by four disulphide bonds. Some of the properties (that are related to this project) of Lysozyme molecules are listed in Table 2.1.

Table 2.1 Properties of Lysozyme molecules

Nominal Molecular Weight	:	14700
Composition	:	contains all the twenty amino acids (Jollès, 1996) in sequence as reported by Prager and Jollès (1996) and Canfield (1963) with leucyl (leucine) as *C*-terminal and lysyl (lysine) as *N*-terminal.
Isoelectric point	:	pH 11.0 (Alderton et al., 1945)
Optimum pH	:	9.2 (Davies et al., 1969)
Stability	:	Stable as a dry lyophilized or crystalline powder. It is stable for years if it is stored at $4^{o}C$ (www.seikagaku.com). Solutions are stable at pH 4-5 for weeks if they are refrigerated. However, the molecular stability is related to the protein folding mechanisms.
Extinction Coefficient, $E_{281.5}^{1\%}$	:	26.4 (Aune and Tanford, 1969)

2.2.2 Crystallization of Protein Lysozyme

2.2.2.1 Solubility of Protein Lysozyme

The number, size and properties of crystals depend strongly on where the initial conditions lie on the solubility phase diagram of that system. Therefore the first step to understand a crystallization process is to study the solubility of that particular system. Solubility is a function of a number of factors including the nature of the solute and solvents, the presence of salts, and other external factors such as heating and stirring.

In particular, the solubility of protein is lowered by the addition of salts or anti-solvent (a second solvent in which the solute is less soluble in) and this explains why precipitation crystallization or anti-solvent crystallization is the most widely used technique for protein crystallization.

Protein Lysozyme can be crystallized into two different structures, tetragonal and orthorhombic. A phase change from tetragonal to orthorhombic form of Lysozyme occurs at around 22-25°C (Jollès and Berthou, 1974). The phase change is manifested in the structural (Cozzone et al., 1975) particularly in the conformational change (Jollès and Berthou, 1974) and catalytic properties of Lysozyme. Thus, the phase change results in a change in the solubility behavior (Ataka and Asai, 1988; Cacioppo and Pusey, 1991a & 1991b).

Cacioppo and Pusey (1991a) measured the solubility of Lysozyme tetragonal crystals at pH 4.0-5.4, and various salt concentrations and temperatures. The solubility was determined using a miniaturized column technique where a pair of columns packed with micro-crystalline protein was equilibrated at the measuring conditions. Over-saturated solution was charged to one of the columns and another was charged with under-saturated solution. The concentration of the eluent from each column was then determined. The solubility of tetragonal form crystals was reported to increase with increasing temperature but decrease with increasing salt concentrations. However the effect of solution pH on solubility varied depending on the salt concentration in the solution. In general, the solubility of tetragonal Lysozyme crystals in solutions with lower salt concentration decreased with increasing pH. On the other hand, at higher salt concentration, a reversed trend was observed.

The solubility of orthorhombic Lysozyme crystals was reported by Ewing et al. (1994) where the measurements were carried out at temperature above 25°C using the same technique as described previously. Similar to the results reported by Cacioppo and Pusey (1991a), the solubility of orthorhombic crystals increased with increasing temperature and decreased with increasing salt concentrations. However, Ewing et al. (1994) showed that the solubility of orthorhombic crystals was less sensitive to temperature change. The solubility of orthorhombic crystals was reported to decrease with increasing pH values, which is the opposite as that of tetragonal crystals.

2.2.2.2 Crystal Morphology

Protein Lysozyme has been crystallized in 1945 by Alderton et al. (1945). Crystallization of Lysozyme was carried out in different buffer solutions and pH ranging from 3.5 to 10.8. Alderton et al. (1945) reported that the crystalline form of Lysozyme varied with the solution pH and the identity of the buffer solutions. Since then, the structure of Lysozyme crystals has been studied by single X-ray diffraction analysis on well formed single crystal. Lysozyme can be crystallized into different crystal structure with addition of different salts into the crystallizing solution. Alderton and Fevold (1946) showed that Lysozyme can be crystallized selectively in needle-like shape with iodide and bromide salts, and in smaller and finer needles with nitrate and bicarbonate salts. However, the attempt to crystallize Lysozyme with acetate, sulfate and tartrate failed. These results implied that the presence of foreign compounds (e.g. precipitant, impurities etc.) will affect the crystal shape of final product as reported by Skouri et al. (1995) and Lu et al. (2003).

Lysozyme crystals can also be obtained in other polymorphs such as orthorhombic (Berthou and Jollès, 1974), monoclinic and triclinic. The formations of monoclinic and triclinic crystals of Lysozyme are less known but it is believed that the inclusion of anion NO_3^- and SO_4^{2-} bound to the enzyme contributed to the formation of these crystal shapes. On the other hand, tetragonal and orthorhombic crystals of Lysozyme are more stable and most commonly studied by researchers. However, tetragonal crystals transform to orthorhombic once the crystallizing condition changed from room temperature (22°C) to above 25°C (Berthou and Jollès, 1974). This transformation is irreversible as the orthorhombic crystals have a wider range of stability (from -4°C to 60°C). Other than the temperature effects on the crystal morphology of Lysozyme, the salts identity and concentration, protein concentration, solution pH and other variables also affect the final crystal morphology (Berthou and Jollès, 1974).

2.2.2.3 Crystallization of Lysozyme under Oil

An approach to crystallize proteins under paraffin oil was first described by Chayen et al. (1990) to prevent evaporation of small-volume trial. An automated micro-batch technique was applied to screen the conditions for protein crystallization. This technique provides advantages (Chayen et al., 1992) over the conventional technique used to study protein crystallization e.g. vapor diffusion, hanging drop etc. Minimum amount of proteins (in micro-scale) was required in each set of experiments in micro-batch technique. Hence, variations in concentration and convection flows can be minimized and better understandings on crystallization kinetics can be further developed. Layers of oil prevent the crystals formed in the solution from physical shock and dissolution (Chayen, 1997). More importantly, samples are protected from

being contaminated by vessel walls or foreign particles/airborne contaminants. Contrarily, this technique has some drawbacks in which crystals formed in the solution under oil are more difficult to harvest. Furthermore, this technique is limited in its application on organic molecules as the crystallizing medium.

Lorber and Giegé (1996) further extended the single oil layer technique to two layers of oil analogous to an ideal non-wetting surface. Sample solutions were mixed at their final concentration before a drop of sample droplet (in micro-liter) was floated in between two layers of silicone oils with different densities. Nucleation occurred in the sample droplet without contacting any solid interface and thus, the nucleation rate was reduced. As a result, single crystals can be grown within the sample droplet and the linear growth rate can be easily measured.

The type and quantity of the oil can affect the results in crystallization of proteins (D'Arcy et al., 1996). D'Arcy et al. (1996) reported that crystallization under paraffin oil required longer induction time than crystallization under lower viscosity silicone oil. However, by mixing of these oils at different composition, the crystallization kinetics in this medium changed with the ratio of mixed oils. This is probably due to the diffusivity of water (which is normally used as the solvent in protein crystallization) in different oil mediums (D'Arcy et al., 1996; Chayen, 1999).

2.3 Two Phase Formation / Liquid-Liquid Phase Separation in Protein Crystallization

Liquid-liquid phase separation in protein Lysozyme system was first discovered by Ishimoto and Tanaka in 1977. They studied the mixing behavior of protein/water

mixture using turbidity measurement, and the coexistence curve and the spinodal curve were determined from the change in laser light intensity with temperature. They found that when the solution was cooled to lower temperature close to its critical point, the solution drastically turned opaque and the laser light intensity decreased abruptly. This corresponded to the onset of the liquid-liquid phase separation or two phase formation in Lysozyme solutions. The solution remained opaque when the solution was further cooled to the temperature lower than the critical temperature.

2.3.1 Phase Diagram of Protein Systems – A Colloidal Approach

The size of colloidal particles is typically in the range of 10 to 10^3 nm. These particles are much larger than atoms and molecules, but small enough that Brownian motion usually dominates gravitational settling, allowing thermodynamic equilibrium to be reached (Jones and Pusey, 1991; Piazza, 1999). It has been shown that the range of attraction between spherical colloidal particles (hard spheres in particular) has a drastic effect on the appearance of the phase diagram. Colloids can appear in three phases depending on the temperature and density of the suspension. These phases are: a dilute colloidal fluid (analogous to the vapor phase), a dense colloidal fluid (analogous to liquid phase) and a colloidal crystal phase. When the range of the attraction is reduced, the fluid-fluid critical point moves toward the triple point, where the solid coexist with the dilute and dense fluid phase. One particular feature of the phase diagram of hard spheres with a short range of attraction is the disappearance of a stable fluid-fluid coexistence curve. A transition between two stable fluid phases of different densities is only possible for relatively long-ranged attractions. For short range interactions, the fluid-fluid coexistence becomes metastable and the coexistence region lies beneath the solubility curve as shown in Figure 2.6(a). This is indeed found in experiments (Illet et

al., 1995; Poon and Haw, 1997) and simulations (Hagen and Frenkel, 1994). In addition, it has been reported that the metastable fluid-fluid coexistence as a function of interaction potentials occupy a large portion in a phase diagram (Dijkstra, 2002), giving flexibilities in altering the solidification process. The observations on the metastability of fluid-fluid coexistence curve are applicable to most of the protein systems as these molecules have short-range attractive interactions due to the charge screening (Steiner et al., 1995). Studies on the phase diagram of protein systems (Broide et al., 1991; Muschol and Rosenberger, 1997; Grouazel et al., 2002) have shown that type of in Figure 2.6(b). Moreover, the range of the effective interactions between protein molecules can be changed by the addition of non-adsorbing polymer (e.g. PEG) (Illet et al., 1995) or by changing the pH or salt concentration of the solvent (Durbin and Feher, 1996; Rosenberger, 1996).

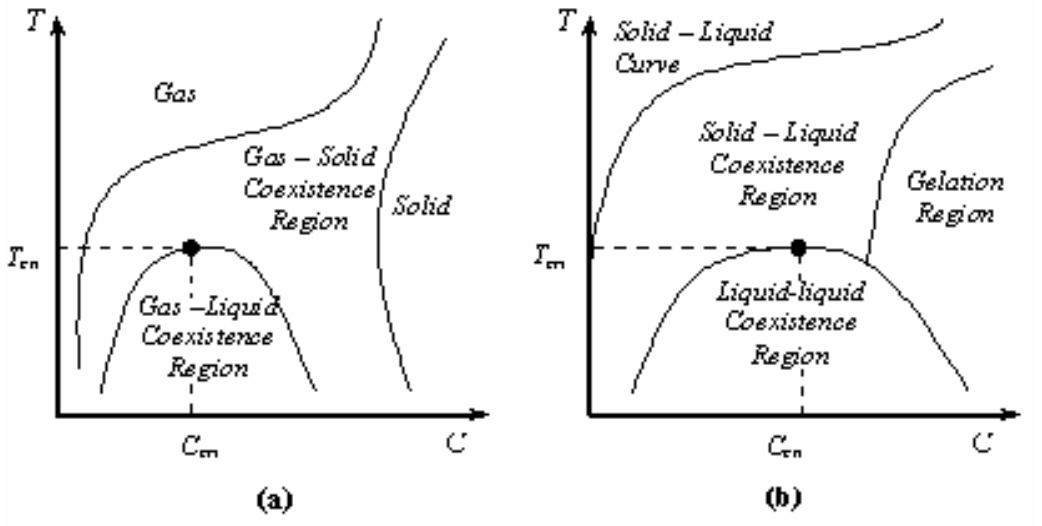

Figure 2.6 (a) General phase diagram of a colloidal system with short-ranged interactions (attraction potentials (Hagen and Frenkel, 1994)) (b) Phase diagram for protein systems. Set of cloud point temperatures, T_{cloud}, form a metastable liquid-liquid phase region which lies beneath the solubility curve. The maximum T_{cloud} is designated as the critical temperature, T_{cri}, with the corresponding concentration as the critical concentration, C_{cri}

Fluid-fluid coexistence of hard sphere in colloidal system is an entropic driven reaction (Kaplan et al., 1994; Steiner et al., 1995). It involves molecular structuring and depends strongly on the molecular interactions when the colloidal particles are brought closer to each other. The interactions between colloidal particles may be affected by additional substances to increase either the repulsion or the attraction forces between colloid particles (Hansen and Pusey, 1999; Dijkstra, 2002). However, the segregation of a mixture into different phases originates from the competition between the enthalpic and entropic contributions to the free energy.

Within the metastable region, the Ostwald rule implies that fluid-fluid phase separation would precede the fluid-crystal transition. Formation of good-quality crystals resulting form phase separation remains a controversial argument (Poon and Haw, 1997; Haas and Drenth, 1999 & 2000; Dixit and Zukoski, 2000). If fluid-fluid separation occurs first, nucleation may be enhanced but it could produce low-quality crystals (less ordered crystals). On the other hand, crystal growth is determined by the average density beyond the fluid-fluid phase separation region. In addition, this region is not commonly seen in colloidal systems. Instead, a gelled state would be formed (Soga et al., 1999). The transition from liquid state to gel state is commonly seen in protein systems in which the gel state is equivalent to the solid region in the phase diagram of colloidal systems.

Colloidal Interactions

Proteins are particles in the colloidal size range, and therefore any attempt to understand and predict protein crystallization would benefit from a description of protein solutions in terms of simple models of interacting colloidal particles. The

molecular interactions in colloidal systems had been studied numerically by adopting different potential models and experimentally by indirect inference from scattering methods where the second virial coefficient (B_2) of osmotic pressure is determined as a function of the nature and strength of the interaction potentials, and thermodynamic parameters such as temperature, ionic strength, pH etc. The second virial coefficient (B_2) of osmotic pressure has been related to the measure of particle interactions in colloidal systems or protein systems in particular. In general, a positive value of B_2 indicates the domination by repulsive interactions while a negative B_2 implies that attractive interactions are dominant. Fluid-fluid coexistence has been shown to occur only within a narrow range of negative values of B_2 (George and Wilson, 1994; Pellicane et al., 2003a) and this range is termed as the 'crystallization slot' (The range has been reported as varying from -0.8×10^{-4} ml.mol/g^2 to -9×10^{-4} ml.mol/g^2 (George and Wilson, 1994; Haas and Drenth, 1998; Zhang and Liu, 2003)).

In modeling the phase boundary of colloidal systems, the DLVO (Derjaguin-Landau-Verway-Overbeek) model has been used as the primary model to predict the solution behavior. This modal assumes that the effective short-range pair interactions between molecules result from uniformly charged molecular surfaces that lead to the screening interactions between the electric double layers around colloidal particles (Pellicane et al., 2003a). The DLVO model predicts well the monotonic decrease of B_2 with ionic strength. However, the virial coefficients change non-monotonically with increasing ionic strength due to the charge distribution on molecular surfaces (Allayarov et al., 2003). This behavior has been modeled by taking into consideration both uniformly charged and discretely charged molecular surfaces.

The phase behavior of colloidal systems has also been modeled as a hard-sphere fluid with an attractive Yukawa interaction (Hagen and Frenkel, 1994). The Yukawa potential can be divided into to two parts: an attractive tail and a repulsive tail (Louis et al., 2002). The attractive tail of the Yukawa potential is related to the 'sticky' interactions between molecules of globular protein whereas the repulsive tail describes the charged suspensions in which the interactions are controlled by the added salt and colloidal charges. The liquid-vapor coexistence curve (equivalent to the liquid-liquid coexistence curve for protein systems) in colloidal systems would vanish if the attractive tail of Yukawa potential is less than one-sixth of the hard-core diameter (Hagen and Frenkel, 1994). Thus, fractal-like aggregates or a gel-like phase which will hinder any phase transitions would be formed and eventually lead to aggregation and eventually (but not necessarily) reorder into the crystalline phase (Piazza, 1999).

The interaction variations on molecular surfaces which is known as aeolotopic (orientation-dependent) interactions, has been studied to understand phenomena such as aggregation and self-assembly during crystallization (Lomakin et al., 1999). This model provides a self-consistent and accurate representation of the liquidus line and the coexistence curve. Moreover, these interactions are responsible for aggregation. When the aeolotopic interactions are strong, metastable aggregates will abound, even though the crystal is the thermodynamically more stable structure. The view is consistent with the observation that, if the virial coefficient is too negative, amorphous aggregation dominates (George and Wilson, 1997). It has been suggested that the isotropic interactions (both repulsion and attraction) between the protein molecules favor crystal formation while the aeolotopic interactions determine the details of the crystal structure.

2.3.2 Two Phase Formation in Protein Crystallization

The interactions between colloidal particles can be classified into direct interactions and solvent-mediated interactions. Direct interactions between colloidal particles determine the fluid-solid transition process. However, studies on crystallization in a finite volume have shown that the fluid-solid transition was due to entropic effects (Jones and Pusey, 1991). This entropy-driven random walk process is due to the self-diffusion of each protein molecule. On the other hand, solvent-mediated interactions or solvation effects are the interactions induced by the solvent molecules between colloidal particles. The latter could explain the effective interactions between protein molecules especially in salting-out systems where precipitant is added to enhance crystallization (Piazza, 1999).

Investigations on the phase diagram numerically (ten Wolde and Frenkel, 1997; Haas and Drenth, 1998; Pellicane et al., 2003b) or experimentally (Ishimoto and Tanaka, 1977; Taratuta et al., 1990; Cacioppo and Pusey, 1991b; Skouri et al., 1995; Broide et al, 1996; Narayanan and Deotare, 1999; Grigsby et al., 2001; Galkin and Vekilov, 2001) for protein Lysozyme agree well with those of colloidal systems for short range interaction colloids. In protein crystallization, salt is commonly used as the precipitant to screen the electrostatic repulsion forces. Both solid-liquid phase separation (Cacioppo et al., 1991a; Ewing et al., 1994) and liquid-liquid phase separation occur (Ishimoto et al., 1977; Taratuta et al., 1990) with the liquid-liquid phase region lying beneath the solubility curve in a typical phase diagram (as shown in Figure 2.6b) for protein Lysozyme system. This indicates that the liquid-liquid phase separation exists as a metastable state in protein solutions. However, the phase diagram of the metastable liquid-liquid immiscibility region depends strongly on the solvent

composition (ionic strength in the solutions). It is possible to have a stable liquid-liquid immiscibility region in a phase diagram if the ionic strength in the solution is high enough to stabilize the two liquid phases (Haas and Drenth, 1999).

Spinodal and Binodal Curves

Phase boundaries provide insights about the molecular interactions of a system. Moreover, the phase diagram represents the equilibrium conditions for all events undertaken in a system. Figure 2.7 shows the liquid-liquid phase region in a (Concentration, Temperature) plane for the Lysozyme system. Upon undercooling to a temperature lower than the cloud point temperature, the solutions are separated into two liquid phases, the protein-rich phase and the protein-lean phase. The protein-rich phase will form as droplets dispersed in a matrix of the protein-lean phase (continuous phase).

The liquid-liquid coexistence curve gives the equilibrium conditions of each phase during liquid-liquid phase separation. This curve is also known as binodal curve. The solute composition in each phase corresponds to its concentration at particular temperature. Thus, its composition can be calculated from the phase diagram by applying the Lever rule. At a temperature slightly lower than the cloud point temperature, a metastable region exists where the occurrence of separated protein-rich phase is delayed by a thermodynamic barrier. On further subcooling, the barrier vanishes and the solution becomes unstable due to the generation of a growth-kinetic controlled phase and possible spinodal decomposition (Cahn and Hilliard., 1958). Spinodal decomposition is known as a process by which a thermodynamically unstable, virtually homogeneous solution transforms within a miscibility gap to a mixture of two

phases that are close to their equilibrium compositions. When this event occurs within a crystallizing solution, a large degree of fluctuations is required to reduce the free energy of the system and the solution becomes metastable supersaturated). The boundary that distinguishes the metastable and unstable region is known as the spinodal curve. In addition, spinodal decomposition can be facilitated by a high salt concentration in the solution (Zhang and Liu, 2003).

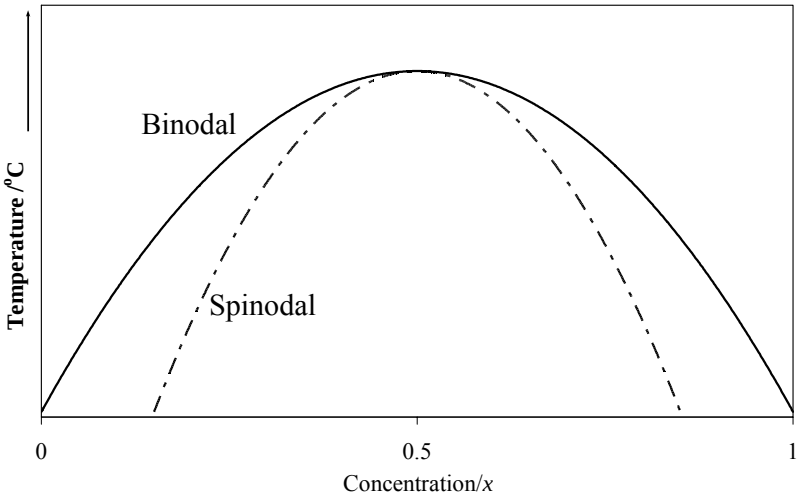

Figure 2.7 Liquid-liquid coexistence curve for Lysozyme system. Spinodal curve as the boundary between metastable region and unstable region

2.3.3 Effect of Process Variables on Cloud Point Curve

2.3.3.1 Effect of Salt Identity and Salt Concentration

Increasing salt concentration will increase the cloud point temperature of Lysozyme solutions while other variables such as pH, buffer solution concentration etc. are held constant. However, the critical concentration of the solutions remains unchanged. The critical concentration has been reported at (230 – 250 ± 10) mg/ml (Taratuta et al., 1990; Muschol and Rosenberger, 1997; Galkin and Vekilov, 2001).

The effects of anions and cations on the cloud point temperature are believed to be due to hydration forces in between the protein molecules and the ions (Grigsby et al., 2001). Specificity of adsorption of different anions and cations on macromolecular surface sites results in different efficiencies of these ions (Ries-Kautt et al., 1989). This specificity determines the so-called Hoffmeister series in the decreasing precipitative efficiency for anions,

$SO_4^{2-} > HPO_4^{2-} > CH_3CO^{-2} \approx$ citrate^{3-} > tartrate^{2-} $HCO^{-3} > CrO_4^{2-} > Cl^- > NO^{-2} > ClO^-$,

and cations,

$Li^+ > Na^+$ and $K^+ > NH_4^+ > Mg^{2+}$

The effect of the salt concentration on the cloud point temperature curve has been modeled successfully using DLVO theory. According to this theory, the cloud point temperature varies linearly with the logarithm of ionic strength at different salt concentrations (Pellicane et al., 2003b). This agrees well with the experimental data (Broide et al., 1996; Muschol and Rosenberger, 1997).

2.3.3.2 Effect of Buffer Solution

Cloud point temperature is not critically dependent on the buffer identity. However, T_{cloud} will decrease with an increasing concentration of buffer solutions. In this case, buffer solutions act as an additional salt in protein solutions and act to screen the charges on the surface of protein molecules (Taratuta et al., 1990; Forsythe and Pusey, 1996).

2.3.3.3 Effect of pH

Cloud point temperature decreases with the increasing solution pH (Broide et al., 1996). The electrostatic interactions between the protein molecules and their surroundings will be affected by the pH of solutions due to the charges on the surface of protein molecules. This is possibly due to the free energy change during the formation of an electrical double layer. Thus the surface residua of the molecules favor a medium which has a lower dielectric constant (adjacent molecules or solvent molecules), which tends to lower the cloud point temperature (Taratuta et al., 1990).

2.3.3.4 Effect of Alcohol

Additional of alcohol at high concentration to protein solution can lead to the formation of amyloid fibrils in the solutions. In addition, alcohol is able to destabilize the tertiary structure of protein molecules. In Lysozyme solutions, the additional of alcohol leads to the decomposition of Lysozyme molecules into monomer, dimer, proto-filament and amyloid fibrils (Yonezawa et al., 2002).

Different types of alcohol have different implications on the protein molecular interactions. Monohydric alcohols have been found to destabilize the protein conformation. Thus, the protein structure can be disrupted easily, causing the increase in its secondary structure. In addition, protein interactions change with the concentration of monohydric alcohols due to the binding of alcohol molecules on the surface of protein molecules (Liu et al., 2004).

2.3.4 Effect of Two Phase Formation on Protein Crystallization

Protein crystallization involves nucleation and crystal growth events which depend strongly on the thermodynamic driving force, supersaturation level, of the system. In conventional way, higher supersaturation level can be achieved either by cooling or additional of anti-solvent or salts to reduce the energy barrier for nucleation. However, highly saturated solution with significance variation of local concentration tends to form aggregates rather than crystals (George and Wilson, 1994; Ilett et al., 1995; Poon et al., 1995; Rosenbaum et al., 1996; Rosenbaum and Zukoski, 1996; Poon, 1997; Muschol and Rosenberger, 1997). In addition, high supersaturation level required for nucleation will affect crystal growth event where nucleation possibly occurs rigorously, and crystal grow rapidly and far from perfection (Durbin and Feher, 1996; Rosenberger, 1996).

The existence of metastable liquid-liquid phase separation has been reported to enhance the nucleation and crystal growth so that a suitable crystal for X-ray diffraction analysis can be obtained. The enhancement is facilitated by the density fluctuations in the vicinity of the critical point of liquid-liquid coexistence curve (ten Wolde and Frenkel, 1997 & 1999; Anderson and Lekkerkerker, 2002). The enhancement is greatest when the critical point is closest to the solubility curve (Galkin and Vekilov, 2000a and 2000b). This will in turn decrease the energy barrier for nucleation that stimulates the formation of critical nuclei (Talanquer and Oxtoby, 1998). The decrease in free energy barrier for nucleation via phase separation (in saturated dense phase) is attributed to a reduction in the interfacial energy due to wetting of crystal nucleus by liquid layer (ten Wolde and Frenkel, 1999). The free energy barrier for nucleation via phase separation has been shown to be lower than

those of nucleation in a conventional way (ten Wolde and Frenkel, 1997). Thus, reduction in the free energy barrier stimulates the formation of crystal nuclei within the dense phase (more concentrated phase). Molecules in that phase are always available for the growth steps and probably have ample time to orientate according to the surface of the growing crystals. Hence, better quality crystals for X-ray analysis can be obtained. Moreover, the supersaturation level, as the thermodynamic driving force for crystallization, is greatly dependent on the locations of the solubility and liquid-liquid coexistence curves in a phase diagram. Hence the crystal growth will be slower when then supersaturation level is low and more ordered crystals can be obtained. It is possible that liquid-liquid phase separation affects the nucleation rate and the crystal growth (Anderson and Lekkerkerker, 2002). However, careful control of the process is needed to avoid growth of imperfect crystals (Durbin and Feher, 1996; Rosenberger, 1996).

Proteins tend to concentrate more in one of the liquid phases than the other during phase separation. This can lead to extremely high protein concentrations and subsequently, a very high supersaturation in one phase. Sica et al. (1996) observed the formation of crystals at the boundary of two liquid phases. The appearance of these crystals at the boundary indicates that some component in the other phase maybe be acting as a "phase transfer catalyst" for the nucleation. The supersaturation in either phase can support crystal growth once growth has started. Nucleation via phase separation was also observed by Chow et al. (2002) where spherulitic or "sea-urchin" crystals were obtained in an impurities-laden Lysozyme system. The presence of impurities during phase separation (Sica et al., 1996) possibly results in heterogeneous nucleation in that system. Nevertheless, the formation of "sea-urchin" crystals has also

been observed in clean systems (Georgalis et al., 1998; Galkin and Vekilov, 2000a and 2001).

CHAPTER 3

CONSTRUCTION OF CLOUD POINT CURVE FOR THE LYSOZYME SYSTEM

3.1 Introduction

Crystallization is an important unit operation in the pharmaceuticals and fine chemicals industry. Good understanding and precise control of the process is of utmost importance in order to obtain products/crystals with the required specifications, as the properties of these products strongly depend on their crystal size, habit and polymorphic form. A key step is to study nucleation and crystal growth events during crystallization, and a detailed understanding of the phase diagram would provide an essential means of tuning the operation conditions.

Phase diagrams of protein systems have been widely studied for bovine γ_{II}-crystalline (Broide et al., 1991; Berland et al., 1992), bovine serum ovalbumin (Grouazel et al., 2002), Taka-amylase A (Ninomiya et al., 2001), Lysozyme (Ishimoto and Tanaka, 1977; Thomson et al., 1987; Taratuta et al., 1990; Cacioppo and Pusey, 1991a; Skouri et al., 1995; Georgalis et al., 1998; Galkin and Vekilov, 2000b) etc. The coexistence of solid-liquid and liquid-liquid phase regions have been reported for these

systems. Moreover, the presence of a metastable liquid-liquid critical point has been reported, which substantially lowered the energy barrier for nucleation, and thus indirectly promoted crystallization (Kern and Frenkel, 2003). Understanding the liquid-liquid coexistence region is thus an integral part of studying the phase behavior of protein solutions, as it may be an important step towards predicting suitable crystallization conditions.

In this chapter, the cloud point curve for liquid-liquid phase separation in Lysozyme system will be studied. Techniques to construct the cloud point curve of Lysozyme system will be discussed. In addition, the role of salts in Lysozyme system will be verified via partitioning test. The experimental results on the liquid-liquid phase separation in Lysozyme system, which comprise of the effect of buffer solution and cooling rates on liquid-liquid phase separation, and the salt partitioning during phase separation, will then be discussed.

3.2 Experimental

The experimental procedure in the construction of cloud point curve for Lysozyme system is divided into three sections, namely solution preparation, cloud point temperature measurements and salt partitioning test.

3.2.1 Solution Preparation

3.2.1.1 Buffered Solutions

An appropriate amount of hen egg white Lysozyme (HEWL) powder (six-time crystallized) purchased from Seikagaku Corp (Lot no. E99201 and E01201) was gradually dissolved in Sodium Acetate solution (pH 5.2±0.1, Sigma-Aldrich), which is

used as the buffer solution, to form Lysozyme stock solution with concentration double its desired final concentration in sample solutions. The dissolution was carried out at 45^{o}C with stirring at 200 rpm. In all the experiments, the pH of the investigating system was 4.5. Therefore, the pH of the stock solution was adjusted to 4.5±0.05 by adding Acetic Acid (ACS reagent, Sigma-Aldrich) or 0.1N Sodium Hydroxide. The pH measurement was done with a pH meter (EUTECH Instrument, CyberScan pH 510).

The stock solution of 6 w/v% salt (Sodium Chloride NaCl, analytical grade, Sigma-Aldrich) was prepared by dissolving an appropriate amount of salts in sodium acetate buffer solution. The pH of salt solution was then adjusted to 4.5±0.05 as in the preparation of Lysozyme solutions. The stock solutions of Lysozyme and salt were filtered through 0.22μm Millipore Millex-GV filter before used.

3.2.1.2 Un-buffered Solutions

Both HEWL and Sodium Chloride solutions were prepared separately by gradually dissolving an appropriate amount of the substance in ultra-pure deionized water (with resistivity 16.3mΩ) according to the desired concentration (double its concentration). The dissolution was carried out at 45^{o}C with agitation. 0.1N Hydrochloric acid or 0.1N Sodium Hydroxide was added to adjust the solution pH to 4.5±0.05. The solutions were filtered through 0.22μm Millipore Millex-GV filter before use.

3.2.2 Cloud Point Temperature (T_{cloud}) Measurements

3.2.2.1 T_{cloud} from the Turbidity and Concentration Measurements

In developing the cloud point curve and to provide understanding on the effect of buffer solution on the oiling out during crystallization, two different approaches were used.

In the first approach, the concentrations of two separated phases were measured using a UV-Vis Spectrometer. The experiments were carried out in a 25ml crystallizer. The crystallizer was cleaned by series of soaking in chromic acid, ultrasonic bath and ultra-purified water to avoid the presence of impurities in the crystallizer. Lysozyme solution was measured out into the crystallizer and incubated at 25^{o}C. An equal volume of the salt solution was measured out in a test tube and incubated at 25^{o}C. The salt solution was then added into the crystallizer and the final solution was left to equilibrate at 25^{o}C for 2-5 minutes. A final solution with the Lysozyme concentration ranges 55mg/ml – 190mg/ml and 3±0.05 w/v% NaCl was then cooled to the temperature where two liquid phases can be clearly seen and this temperature was recorded as the cloud point temperature. The sample solution was then left at that temperature. A small amount of the liquid from each phase was withdrawn and diluted to 100x or 1000x for concentration measurement using a UV-Vis Spectrophotometer (UV-2550, Shidmazu) at the wavelength 280nm with an extinction coefficient of 2.64 absorbance units per 1mg/ml solution (Sophiaopoulus et al., 1962). The schematic diagram for the experimental setup to determine the cloud point temperature via concentration measurement in both buffered and un-buffered solutions is shown in Figure 3.1.

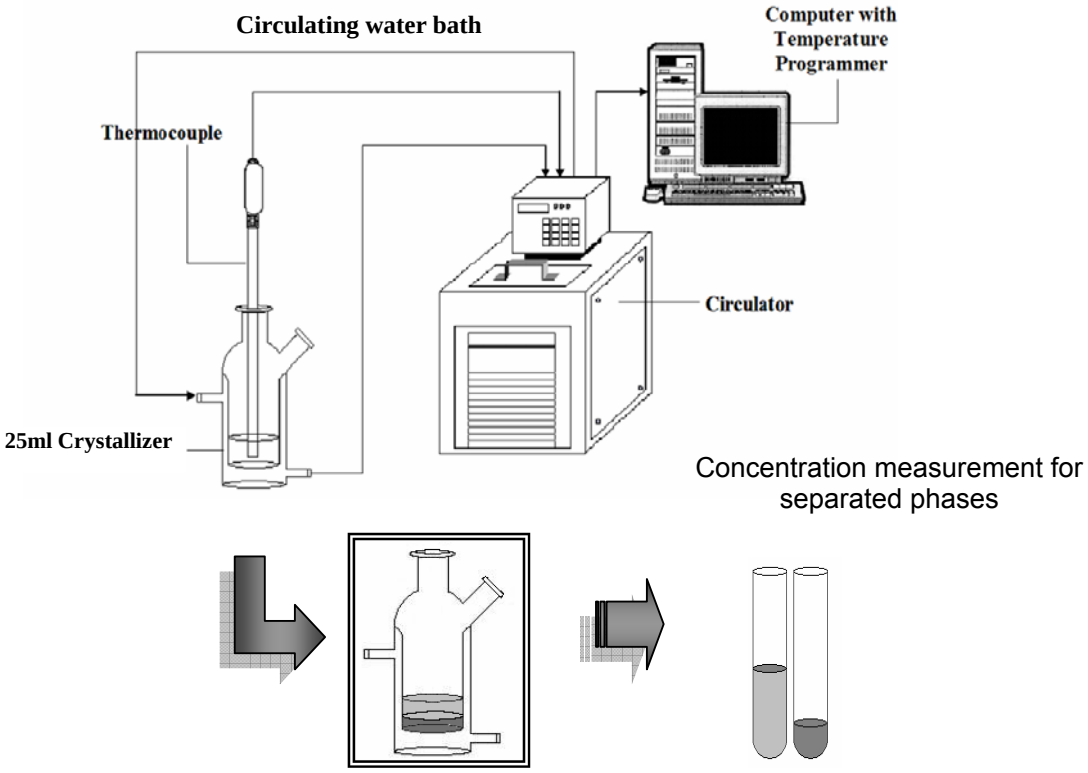

Figure 3.1 Concentration measurement for two liquid phases after the Lysozyme solution was cooled and turned cloudy. Upon observing the formation of two distinctive layers, small amount of the solution from each phase was drew out and diluted into a sample cell. The concentration was then measured at the wavelength 280nm with UV-Vis spectrophotometer

In the second approach, the cloud point temperature was determined using a calorimeter (Brinkmann Fibre Optic Colorimeter Digital Model 920) at the wavelength (λ) of 540nm. The final solution (Lysozyme concentration ranged 55mg/ml – 190mg/ml and 3±0.05 w/v% NaCl) was prepared as in the first approach mentioned previously (except the solutions were measured into Pyrex® test tubes which have been pre-washed in chromic acid, ultrasonic bath and ultra-purified water) which were then incubated in a bath (3:1 mixture of Ethylene Glycol and water) at 25^{o}C. The solution was left to equilibrate at 25^{o}C for 2-5 minutes. Salt solution was added into the Lysozyme solution and the calorimeter probe window was then immersed beneath the final solution level. The mixed solution was again left to equilibrate at 25^{o}C for 2-5

minutes and followed by cooling to 0^{o}C. The absorbance of the solution was recorded as a function of time. An instantaneous change in the absorbance indicates the onset of the cloudy state of the solution, thus, the temperature at this point is taken as the cloud point temperature.

3.2.2.2 Effect of Cooling Rates, using Polarized Microscope and Micro-DSC

Different cooling rates have been applied to the Lysozyme solution in order to have a better understanding on the kinetics effects of two phase formation in protein crystallization.

Micro Batch Experiments

The experiments were first carried out in a micro-batch system. Buffered solutions were used to determine the effect of cooling rates to the cloud point curve. The stock solution was left to equilibrate to the experimental temperature (25^{o}C) in a thermostatic water bath prior to mixing. Upon mixing, a drop of the final solution (1.2-1.5µl) was sandwiched in between a silicone oil layer (specific gravity 1.075) and a paraffin oil layer (specific gravity 0.86) in a quartz crucible (Linkam Scientific Instrument, model no. HSF-91). In this set of experiment, the crucible which was used as the medium for observations on protein crystallization, was cleaned with 2-propanol, soaked with chromic acid and cleaned with ultra-purified water. The experimental setup is shown in Figure 3.2. This method is known as double-oil layer method and is applied to prevent the evaporation of the sample (Chayen, 1997; Lorber and Giegé, 1996) and to observe the crystallization events under a well-controlled environment (Lorber and Giegé, 1996; Chayen, 1999). The crucible was then placed inside a temperature-controlled stage (Linkam, THMS600) on a polarized-light

microscope (BX51, Olympus). Liquid Nitrogen was supplied and circulated in the stage for cooling purpose. The observations with the microscope were converted to digital images through a color video camera (JVC KY-F55B 3-CCD), and captured and processed by an image analysis software (AnalySIS). In all the experiments, the concentration of NaCl was kept at 3 w/v% and the concentration of Lysozyme varied from 15 mg/ml to 190mg/ml.

Different cooling rates (from 0.05^{o}C/min to 1.5^{o}C/min) were applied to the samples in order to understand the kinetic effect on the phase separation phenomenon. The solution was first rapid-cooled to 8^{o}C (at 10 to 15^{o}C/min), then followed by cooling to -10^{o}C at different rates. Real time images were acquired at a regular time interval during the cooling process. The onset of the appearance of oil droplets was taken to be the cloud point temperature, T_{cloud}. The experiments were repeated in triplicate.

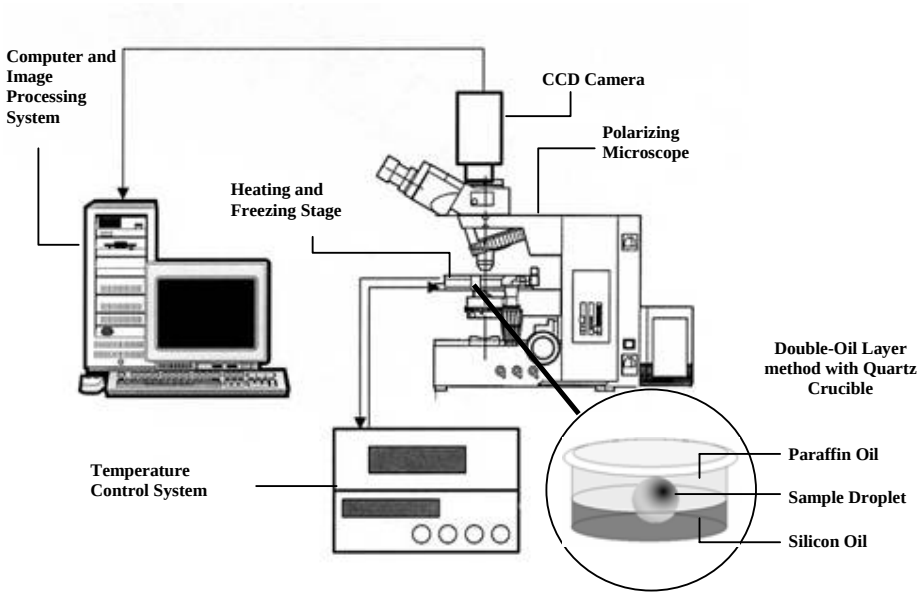

Figure 3.2 Experimental set up in micro-batch system. Sample droplet is sandwiched by two layers of oils with different densities

Micro Differential Scanning Calorimetry

In order to further validate the T_{cloud} values determined in the micro-batch experiments, the heat flow of Lyszome solutions during cooling was monitored using a micro-DSC (Setaram micro-DSC III). The sample solutions were prepared by mixing of Lysozyme solution and salt solution at 25^{o}C. The final solution was left to equilibrate for 2-5 minutes before 0.4-1 ml of the solution was introduced into a micro-DSC vessel. An identical amount of sodium acetate solution (pH 4.55, 0.1 M) was placed in to a reference cell. The cells were placed into the furnace of micro-DSC and the experiments were started at 25^{o}C. The sample was kept to equilibrate at 25^{o}C before it was fast cooled to 8^{o}C (at 1^{o}C/min). The sample was then cooled to –10^{o}C at different rates (ranged 0.25^{o}C/min to 0.75^{o}C/min) and the heat flow of the samples was recorded. After each run of experiments, the vessels were soaked with 2-propanol and cleaned with acetone. It was then followed by cleaning with chromic acid and deionised water before drying in an oven. The cooling at 0.05^{o}C/min and 1.5^{o}C/min as used in the micro-batch experiments cannot be applied in the experiments using micro-DSC due to the constraints in cooling capability of the instrument. The cloud point temperature was determined as the temperature at which a deflection in the heat flow occurred, which indicated that an endothermic event has taken place (Darcy and Weincek, 1999 and Lu et al., 2004). The experiments were carried out in triplicate.

3.2.3 Partitioning Test

The partitioning test of the sodium ions was carried out to understand the effect of salts, which was used as the precipitant, during liquid-liquid phase separation. A Atomic Absorbance Spectrometer (Shidmazu AA-680) with Na light source as the analytical element (analytical wavelength 589nm) was used to measure the concentration of

Sodium ions in the solutions. Standard solutions with sodium concentration ranged from 0.75ppm to 1ppm were prepared. Once the calibration curve had been established, measurement on sodium contents in sample solutions can be performed.

The following sample solutions were prepared:

1. Crystallizing solutions before and after the formation of tetragonal Lysozyme crystals,
2. Crystallizing solutions before and after the formation of orthorhombic Lysozyme crystals,
3. Crystallizing solutions before they turned cloudy (before the liquid-liquid phase separation event), and
4. Two liquid solutions (namely protein-rich phase and protein-lean phase) after the phase separation.

Each sample was aspirated once the constant absorbance is achieved and the measurement was repeated to obtain the average absorbance of the sample.

3.3 Results and Discussion

3.3.1 Phase Separation in Buffered and Un-buffered Solutions

The formation or occurrence of phase separation in a Lysozyme solution is shown in Figure 3.3. In Figure 3.3(a), the phase boundary in Lysozyme solution can be seen when phase separation was first took place after being cooled to the temperature lower than its cloud point temperature. The instantaneous temperature at this point is taken as the cloud point temperature. The solution concentrations for both layers were measured and, as expected, the protein-rich phase settled as the bottom layer while the protein-lean phase with the lower density formed the top layer (Lafferrère et al., 2002; Bonnett et al., 2003). When the solution was further cooled to a lower temperature, it

has a tendency to form a milky solution (as pointed with arrow in Figure 3.3b) rather than two distinct phases. The milkiness of solution depends on the solution temperature. The solution remained milky when it was kept below its cloud point. It is possible that upon further cooling after the phase separation has occurred, Lysozyme molecules diffuse across the interface to attain a new equilibrium.

The formation of the two distinctively separated liquid phases can be understood in term of simple fluid theory in which the protein molecules are treated as a hard sphere square well colloidal system with short-range interactions (Lomakin et al., 1999; Vliegenthart et al., 1999; Dixit and Zukoski, 2000; Kern and Frenkel, 2003). When the interaction range is low (about quarter (Daanoun et al., 1994; Rascòn et al., 1995) or one-third (Dixit et al., 2001; Kern and Frenkel, 2003) of the diameter of protein molecules, which is 1.7nm (Haas and Drenth, 1999) for Lysozyme molecules), it leads to a lower critical temperature and a higher critical density that in turn affect the segregation of protein molecules. The highly anisotropic protein molecules (Muschol and Rosenberger, 1997) tend to stick together randomly due to their anisotropic behavior. The molecules will then gradually reoriented to align in aggregates. The formation of two liquid phases has been related to the cluster formation in precrystalline solutions (Tanaka et al., 1999; Zhang et al., 2003; Sorensen et al., 2003) according to the diffusion-limited clusters aggregation (DLCA) model. However, the formation of liquid-liquid phase transition is metastable in protein system.

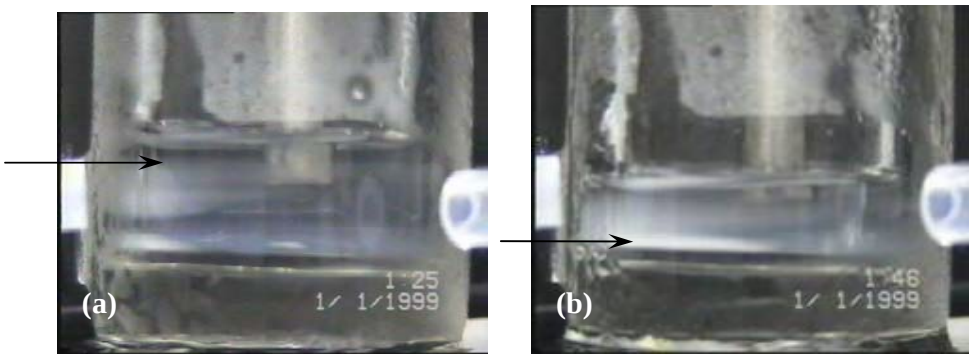

Figure 3.3 (a) The phase boundary (pointed with arrow) can be seen at the beginning of phase separation. The temperature at this point is known as the cloud point temperature; (b) Upon cooling to lower temperature after the phase separation taking place, the solution gradually turned milky (pointed with arrow) instead of two distinct liquid phases

The two liquid phases formed during the measurement were then separated and allowed to crystallize separately. Tetragonal crystals were expected to form at the given temperature (<25^{o}C). Figure 3.4 shows the crystals of protein Lysozyme formed from the two individual phase solutions. More crystals with smaller size were formed in the protein-rich phase while fewer but bigger crystals formed in the protein-lean phase. As discussed in Chapter 5, the protein-rich phase exists as the oil droplets (disperse phase) in the matrix of protein-lean phase regardless of the initial protein concentration. These droplets have the same Lysozyme concentration, and therefore attain a same concentration driving force that leads to stimulated nucleation of Lysozyme crystals. Previous studies have demonstrated that nucleation is first initiated within the droplet phase (ten Wolde and Frenkel, 1997 & 1999; Haas and Drenth, 2000). This could explain why more crystals are obtainable in the protein-rich phase. The crystals were then grown and crystal clusters was observed, probably as a result of the high nucleation rate in the protein-rich phase.

As compared to the protein-rich phase, only few nuclei were formed in the protein-lean phase with relatively lower supersaturation level. The nucleation in this phase would be similar to crystallization from bulk phase. The nucleation rate for each nucleus may be different depending on the local concentration or density variations (ten Wolde and Frenkel, 1997 & 1999; Anderson and Lekkerkerker, 2002; Manno et al., 2003). In addition, higher concentration driving force or supersaturation level is required to achieve the formation of critical nucleus in solution. Thus, the number of crystals formed would subsequently determined by the number of nuclei formed.

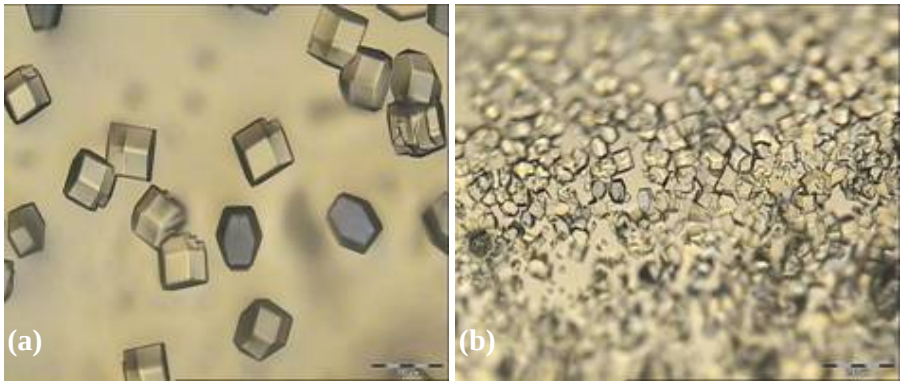

Figure 3.4 (a) Less number but bigger crystals formed in protein-lean phase, and (b) many smaller crystals formed in the protein-rich phase

The measurement of T_{cloud} was first carried out using a colorimeter in which the turbidity of the cooled samples was recorded with the corresponded time. Figure 3.5 shows the plots from turbidity measurements for buffered Lysozyme solutions. There was an instantaneous deflection in absorbance when the sample solutions were cooled to a sufficiently low temperature and turned cloudy. Upon removal from the incubation bath, the solutions turned clear. This further demonstrates that the measured turbidity of Lysozyme solutions was indeed due to metastable liquid-liquid phase separation.

Figure 3.6 shows the cloud point temperatures measured from two different approaches mentioned in section 3.3.2.1 for buffered solutions. The results from both approaches were comparable. As compared to the data reported by Muschol and Rosenberger (1997), the cloud point temperatures obtained in this investigation were (5 – 10) ^{o}C higher. Discrepancies in the measured cloud point could be due to the differences in sample preparations. Salt solution was added to Lysozyme solution after equilibrated at the initial experimental temperature in this study, while Lysozyme powder was dissolved directly into the buffer/salt solutions as reported by Muschol and Rosenberger (1997). Mixing of solutions could change the entropy of a system since the entropy is related to the order of a system during phase transition. This mixing effect in conjunction to other aspects (e.g. protein molecular interactions, folding, etc.) may affect the liquid-liquid phase separation event during cooling. Despite the differences in the measured cloud point temperatures, it appears that the measured critical concentration of Lysozyme at ~210-230mg/ml is comparable to those reported by other researchers (Taratuta et al., 1990; Muschol and Rosenberger, 1997; Galkin and Vekilov, 2001).

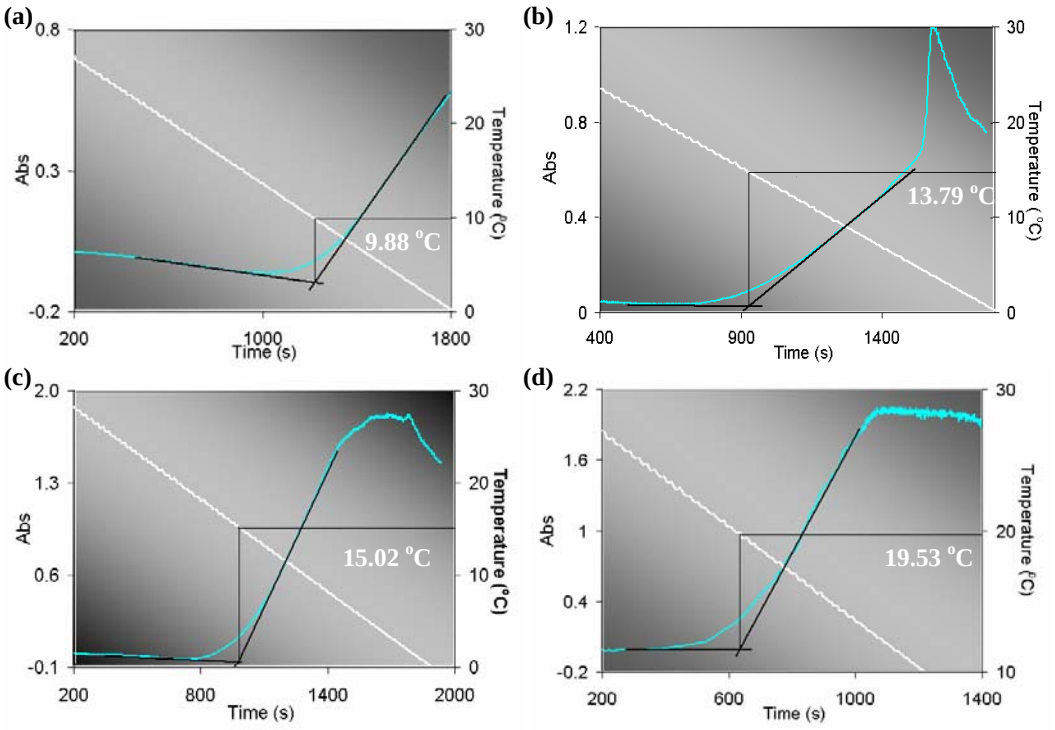

Figure 3.5 Absorbance of buffered Lysozyme solutions (pH 4.55) was recorded as a function of time. The solution concentrations were 3±0.05 w/v% NaCl and (a) 81.35mg/ml lys, (b) 116.85mg/ml lys, (c) 163.96mg/ml lys, and (d) 190.97mg/ml lys. Curves in the graphs indicate the absorbance and the straight lines indicate the temperature flow of the investigating system. Cloud point temperature was determined as the onset of deflection in the measured absorbance

No data was obtained in the turbidity measurement of Lysozyme solutions with concentrations higher than 250mg/ml. The solutions became gel-like once mixed with NaCl solution beyond this concentration. According to the generic phase diagram proposed by Muschol and Rosenberger (1997), there is no clear boundary between the liquid-liquid coexistence region and the gelation region in the vicinity of higher concentration of protein solutions. Thus, rapid crystallization and gelation would prevent the formation of two liquid phases particularly in solutions with high protein concentration.

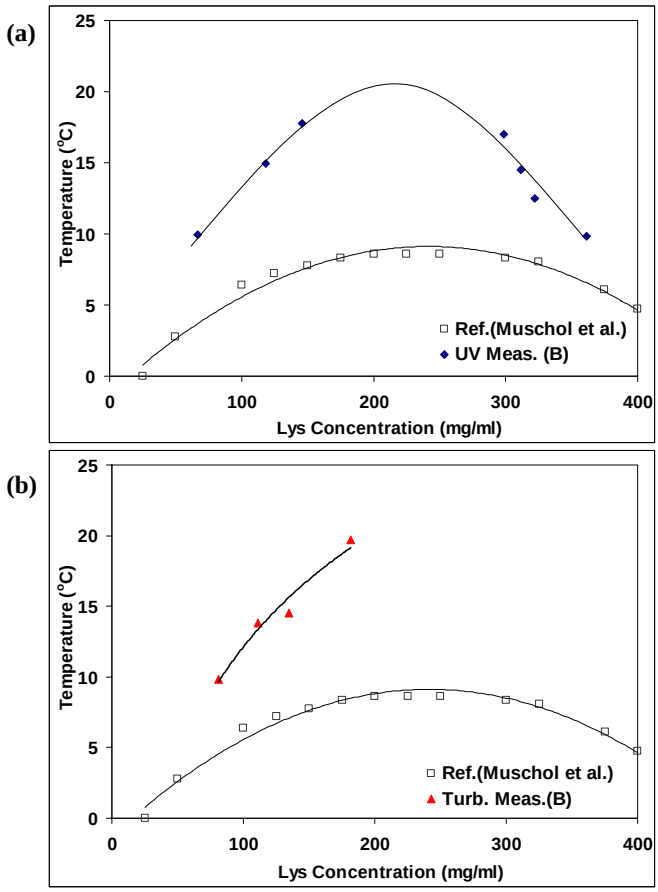

Figure 3.6 Determination of cloud point temperatures for buffered solutions from the two approaches: (a) concentration measurement of each liquid phase (shown as diamond dots); and (b) cloud point temperature determined from turbidity measurement (shown as triangle points). Line was drawn to illustrate the pattern for the experimental data

The cloud point curve was further investigated with un-buffered solutions. Figure 3.7 shows the cloud point curve in un-buffered solutions determined by two approaches. As in the results for buffered solutions, cloud point temperatures for un-buffered solutions are also higher than those reported by Muschol and Rosenberger (1997). However, when comparing the results from the turbidity measurements for both buffered and un-buffered solutions, the cloud point temperatures were comparable (Figure 3.8), with a maximum difference of approximately 3^{o}C was recorded. It has been reported that sodium acetate, though a weak precipitant (Ries-Kautt et al., 1989),

may increase the ionic strength in buffered solutions. However, the buffer effect on the cloud point temperature depends on the identity of buffer solutions, pH, the concentration of buffer solutions (Taratuta et al., 1990) and the net surface charge of Lysozyme molecules (Forsythe and Pusey, 1996). Lysozyme at pH 4.5 has 10-12 net positive charges on its surface (Rosenberger, 1996). At pH around neutral, Lysozyme has a net positive charge that may repel positive ions. Therefore, anions have a stronger effect on the cloud point temperature. It is believed that these net surface charges of Lysozyme molecules drive the phase transition in the observed systems.

The differences in the measured cloud point temperature are believed to be due to the buffering effect. Sodium chloride is the only salt used in this project and the pH of solutions was maintained at 4.5±0.05. The effect of anions, as reported by Taratuta et al. (1990), Broide et al. (1996) and Grigsby et al.(2001) is unlikely contributed to the differences in cloud point temperatures between the buffered and un-buffered solutions.

In all the experiments explained from this point onwards, the buffered solutions will be used as the investigating system as they exhibited a greater consistency of pH in the Lysozyme solutions.

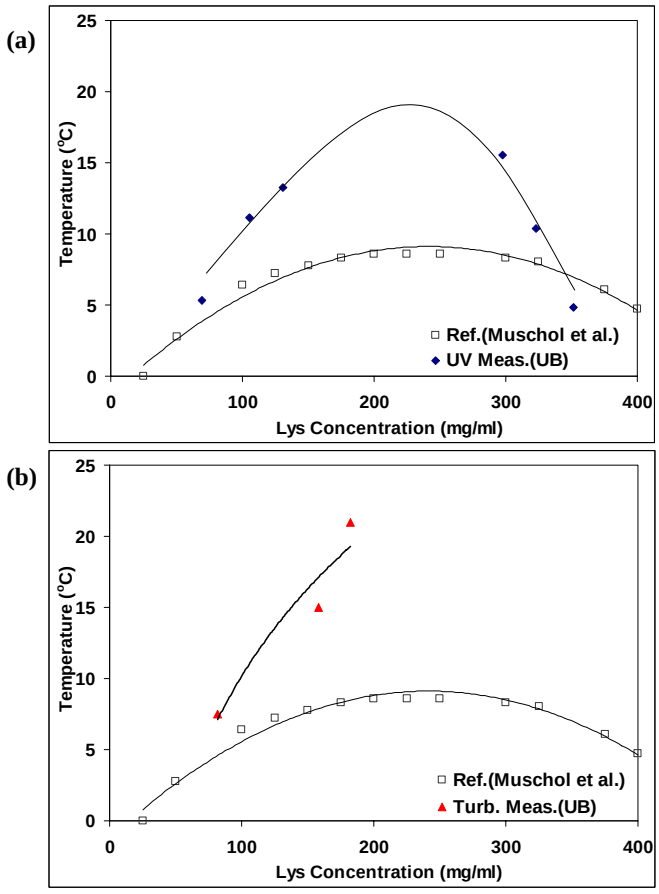

Figure 3.7 Cloud point curve for un-buffered solutions developed from the two approaches: (a) concentration measurement of each liquid phase (shown as diamond dotes); and (b) cloud point temperature determination from turbidity measurement (shown as triangle points). Line was drawn to illustrate the pattern for the experimental data

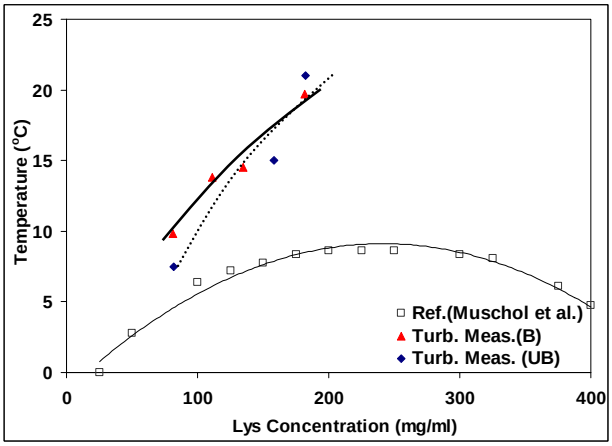

Figure 3.8 Comparison of cloud point curves for buffered (▲) and un-buffered (♦) solutions. Lines were drawn to aid the eyes in comparing the data points

3.3.2 Effect of Cooling Rates on the Cloud Point Curve

Figure 3.9 shows the evolution of oil droplets formation in Lysozyme solutions during cooling in the micro-batch system. The protein-rich phase exists as oil droplets dispersed in the continuous phase (Figure 3.9a). In some cases, crystals might be formed prior to the existence of oil droplets (Figure 3.10). Upon cooling to lower temperature, the amount of droplets formed increased drastically and the solution turned opaque (as those shown in Figure 3.3). The cloudiness of sample blocked the passage of the transmitted light of microscope, resulting in the dark image in Figure 3.9b. Upon reheating, the number of protein-rich droplets decreased and the solution became clear again as shown in Figure 3.9c and 3.9d.

Figure 3.11 shows the cloud point temperatures of Lysozyme solutions at different cooling rates from the micro-batch experiments. The trend of the data is not clear, but it appears that cloud point temperatures are influenced by the cooling rates. The results suggest that between 0.5^{o}C/min to 0.75^{o}C/min, the cloud point curve is situated at its lowest position beneath the solubility curve in a phase diagram. This may be useful in devising a method to control the nucleation rate in cooling crystallization by cycling through two-phase region (Muschol and Roseenberegr, 1997; ten Wolde and Frenkel, 1999; Galkin and Vekilov, 2001). Moreover, it is necessary to have a detail understanding of the phase diagram if two phase formation is to be avoided owing to obtain desired crystal morphology.

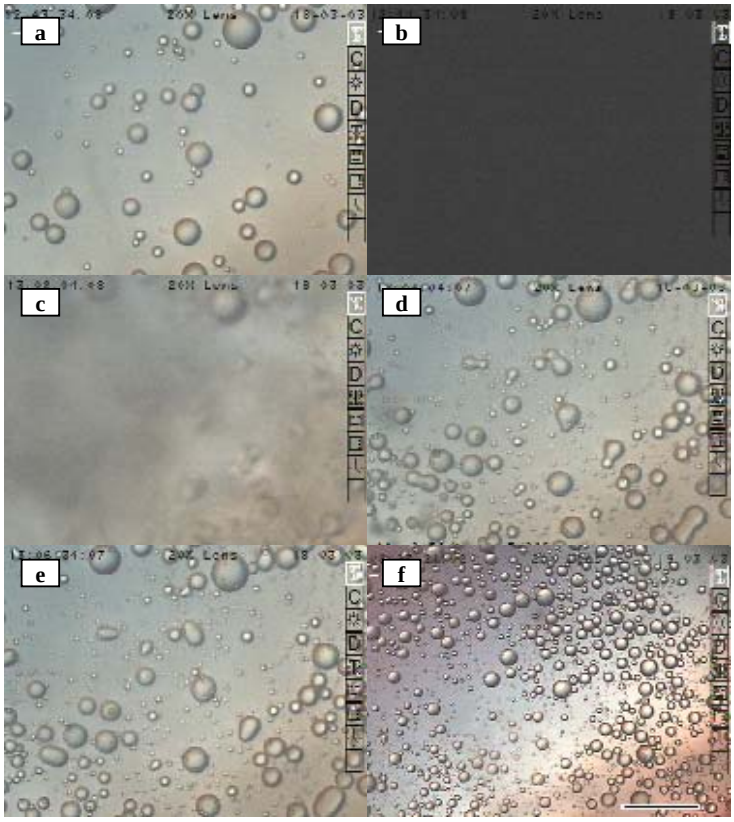

Figure 3.9 Lysozyme solution at (a) –8.9 °C, (b) -10 °C, (c) 0.2 °C, (d) 5.2 °C, (e) 11.5 °C, and (f) 21.3 °C. The formation of the oil droplets as the dispersed phase indicates the onset of the liquid-liquid phase separation or the two phase formation phenomena. The scale bar is corresponding to 100µm for (a) – (e) and 200µm for (f)

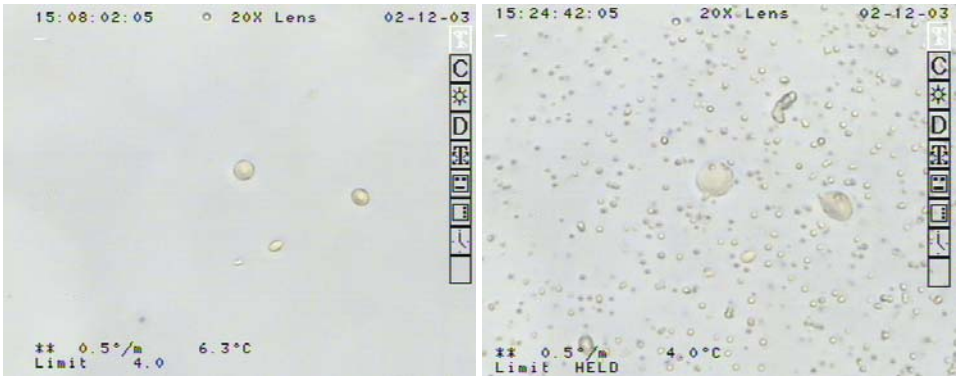

Figure 3.10 Crystals formed prior to the formation of oil droplets in the matrix of continuous phase (Lysozyme solution with 121.4mg/ml Lysozyme and 2.98 w/v% NaCl, at 0.5°C/min cooling). Nucleation and crystal growth occurred simultaneously in this case. New crystals were expected to nucleate in the vicinity of solute-rich phase and the number of oil droplets may decrease due to the Ostwald ripening phenomenon (Davey and Garside, 2000), if solution was kept at constant temperature

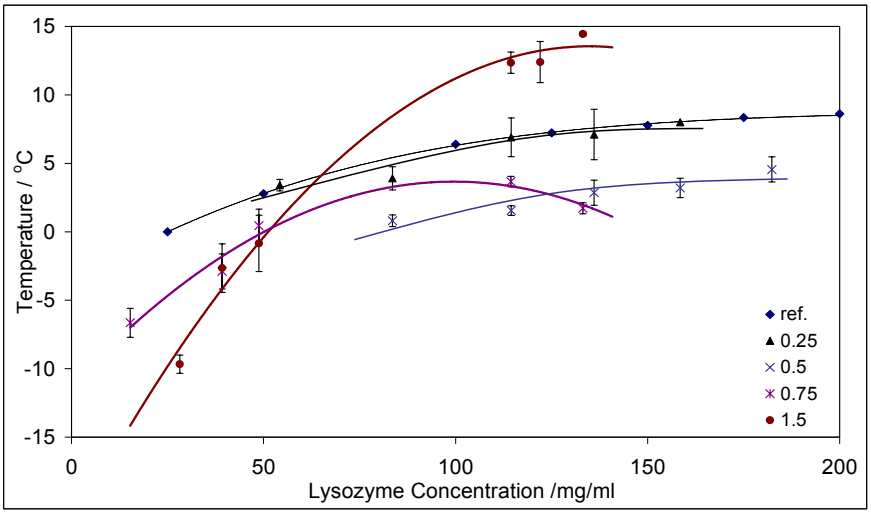

Figure 3.11 Cloud point temperatures of Lysozyme solutions cooled at 0.25 – 1.5°C/min. Lines were drawn to aid the T_{cloud} comparison between the experimental data and the data from Muschol and Rosenberger (1997). Only typical error bars are shown in the diagram. The solubility curve is located well above the cloud point curve, which is not shown in the figure

The formation of the dispersed phase is believed to be due to the interaction of protein molecules as a result of the fluctuations in local density (ten Wolde and Frenkel, 1997; Manno et al., 2003). However, the effect of cooling rates on the crystallizing solutions requires further investigations. A possible explanation for this effect could be the different folding ability of Lysozyme molecules at different cooling rates. Cloud point temperatures have been reported to be a function of the interaction strength between protein molecules or the concentration of protein solution (Muschol and Rosenberger, 1997). Globular proteins, such as Lysozyme, with their folded structure are possibly bound by surface charges, thus reducing the likelihood of attractive interactions. At different cooling rates, the molecular folding mechanism could be different, thereby altering the molecular interactions.

In addition to the cooling effects, variations in achieving equilibrium for the Lysozyme systems at different cooling rates should be taken into consideration. Moreover, fluctuations in water properties (water being the major component in protein solutions) upon cooling below its melting point may affect the kinetics of liquid-liquid phase separation and crystallization. It is possible that a complex combination of factors such as the enthalpy/entropy change of the system in reaching phase equilibrium, the molecular interactions and restructuring, and other kinetic phenomena are responsible to the effect of cooling rates on the cloud point temperature or the metastable liquid-liquid phase region for Lysozyme system.

Figure 3.12 (a) The formation of tiny crystals upon cooling at 0.05°C/min; (b) the tiny crystals grew to bigger crystals

However, at very slow cooling rate, e.g. 0.05^{o}C/min, the cloud point temperature could not be determined (Figure 3.12). Tiny crystals were observed, which grew larger as the solution was further cooled at slow rate. No oil droplets were observed in the sample solutions. It is believed that the slow cooling hinders the formation of solute-rich phase by favoring homogeneous nucleation. Nevertheless, the explanation for this effect requires further investigations.

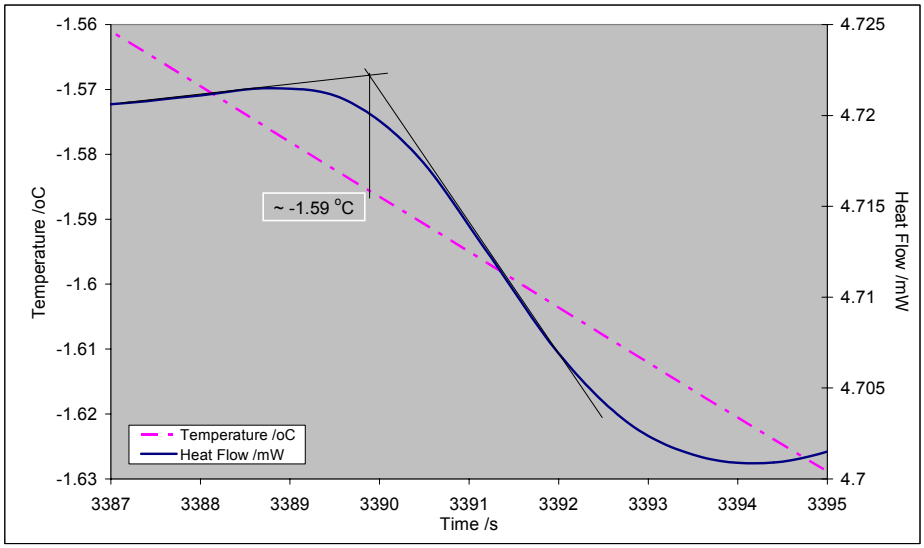

Figure 3.13 Heat flow in Lysozyme solutions (48.82mg/ml Lysozyme and 3.01 w/v% NaCl) during cooling at 0.5°C/min from 8°C to -5°C. A deflection in the heat flow at low temperature revealed the liquid-liquid phase separation is probably occurred during cooling. Thus, the cloud point temperature for this sample is -1.59^{o}C

The cloud point temperature of Lysozyme solutions was further determined using a micro-DSC. Heat flow of the solutions during cooling was measured as a function of time. A typical change in the heat flow during cooling of Lysozyme solutions is shown in Figure 3.13. A sudden-drop in the heat flow occurred during the cooling process, indicating that a phase transition event has taken place (Darcy and Weincek, 1999; Lu et al., 2004). This deflection is associated with a latent heat of demixing (liquid-liquid phase separation). A cloudy solution was observed when the sample was taken out from the calorimeter. The sample became clear upon returning to room temperature. This observation demonstrated that the heat change monitored was indeed due to the formation of a metastable liquid-liquid state. Figure 3.14 shows the cloud point temperatures obtained from the micro DSC experiments together with the values obtained from the micro-batch experiments. The results from the two methods are generally consistent, particularly at cooling rates of 0.25^{o}C/min (Figure 3.14a) and

0.5°C/min (Figure 3.14b), supporting the observation of two phase formation at different cooling rates.

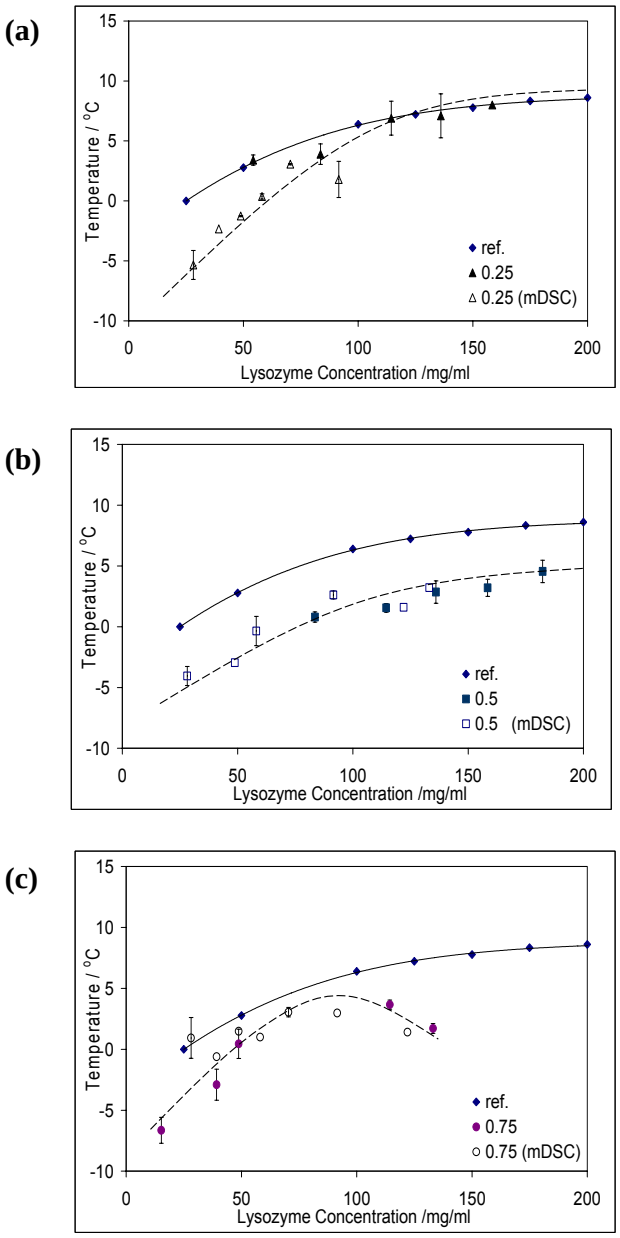

Figure 3.14 Cloud point curves for Lysozyme solutions determined from the micro-batch experiments and micro-DSC measurements. Solid symbols represent the cloud point temperatures obtained from the micro-batch experiment for cooling rates of (a) 0.25°C/min (▲), (b) 0.5°C/min (■) and (c) 0.75°C/min (●), whereas the open symbols represent the cloud point temperatures obtained from the micro-DSC measurements at (a) 0.25°C/min (Δ), (b) 0.5°C/min (□) and (c) 0.75°C/min (○)

3.3.3 Salt Partitioning in Crystallizing Solutions

The partitioning of salt during crystallization was investigated in order to better understand its role in the process. Table 3.1 shows the salt concentration of Lysozyme solution under different conditions, measured by AAS. The results showed that there was no significant difference in the salt concentration over all crystallizing solutions. In addition, for the phase separated solutions, the partition coefficient (K) was found to be ~1, indicating the salt concentration remained comparable before and after the phase separation event was taking place. Therefore, it can be deduced that salt concentration does not play a significant role in the phase separation of Lysozyme solutions (Vekilov et al., 1996).

Table 3.1 Salt partitioning in Lysozyme solutions under different conditions

Solutions Description	Salt Concentration (w/v %)	
	Measured before the mentioned event	Measured after the mentioned event
*Cooled until phase separation is achieved	3.3334	Top layer : 3.3447 Bottom layer : 3.3294
Incubated at 15^{o}C, tetragonal crystals have formed	3.3594	3.3405
Incubated at 30^{o}C, orthorhombic crystals have formed	3.2961	3.2814

*K~1. Partition coefficient, K, for salts in the phase separated solutions is defined as C_t/C_b (Jönsson and Johansson, 2003) where C_t and C_b are the salt concentration in top layer and bottom layer respectively.

3.4 Conclusions

The cloud point curve was studied for protein Lysozyme system with sodium chloride as precipitant. This study is to provide a better understanding of the factors, e.g. buffer solution, cooling rates and salt partitioning that determine the liquid-liquid equilibrium state of Lysozyme system during crystallization.

The use of buffer solution to stabilize the solution pH was found to affect the cloud point temperature of Lysozyme solutions. The presence of acetate ions would increase the ionic strength in the solutions, thus, increasing the cloud point temperature. Besides, it was found that the rate of cooling has an effect on the cloud point temperature for liquid-liquid phase separation of Lysozyme solutions; therefore the cloud point curve depends on the kinetics of the experiments. These findings may provide a pathway to control the crystallization process if the liquid-liquid phase separation lead to undesirable impacts on crystals. However, the cooling effects remain as a potential factor in altering the liquid-liquid phase separation and future research should be carried out on the molecular interactions and diffusions in order to have an insight into the phase transition kinetics.

CHAPTER 4

LYSOZYME CRYSTAL MORPHOLOGY AND POLYMORPHISM

4.1 Introduction

Crystal morphology is also known as crystal habit or shape. As crystallization processes play an important role in the manufacture of pharmaceuticals, both in the separation and purification steps, the shape of crystals and their size distribution would be a vital parameter in controlling the ease and efficiency of these steps. For example, thin and plate-like crystals will form a low permeability filter cake in a filter medium that will decrease the efficiency of filtration. On the other hand, a porous and easily-washed filter cake will be formed by the packing of low aspect ratio crystals; hence, it can be separated easily from the mother liquor. Crystals may form in different shapes depending on numerous factors such as temperature, supersaturation and subcooling, the presence of impurities, agitation, solvents used, etc., by which the relative growth rate of different faces of a crystal can be altered (Grimbergen et al., 1999a & 1999b; Davey and Garside, 2000; Wood, 2001). In addition, two phase formation or the liquid-liquid phase separation during crystallization could affect the crystal morphology (Bonnett et al., 2003; Laffèrrere et al., 2002).

Polymorphism is the ability of a substance to exist as different crystalline states that have different arrangements of the molecules in the crystal lattice. A commonly known example of polymorphism is the case of carbon, which can exist in crystalline form as either in graphite or diamond. The occurrence of polymorphism is driven by thermodynamic (e.g. Gibbs energy, surface/inter-phase tension, etc.) and kinetic (e.g. molecular interactions) factors (Giron, 1995). Polymorphism has a pronounced influence on the properties of pharmaceutical materials due to the internal solid state structure (Giron, 2003). Thus, the chemical and physical properties (determined by kinetics, thermodynamics, packing, interfacial phenomena etc.) as well as the mechanical properties of polymorphs would be different (Yu et al., 2003). In addition, the performance of pharmaceutical materials (including stability, dissolution and bioavailability), especially in drug applications, is highly dependent on crystal morphology. The unexpected appearance or disappearance of polymorphs in drugs may lead to serious impacts in therapeutic applications. This would subsequently affect the product development and production as in the case of ritonavir (Bauer et al., 2001) and ranitidine hydrochloride (http://www.gsk.com/media/glaxo97.htm).

As Lysozyme is well-known as a natural antibiotic and as an aid in the diagnosis of disease, it is important to understand the crystal morphology and polymorphism of Lysozyme in accordance with its applications. First, the experimental work to observe different crystal morphologies of Lysozyme and to characterize these crystal morphologies will be explained in the experimental section. This includes the growing of Lysozyme crystals at varying temperatures and the use of crystal characterization techniques such as scanning electron microscope (SEM), optical polarizing microscope, X-ray powder diffractometer (XRPD) and Fourier-transform

infra red spectrometer (FTIR). It is then followed by the results and discussion on different crystal morphologies obtained in this investigation. The effect of two phase formation on crystal morphology will also be discussed. Lastly, the characteristics of Lysozyme crystals such as polymorphism, anisotropic behavior and its molecular functional groups will be discussed.

4.2 Experimental

4.2.1 Crystal Growth

Tetragonal and Orthorhombic Crystals

Tetragonal and orthorhombic crystals were grown from Lysozyme solutions at 20^{o}C and 35^{o}C respectively. The mother liquor was prepared by mixing of Lysozyme solution and salt solution to the desired concentrations (varying Lysozyme concentration and 3 w/v% salt) in a test tube. The solutions were then incubated at the final temperature in a water bath (Julabo F25-HP). Crystals were formed within 1 day in both cases. Images of theses crystals were then recorded using an optical microscope (BX51, Olympus). The solutions (with crystals inside) were placed in a sonic bath for approximately 1 minute to remove those crystals that formed on the wall of test tubes. The crystals were then separated from the mother liquor by vacuum-assisted filtration and washed with a saturated Lysozyme solution (saturated at room temperature) to ensure the crystals obtained were clean from impurities (Lorber et al., 1999). Lastly, the crystals were dried in an oven at 40^{o}C.

Crystals from Two Phase Formation

The effect of two phase formation on crystal morphology (habit or shape) was observed microscopically using an optical microscope, and macroscopically in scale-up experiments.

Crystal morphology was observed using an optical microscope according to the procedures mentioned in section 3.2. However, they are briefly explained here again. The sample solutions were prepared by mixing known proportions of Lysozyme solution and salt solution. After incubating at 25^{o}C for 2-3 minutes in a water bath, a drop (1.2-1.5 μl) of sample solution was drawn out and placed in between two layers of oil (with different densities) in a crucible (Double-oil layer method) (Lorber and Giegé, 1996; Chayen, 1997). The crucible was then placed on a microscope stage mounted with a temperature control element. The sample droplet was heated to 45^{o}C or 50^{o}C to ensure that no crystal phase exist in the droplet. The sample droplet was then cooled to a lower temperature (lower than 5^{o}C) at which the oil droplets could be seen forming within the sample droplet and the temperature of the sample was kept constant. If the sample turned cloudy and became invisible under microscope, the sample would be heated slowly until the dispersed solute-rich phase could be observed. The two phase formation and its changes were then observed and recorded using the program (AnalySIS®) interfaced with the optical microscope.

These micro-batch experiments were then scaled up to 5 ml scale in order to obtain sufficient quantities of Lysozyme crystals for characterization. The experiments were carried out by incubating the Lysozyme solution (114.4 mg/ml Lysozyme and 3±0.05 w/v% NaCl, by mixing Lysozyme solution and salt solution) at 25^{o}C in a

circulating water bath (Julabo F25-HP) for 2-3 minutes. Sets of experiment were carried out where the solution was cooled at 0.5^{o}C/min to different final temperatures (1^{o}C and 5^{o}C) at which the liquid-liquid phase separation was expected to take place. For each set of experiments, the solution was kept at that final temperature for at least 15 hours. After which, small samples of the solution were periodically drawn out and filtered after another 2, 3 and 14-15 hours. The crystals were then filtered and dried in a vacuum oven (BÜCHI glass oven B-850).

4.2.2 Characterization of Lysozyme Crystals

4.2.2.1 Scanning Electron Microscopy

A small amount of sample crystals was sprinkled on the carbon-tape coated stubs using a spatula. The particles that did not adhere to the carbon tape on the stub surface were removed by gently tapping the stub on a flat surface (or the surface of a table). The layer of adhered sample was coated with a platinum-coater (CRESSINGTON Sputter Coater 208HR). The thickness of the coated platinum layer was controlled by the coating time set in the thickness controller unit. The samples were then observed using a scanning electron microscope (JEOL JSM 6700F).

4.2.2.2 X-ray Powder Diffraction (XRPD)

Crystals were ground to powder using a pestle and mortar, and then filled into a circular sample holder of the X-ray powder diffractometer (Bruker AXS D8 Advance) carefully, so that the holder was fully filled and compacted. The sample was then scanned from 2^{o} to 40^{o} (2θ) at a rate of 0.02 degree (2θ, ^{o})/min. The sample spectra were analyzed using the DiffractPlus program.

In order to further analyze the phase transition during liquid-liquid phase separation, the solution samples were scanned using the X-ray powder diffractometer. The sample solution was filled into a metal sample holder. The sample (with the sample holder) was then placed onto the 'low-temperature' stage of the diffractometer where the stage was connected to a cooling system (liquid nitrogen as the coolant). The sample solution was first cooled to 5^{o}C before being scanned from 10^{o} to 90^{o} (2θ) at 0.2 degree (2θ,^{o})/min.

4.2.2.3 Fourier-Transform Infrared Spectroscopy (FTIR)

The molecular structure or the functional groups of protein Lysozyme was studied spectroscopically using a Fourier-Transform Infra Red spectrometer. This study was carried out using three different IR spectrometers, (i) conventional FTIR spectrometer (BioRad), (ii) mercury-cadmium-telluride (MCT) IR spectrometer (Equinox55, Bruker) and (iii) reaction IR spectrometer (ReactIR 4000, Mettler-Toledo), with different operating principles.

First, in using the conventional FTIR spectrometer, the crystals were first ground into powder before being mixed with Potassium Bromide (KBr) in the ratio of approximately 1:100. The mixture was then introduced into a die and palletized using a press at a pressure of about 5-8 kPa. A pellet consisting of only pure KBr was prepared as the baseline reference. The pure KBR pellet was first placed into the sample holder of the instrument. It was then scanned (64 scans/analysis) for the range of wavenumber from 600cm^{-1} to 4000cm^{-1}. A background spectrum was obtained. The sample pellet was then scanned at the same speed and wavenumber (cm^{-1}) range as those applied in

obtaining the background spectrum. The spectrum of the sample was then subtracted from the background spectrum using WinIR software.

The MCT-IR spectrometer is a diffuse reflectance FTIR method. The spectra from this spectrometer can be obtained via diffuse reflectance of the samples, based on the principle of measuring radiation that penetrates into the interior of the sample and being scattered and reflected. Before using this instrument, the spectrometer needs to be purged with nitrogen gas before the measurements can be carried out. 1-2 g of the crystals was ground into powder and placed into a sample crucible. KBr was placed into another sample crucible as the reference material. Both crucibles were tapped gently before being placed into the sample chamber of the spectrometer. The measurement was started by collecting background spectrum of KBr with 100 scans/analysis and 4 cm light path length. The spectra were then analyzed using Opus I software. This IR technique has advantages over the conventional FTIR spectrometer in the ease and consistency of the sample preparation. In this technique, the sample is not required to be mixed and made into pellet form with KBr powder in which the mixing ratio may be varied. However, the spectra would be complicated by optical geometry effect, sample preparation, particle size, sample concentration, etc. (http://www.google.com/ with the searched page http://147.46.41.146/~1ii/DRIFT.htm; http://www.ct.chemie.tu-darmstadt.de/ak_vogel/hetkat/drifts_en.html).

Solution samples were analyzed with reaction IR spectroscopy. This technique is especially useful in tracking the critical reaction species in real time using characteristic infrared fingerprints. Thus, it is able to identify and track the reactive and unstable intermediates materials in a reaction, and to provide in situ measurement and

investigation on the reactivity and selectivity in a reaction medium (http://www.mt.com/mt/product/). In using this spectrometer, a sample solution was prepared by mixing of Lysozyme solution and salt solution in a 10ml vial and was incubated in a water bath at 25^{o}C. The probe was then inserted into the solution vial. Another set of the sample solution was prepared under the same conditions but with a temperature probe inserted in order to monitor the temperature change within the solution during cooling. After incubated for 2-3 minutes, the solutions were cooled to 5^{o}C at 0.5^{o}C/min. the spectrum of the solution was acquired at a regular time interval and the changes in spectra pattern were recorded with intuitive Windows-based software.

4.2.2.4 Cross-Polarization on Lysozyme Crystals

A polarized microscope (BX-51, Olympus) was used to identify the anisotropic behavior of Lysozyme crystals. Crystals were placed on a microscope slide before placing the slide on the microscope stage. The observation was done through the binocular lens of microscope. Then, the polarizer and analyzer of the microscope were tuned by crossing each other in such a way that a dark screen can be observed. The crystals appeared transparent under cross-polarization. The microscope stage was then rotated accordingly and changes in the color of crystals were observed and the images of the crystals were captured.

4.3 Results and Discussion

4.3.1 Lysozyme Crystal Morphologies

4.3.1.1 Morphologies of Lysozyme

Lysozyme crystal habit and morphology have been observed microscopically. The habit of the crystals depends on the crystallization conditions such as temperature, solvent used, additives, impurities etc (Wood, 1997; Mullin, 2001). Figure 4.1 shows the images of tetragonal and orthorhombic crystals observed under a polarizing microscope, crystallized at different temperature. It has been reported that the tetragonal crystals formed when the crystallizing solution is cooled to below 25^{o}C while the orthorhombic crystals formed in the solution at temperature above 25^{o}C (Cacioppo et al., 1991a; Ewing et al., 1994). However, Lysozyme crystal morphologies depend on other factors such as salt concentration, solution pH. Two other morphologies of Lysozyme crystals (monoclinic and triclinic) were also been identified and reported (Harata, 1994; Ho et al., 2001; Legrand et al., 2002; Harata and Akiba, 2004). However, these two morphologies were not observed in this project due to the differences in crystallization conditions.

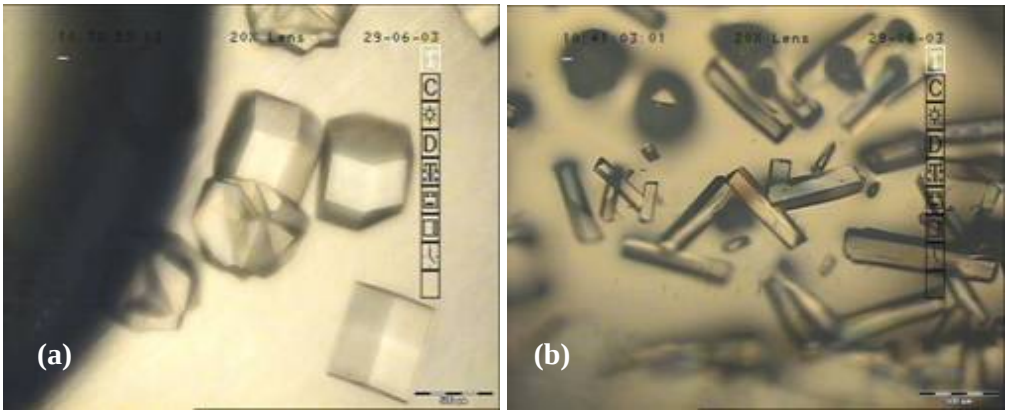

Figure 4.1 (a) Tetragonal Lysozyme crystals at 15°C (b) Orthorhombic Lysozyme crystals at 35°C

Interestingly, an unstable crystal habit was observed when the solution was cooled to a lower temperature at which two phase formation occurred. Under these conditions, oil droplets were first formed when the Lysozyme solution was cooled to 5^{o}C and reheated to 6.6^{o}C as shown in Figure 4.2(a). Cup-like and/or spherical crystals, as shown in Figure 4.2(c), can be seen forming in the Lysozyme solution after the solution was reheated to higher temperature and the number of oil droplets decreased (Figure 4.2(b)). These crystals have been observed to transform into tetragonal crystals upon reheating the crystallizing solutions back to room temperature. Moreover, these crystals appeared after the phase separation occurred in several sets of experiment and the crystal shape transformation from spherical to tetragonal has been observed at different temperatures. The effect of the two phase formation on the crystal habits and morphologies will be further discussed in the following section.

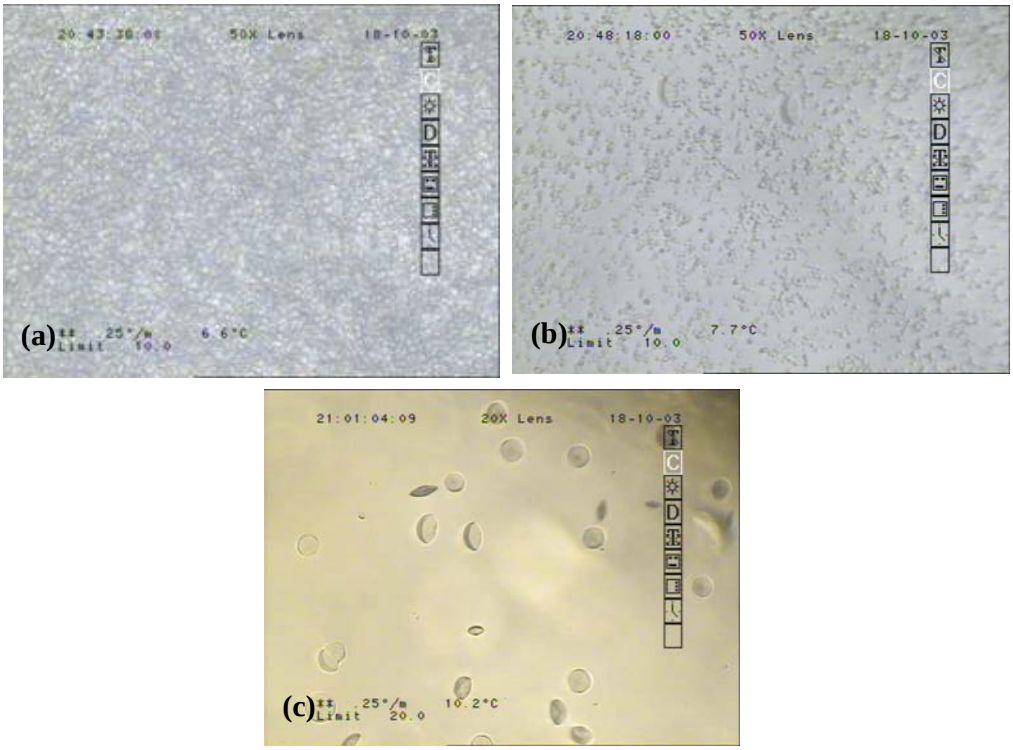

Figure 4.2 (a) Formation of oil droplets in cloudy solution (b) Oil droplets re-dissolved when the solution is heated (c) Cup-like and spherical crystals can be clearly seen after all the oil droplets disappeared

In some cases, spherulites (needle-like) or sea-urchin like crystals were observed preceding the formation of either tetragonal or orthorhombic crystals. The formation of these crystals has been observed and reported as a consequence of liquid-liquid phase separation (Skouri et al., 1995; Georgalis et al., 1998; Galkin and Vekilov, 2000a & 2001) or due to the presence of foreign micro-impurities (Chow et al., 2002). As shown in Figure 4.3, sea-urchin like crystals were formed in the Lysozyme solutions under different conditions. In addition, these crystals coexisted with either oil droplets or tetragonal crystals, indicating that the spherulites or sea-urchin like crystals were formed regardless of the occurrence of two phase formation in Lysozyme solution. Besides, the solutions were prepared with micro-filtered buffer solution; therefore the presence of impurities could be eliminated. Hence, the formation of needle like or sea-urchin like crystals is probably due to the high concentration of salt in Lysozyme solution.

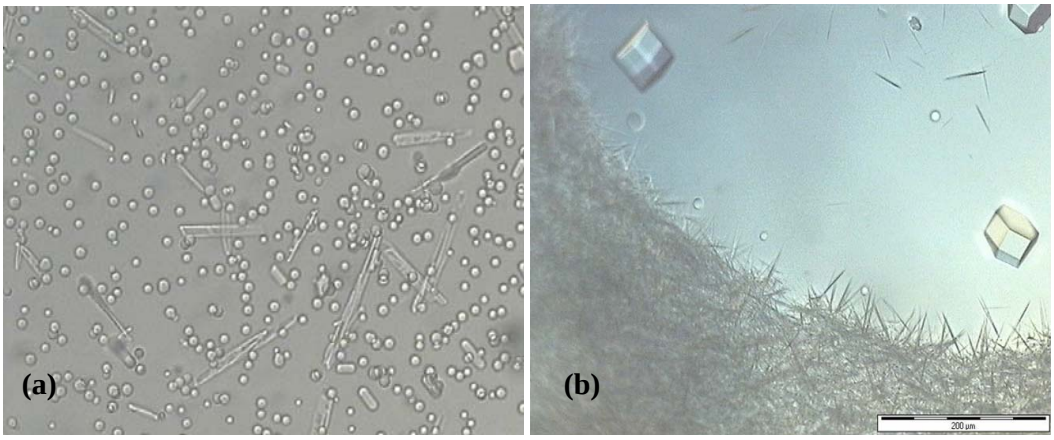

Figure 4.3 Formation of needle-like crystals in solutions with higher salt concentration; (a) needle-like crystals coexisted with oil droplets in Lysozyme solutions (10wt% Lysozyme and 5wt% NaCl, pH 4.5 and at 22°C), and (b) needle–like crystals coexisted with tetragonal crystals (solutions with 8wt% Lysozyme and 6wt% NaCl, pH 4.5 and at 35^{o}C)

The relationship between the solution compositions to the formation of different crystal morphologies has been proposed in a morphological phase diagram (Tanaka et al., 1996). The formation of needle-like or sea-urchin like crystals was observed in the region of high salt concentration in that morphological phase diagram.

4.3.1.2 Effect of the Oiling Out Phenomenon on Crystal Morphology

Crystal Growth from the Solute-Rich Phase

Figure 4.4 shows the evolution of two phase formation and subsequent crystal growth in Lysozyme solutions (136.05mg/ml Lysozyme and 3.01w/v% NaCl) at different temperatures. The solutions were first cooled to the experimental temperature below their respective cloud point temperature and the changes were observed under a polarizing microscope. The solutions were observed to turn cloudy below their cloud point temperature and turned clear again upon being reheated slightly above T_{cloud}. The protein-rich oil droplets can be clearly seen initially (images (a)-(c)) dispersed in the matrix of the continuous phase. It is believed that nucleation first took place within the droplets (ten Wolde and Frenkel, 1997 & 1999; Haas and Drenth, 1998; Anderson and Lekkerkerker, 2002) due to its high supersaturation level. Some droplets formed into what appear to be spherically-shaped crystals. The crystals acquired a spherical shape possibly due to the growth being limited by the volume of the oil droplets. As the supersaturation is gradually reduced during the crystallization, the overall composition eventually moved out of the two phase region, the oil droplets disappeared and the crystals continued to grow in the remaining supersaturation (images (d)-(f)). However, as the growth is no longer constrained by the volume of oil droplets, the crystals gradually transformed into tetragonal shapes (images (g)-(h)). This shows that spherical crystals are metastable and they could be the precursors to the stable

tetragonal form when liquid-liquid phase separation is followed by nucleation in the droplets.

The occurrence of the metastable spherical crystals still remains not well understood and further investigations are needed to provide more understanding of their formation and to determine if they arise from the phase separation in Lysozyme solution. The formation of these spherical crystals imposes difficulties in controlling the crystal shapes as a consequence of the two phase formation.

In order to reproduce the 'metastable' spherical crystals, its formation as observed in the micro-batch system as discussed previously, was extended to a scaled-up system. In this system, the Lysozyme solutions were cooled to two final temperatures individually, 1°C and 5°C, and the solutions were maintained at that final temperature for at least 14-15 hours.

Figure 4.5 shows the SEM micrographs of the crystals that were formed in the scaled-up Lysozyme solutions. In Figure 4.5(a), spherical crystals were obtained from Lysozyme solutions after cooling at 1°C for 2 hours. It is postulated that the formation of spherical crystals is nucleated within the oil droplet phase and gradually grew within the droplets (ten Wolde and Frenkel, 1997 & 1999; Anderson and Lekkerkerker, 2002) into a spherical shape of approximately 10μm diameter due to the volume constraint imposed by the oil droplets. Lysozyme molecules are available within the oil droplets, thus the molecules have ample time to move from the surrounding and oriented on the growing surface. Upon depletion of the molecules within the oil droplets, Lysozyme molecules from the bulk phase (continuous phase during liquid-liquid phase separation)

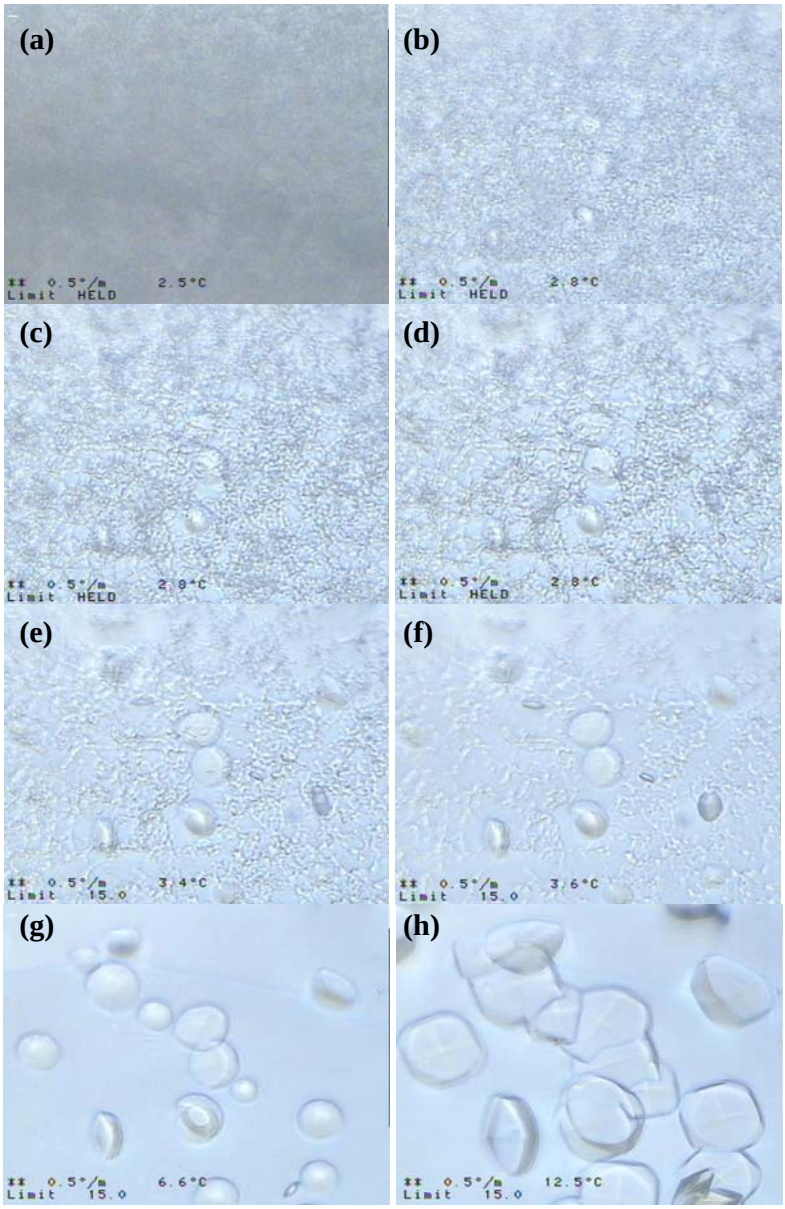

Figure 4.4 Time evolution of spherical crystals formed after the two phase formation. The solution (136.05 mg/ml Lysozyme and 3.01 w/v% NaCl, cooled from 8°C to 2.5 °C, followed by reheating to 2.8±0.1°C) was kept at 2.8±0.1°C after observing the appearance of the oil droplets. The spherical crystals reverted into the stable tetragonal form after the solution was left to warm at 15°C

will diffuse to the growing surfaces. The growth rate in this stage may be different for different faces of the spherical crystals. Thus, the spherical crystals will transform into disc-shaped crystals as shown in Figure 4.5(b) where the crystals were left to grow for a longer period (14 hours) at 1°C.

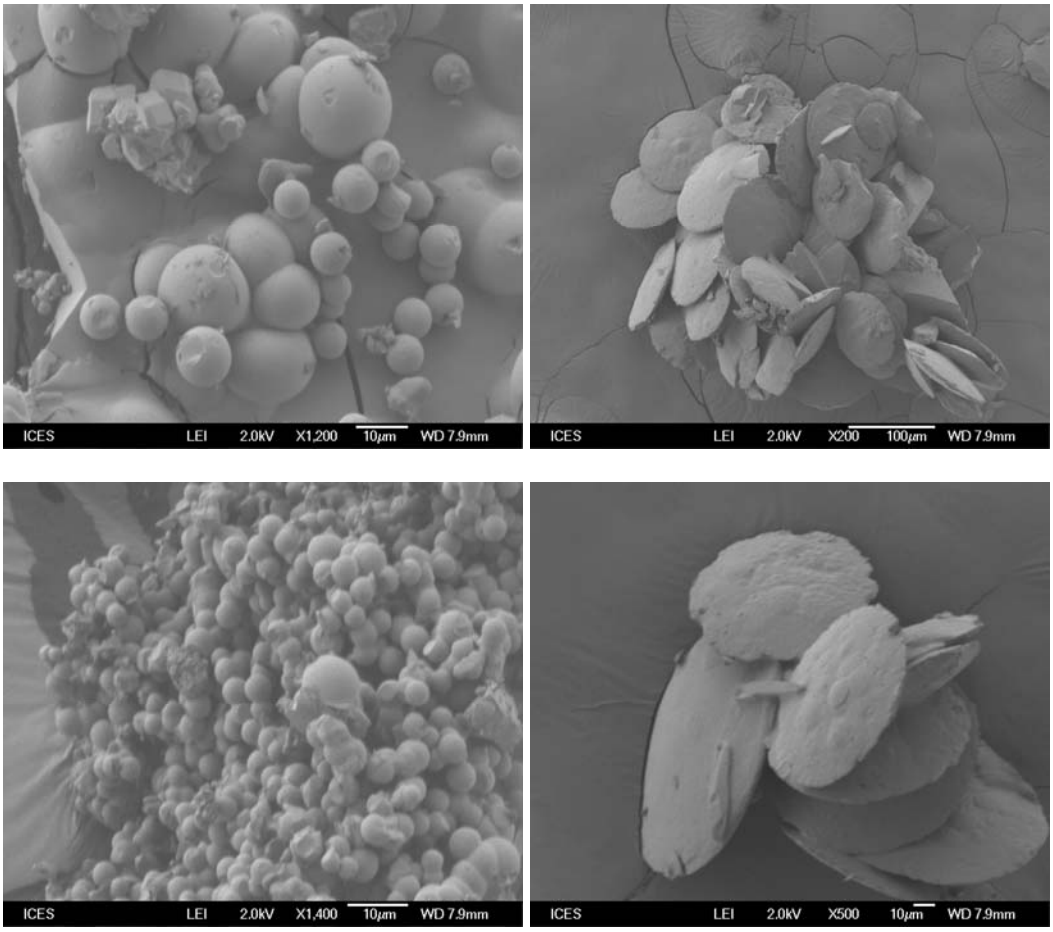

(a) **(b)**

Figure 4.5 Spherical Crystals obtained from Lysozyme solutions (114.41 mg/ml Lysozyme and 3 w/v% NaCl) which had been maintained at 1°C for (a) 2 hours and (b) 14 hours

Lysozyme solutions with the same concentration as that used for Figure 4.5 were cooled to 5°C in another set of experiments. The solutions were maintained at that temperature for 2, 3 and 15 hours respectively. The resulting crystals were

harvested and observed with SEM imaging. Figure 4.6(a) shows the SEM micrographs of the spherical crystals obtained after maintaining at 5°C for 2 hours. Again, unusual and distinctly spherical crystals in the size range 1-6μm can be clearly seen. The dominant crystal size agrees well with the droplet sizes measured by FBRM (which will be further discussed in Chapter 5), and this confirms the view that the spherical crystals grew from within the spherical oil droplets, and that their shape was influenced by the droplet interface.

The tiny spherical crystals subsequently grew to larger spherical crystals with a deformed ellipsoidal or disc-like shape, as shown in Figure 4.6(b). Finally, the crystals transformed into the stable tetragonal form (Goergalis et al., 1998) after being left to grow for a longer period of time (Figure 4.6(c)). These results illustrate an interesting possibility of controlling crystal shape and habit by inducing the formation of oil droplets, followed by nucleation within the droplets.

With the same solution compositions but cooling to two different final temperatures (1^oC and 5^oC), Lysozyme crystals have the same morphology at the early stage of its formation. However, when the crystals were grown in the cloudy solutions for a longer period, the final crystal habit would be different as seen in Figure 4.5(b) and Figure 4.6(c). Transformed tetragonal crystals were obtained in the solutions which had been kept at 5^oC for 15 hours whereas flat and disc-like crystals were obtainable when the solution was cooled at 1^oC for 14 hours. This discrepancy would be arisen from the fact that these crystals were obtained via two different pathways as shown in Figure 4.7.

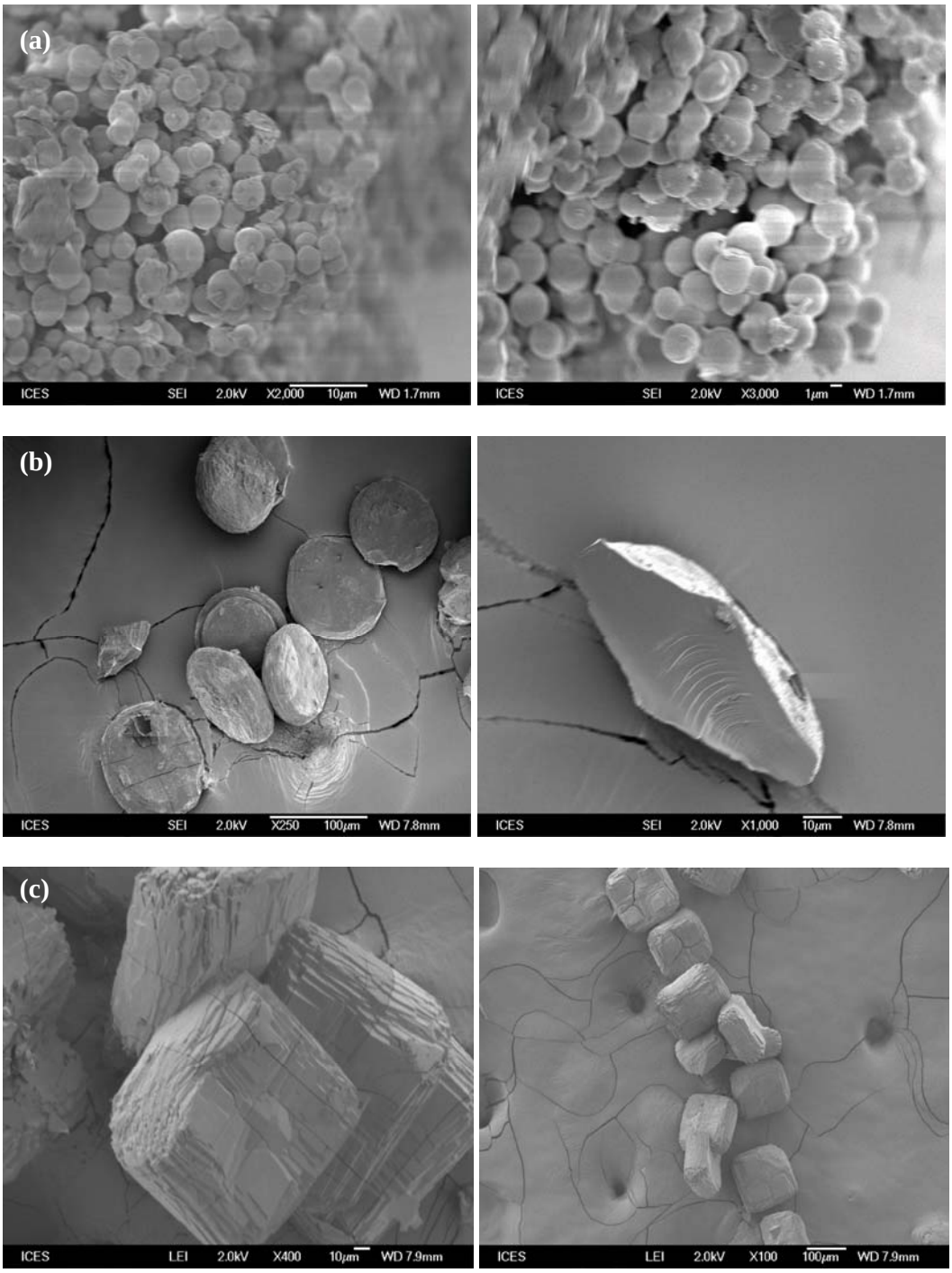

Figure 4.6 SEM micrographs show the spherical crystals obtained after the Lysozyme solution (114.4 mg/ml Lysozyme and 3±0.05 w/v% NaCl) was maintained at 5°C for (a) 2 hours, and (b) 3 hours. (c) The spherical crystals transformed into tetragonal form after the solution was cooled at the final temperature for 15 hours

As the final temperature in both solutions was lower than its cloud point temperature, two phase formation or liquid-liquid phase separation was expected to occur. Nucleation and subsequent crystal growth are postulated taking place within the oil droplets (point A in Figure 4.7). As the Lysozyme molecules diffused and attached to the growing crystals, the supersaturation level depleted within the oil droplets. The crystals will gradually grow from droplet phase to the bulk liquid phase. Hence, the shape of crystals no longer constrained by the oil droplets and the subsequent growth will rely on the mass transport between solid and bulk liquid phase. Depletion of Lysozyme concentration may lead the solutions moving out from the liquid-liquid phase separation region in the phase diagram (point B). However, this transformation also depends strongly on the temperature of the system.

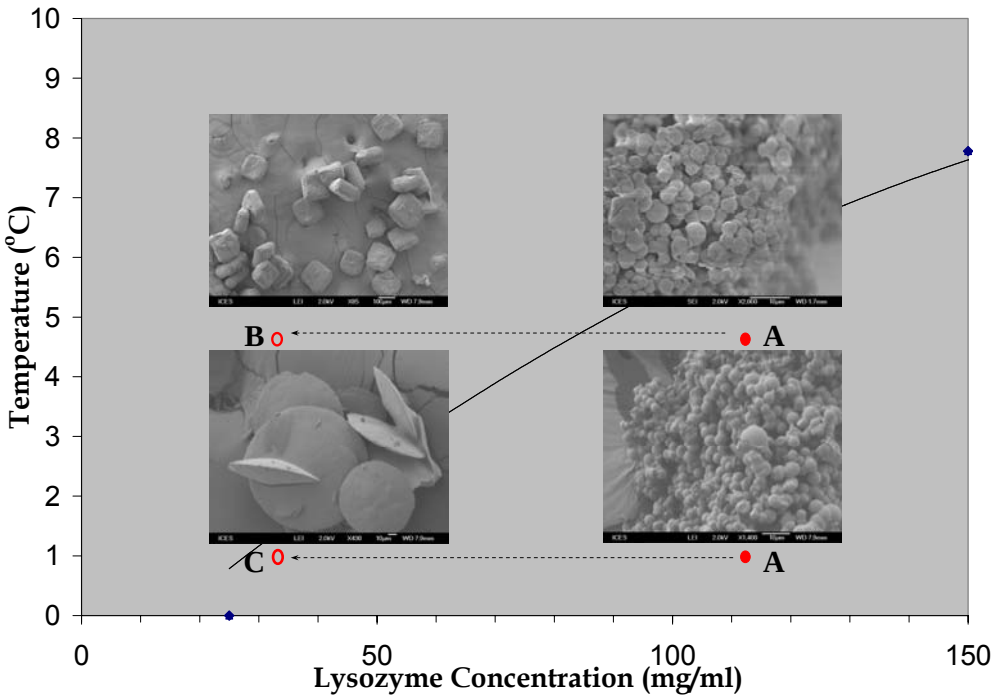

Figure 4.7 Lysozyme crystals formed via different pathways in the liquid-liquid phase separation region of Lysozyme phase diagram, exhibited different crystal morphologies. Solid curve shows the liquid-liquid coexistence curve reported by Muschol and Rosenberger (1997)

In the case of keeping the crystallizing solutions at 5^{o}C, depletion in Lysozyme concentration may change the crystallization behavior by crossing from the two-liquid phase into the single-liquid phase region of the phase diagram. Crystal morphology depends on the environment in which it is grown. This could explain the crystal transformation from spherical to tetragonal shape in that case. On the other hand, with the given period of cooling at 1^{o}C, the solutions probably remained at two-liquid phase region (point C). Thus, the spherical crystals formed initially may retain their shape but will grow to disc-like crystal beyond the confined oil droplets. The subsequent growth will depend on the ease of molecular attachment into the growth surface and the diffusion of Lysozyme molecules towards these surfaces (Georgalis et al, 1998).

4.3.2 Polymorphic Forms of Lysozyme

The peaks appearing at specific angles of X-ray diffraction spectra signify the relative location of molecules in a crystal lattice, conformations and the molecular structure (Wood, 1997). Thus, polymorphs of a material will show different patterns in XRPD spectra. Two polymorphs of Lysozyme crystals are known to exist, that is orthorhombic and tetragonal crystal (Weiss et al., 2000; Sauter et al., 2001). These polymorphs have different lattice dimensions due to the different packing of molecules during the growth event in crystallization.

Lysozyme crystals were compared qualitatively in this project using X-ray Powder Diffraction (XRPD) method. Powdered Lysozyme crystals were scanned and the results are shown in Figure 4.8. For the spherical crystals, the powder diffraction pattern showed some significant peaks (with corresponding 2θ) that are not observable in the pattern of tetragonal and orthorhombic crystals (pointed in arrows in Figure 4.8).

It is postulated that spherical crystals most likely formed another polymorph. However, the stability of this polymorph system may vary. It has been reported that an unstable Lysozyme polymorph may be formed by nucleation in the solute–rich phase (Bhamidi et al., 2001). The unstable polymorph is possible to transform in time to a more stable polymorphic form (Wood, 1997; Bhamidi et al., 2001). Fluctuations shown in the acquired spectra in Figure 4.8 most likely originated from the sample itself as the background signal (empty sample holder) was acquired and subtracted from the samples' signal for each measurement. The fluctuations in acquiring the spectrum of Lysozyme crystals have also been observed and reported by Bhamidi et al. (2001).

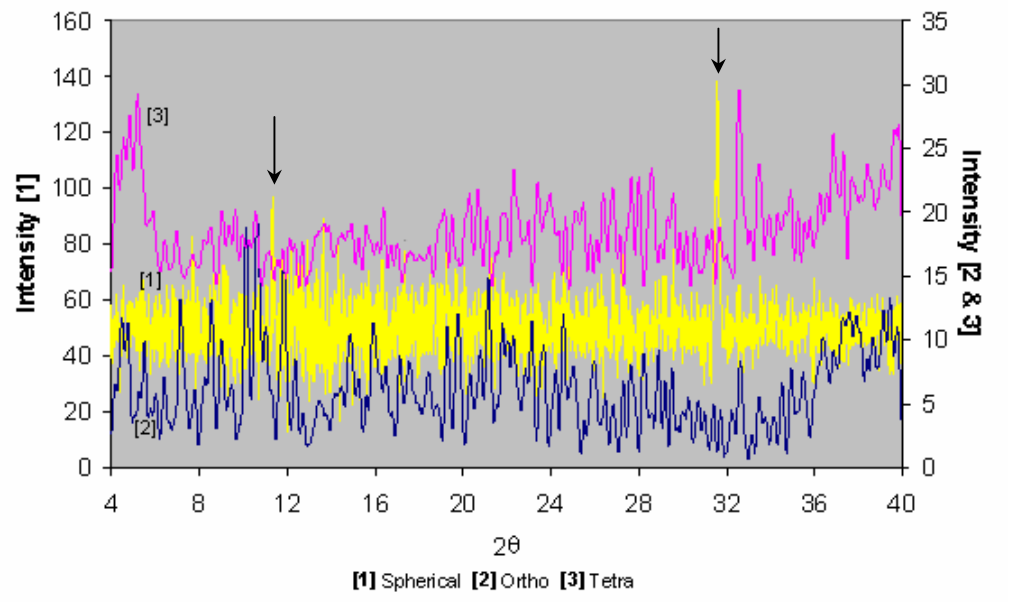

Figure 4.8 Different powdered XRD patterns for Lysozyme crystals, (1) spherical crystals, (2) orthorhombic form, and (3) tetragonal form signifying the polymorphic systems in Lysozyme. Spherical crystals may exist in the unstable polymorphic form as polymorphism tends to change with time where the crystals were grown (Wood, 1997)

The powder diffraction pattern of a cloudy Lysozyme solution was also determined. Figure 4.9 shows the pattern for the cloudy solution as compared qualitatively to that of tetragonal crystals. The characteristic peaks in the spectrum of

Lysozyme solutions appeared at different measuring angles (2θ) from that of Lysozyme crystals. It is likely that the particles formed in the Lysozyme solutions during cooling were of different structure than the tetragonal crystals of Lysozyme.

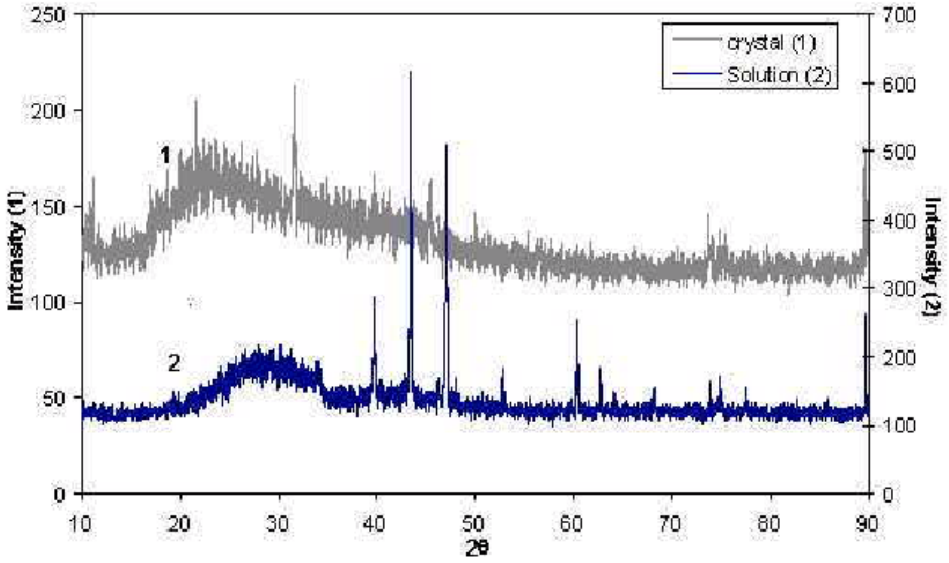

Figure 4.9 Qualitative comparison of powdered XRD pattern between the tetragonal crystals and the cloudy Lysozyme solutions further explained the possibility of forming another polymorph of Lysozyme during liquid-liquid phase separation

4.3.3 Functional Groups of Lysozyme Molecules

The characteristic functional groups of Lysozyme crystals were analyzed by infra-red (IR) spectroscopy. Figure 4.10 shows the spectra of Lysozyme crystals from three different IR spectrometers. These spectra show peaks at the wavenumber of 1535-1543 cm^{-1}, 1652-1655 cm^{-1} and 3284-3308 cm^{-1}. The existence of the amide linkage within the Lysozyme molecules is indicated by the peaks at the wavenumber range 1535-1543 cm^{-1}, 1652-1655 cm^{-1}, while the existence of the carboxyl group in Lysozyme molecules is indicated by the peak at 3284-3308 cm^{-1}. Analyses of the spectrum from three different IR spectrometers gave the same indications of the characteristic functional groups in Lysozyme crystals. However, the signal intensities were different.

Measurement with React IR gave the strongest signal as compared to the other spectrometer. But, it showed much noise at 2100-2200 cm^{-1} possibly due to the IR absorption of the diamond probe tip. On the other hand, spectrum from MCT-IR and FTIR showed a peak at 2360 cm^{-1} which is a characteristic functional group of KBr that was used as the background reference.

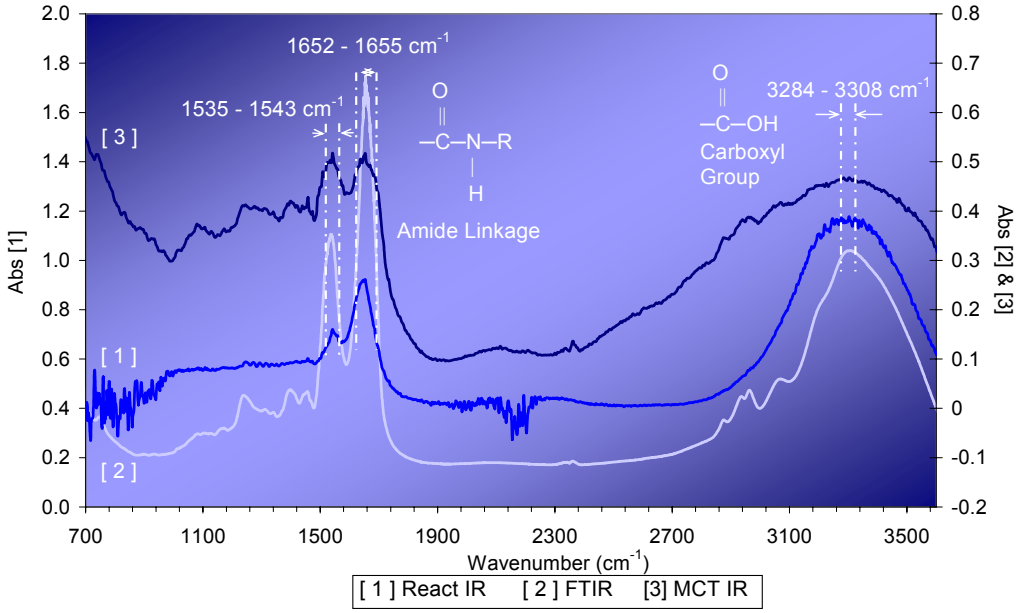

Figure 4.10 IR spectra of Lysozyme crystals from [1] React IR spectrometer, [2] FTIR spectrometer and [3] MCT IR spectrometer

One difference was observed for the band of carboxyl group when comparing the IR spectrum of Lysozyme from this investigation to the spectrum obtained from a reference (http://spectra.galactic.com/SpectraOnline/) as shown in Figure 4.11. The spectrum from this study has a broader band and the band was shifted to a lower wavenumber (3284-3308 cm^{-1}) as compared to the spectrum from the reference (3400-3450 cm^{-1}). This is probably due to the hydrogen bonding (either intermolecular or intra-molecular bonding) that tends to produce significant band broadening and to

lower the mean adsorption frequency (Coates, 2000). Furthermore, the form of hydroxyl group present within the molecules (either in hydrates, water solutions, amino compound, carboxylic acid compound, alcohol compound, etc.) is related to the crystalline structure of a compound and the symmetry of certain aspects of the molecular structure. Samples used in the reference were in solution form whereas Lysozyme crystals were used in this investigation. The difference in sample preparation would contribute to the deviation in the spectrum. Thus broader and shifted characteristic band of carboxyl group in this case are more likely due to the presence of hydrogen bonding. However, the type of hydrogen bonding in Lysozyme crystals is needed to be investigated to support the previous arguments. In addition to the factors that affect the molecular IR absorption, pressure, concentration of solute and solutions, and the spectroscopy methods used may play an important role in changing the band distribution of spectrum (Coates, 2000).

4.3.4 Cross-polarized Microscopy on Lysozyme Crystals

The optical properties of Lysozyme crystals were observed under a polarizing microscope. Samples were placed on the rotating stage of the microscope and the polarizer was tuned to cross each other while observing the crystals.

Figure 4.12 shows the effect of cross-polarizing on Lysozyme crystals and salt crystals. Lysozyme crystals remained transparent whereas the salt crystals became invisible under cross-polarized condition. This behavior is due to the anisotropic behavior of Lysozyme crystals where its properties may vary with the directions of measurement. When lights enter the crystal, it splits in to two rays and travel at different speeds. The splitting of light into two components (an ordinary light ray and

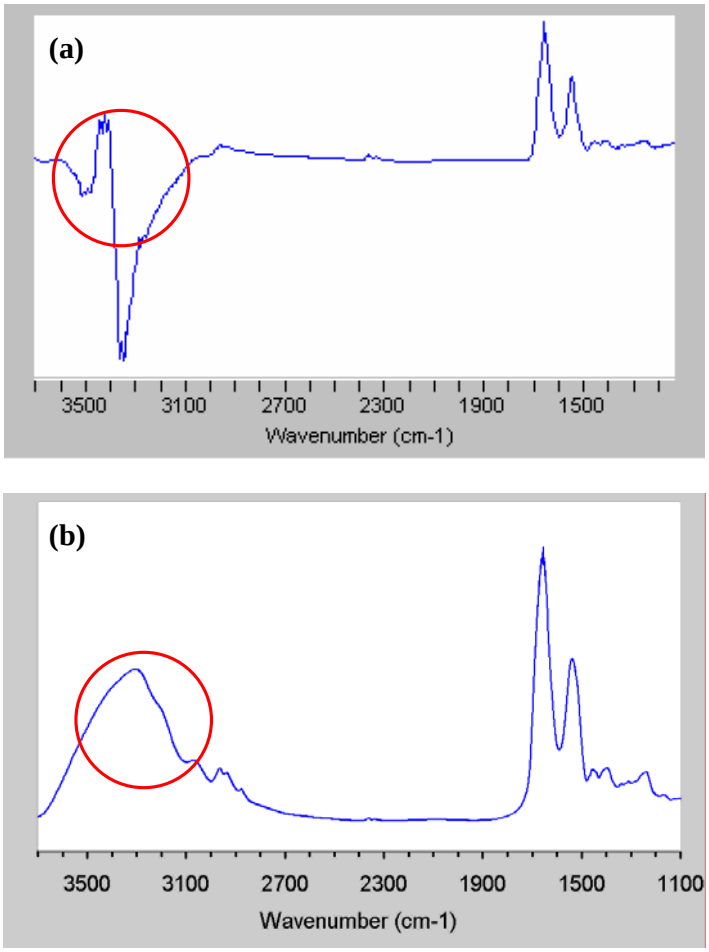

Figure 4.11 Difference in band width and shift in wavenumber above 3000cm^{-1} (carboxyl group) between the reference spectrum and the spectrum from experiment suggested the effect of hydrogen bonding in the vibrational behavior of Lysozyme molecules

an extraordinary light ray) by a crystalline substance is known as birefringence. Birefringence is also known as "double refraction" and it will result in two refraction indices of a crystalline material. One light ray is slowed down and color changed compared to another light ray. Birefringence is caused by the atoms in a crystal in which it has stronger bonds with one another in one direction and weaker bonds with one another in a second direction. Hence, the light transmitted out of the anisotropic Lysozyme crystals changes in its vibrational direction and the crystals remain visible when another polarizer is placed at right angle to the first polarizer. The visible

Lysozyme crystals can be observed. On the other hand, the vibrational direction of the light transmitted through an isotropic crystal like salt will be the same as those of the incident light. The light will be blocked when another polarizer is placed above the crystals and the crystals become invisible. This phenomenon is known as extinction.

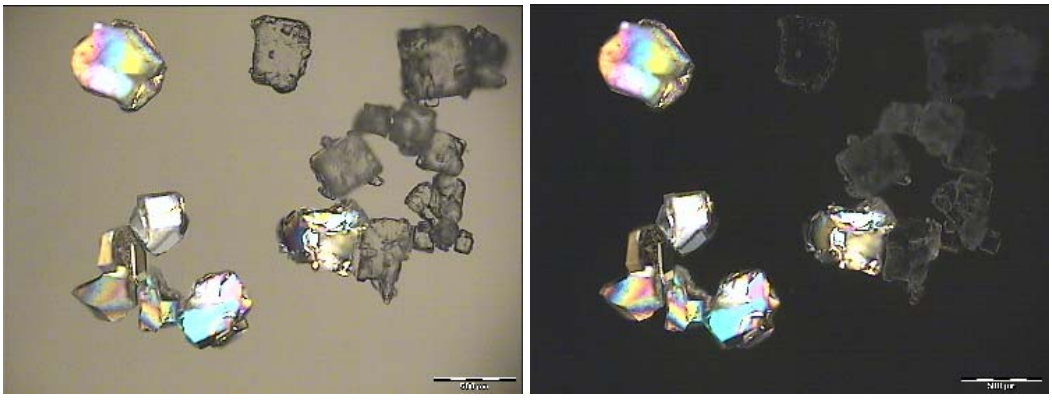

Before Cross-polarized **After Cross-polarized**

Figure 4.12 Influence of polarized light setup on Lysozyme crystals and salt crystals using Polaroid filters

Under cross-polarized condition, the microscope stage was rotated and the changes in the crystals were observed. Figure 4.13 shows the micrographs of Lysozyme and salt crystals when the stage was rotated 360^{o}. Variation in color intensities of Lysozyme crystals can be observed whereas the salt crystals remained invisible. The ability of a crystal to absorb different wavelengths of transmitted light depends upon its crystallographic orientations. As a result, the crystals appear to have different colors depending on the direction in which they are observed, i.e. according to the direction of vibration of the waves that passed crossing them. This phenomenon is known as pleochroism (http://www.uwgb.edu/dutchs/PETROLGY/).

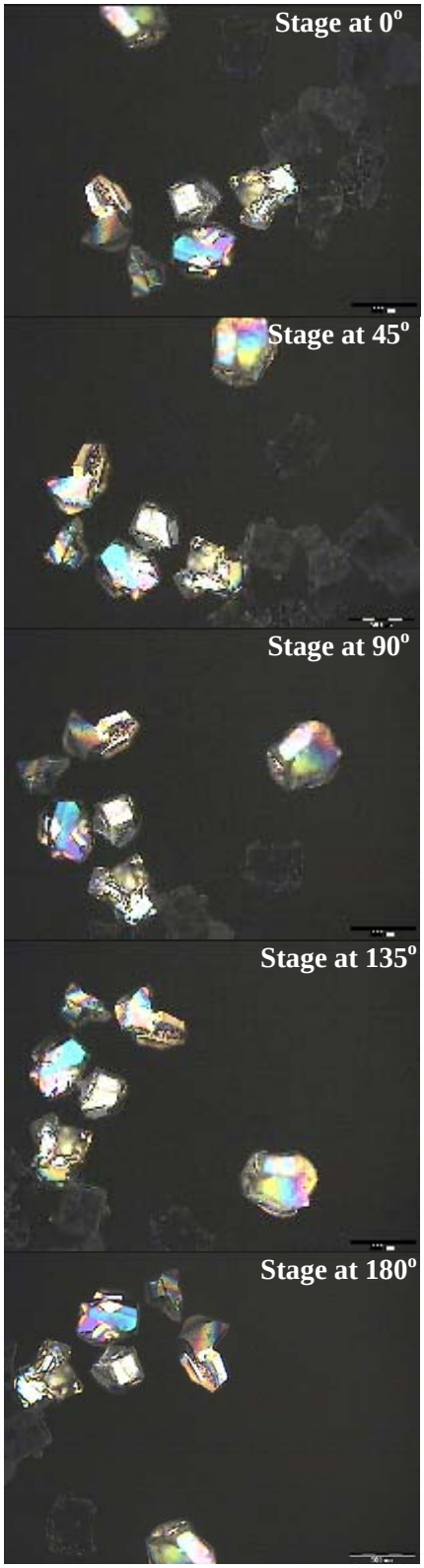

Figure 4.13 Pelochroism in Lysozyme crystals was observed where the color intensity of the crystals was changed when the microscope stage was rotated

4.4 Conclusions

Lysozyme crystal morphologies have been studied and shown in this chapter. It was found that an interesting crystal morphology, which has a different shape from the normally known tetragonal and orthorhombic crystals, was formed in Lysozyme solutions when the solution was cooled to the liquid-liquid phase separation region. These crystals, namely spherical crystals, were postulated to be formed as a consequence of two phase formation in Lysozyme solutions. The high supersaturation level of the droplets phase may enhance the nucleation (ten Wolde and Frenkel, 1997 & 1999, Haas and Drenth, 1998 and Anderson and Lekkerkerker, 2002), and the subsequent crystal growth would take place in the confined oil droplets and the crystal shape would be constrained by the droplets. In addition, these crystals have been shown to transform into the tetragonal morphology as a function of temperature and Lysozyme concentration. These findings suggest that crystal morphology of Lysozyme can be altered or affected by the formation of oil droplets in Lysozyme solutions. Furthermore, the transformation of spherical crystals to tetragonal crystals suggests the metastability of spherical crystals. However, the formation of those crystals still remains unclear and not well-defined. Therefore, future studies will be focused on the phase equilibria in droplet phase and the crystallization kinetics within the oil droplets. Moreover, investigations on the solubility and stability of spherical crystals as compared to those of tetragonal and orthorhombic crystals could be carried out. These are needed to develop a deeper understanding on the effects of two phase formation on crystal morphology.

CHAPTER 5

CHARACTERISTICS AND EFFECTS OF TWO PHASE FORMATION

5.1 Introduction

Oil droplets form when liquid-liquid phase separation occurs in a crystallizing solution. This phenomenon has been observed in macromolecular systems such as proteins γ-crystalline bovine (Broide et al., 1991), Lysozyme (Ishimoto et al., 1977; Petsev et al., 2003), and bovine pancreatic trypsin inhibitor, BPTI (Grouazel et al., 2002) and polymers (Wiltzius and Cumming, 1991; Shang et al., 2003) and in systems of smaller molecules (Lafferrère et al., 2002; Bonnett et al., 2003). Crystallization of protein Lysozyme in the vicinity of liquid-liquid phase separation has been shown to enhance the nucleation rate (Galkin and Vekilov, 2000a & 2001; Nicolis and Nicolis, 2002) and to promote the formation of spherulites or sea-urchin like crystals (Georgalis et al., 1998; Chow et al., 2002). However, these reports provide no further information on the characteristics of oil droplets. In addition, the effect on crystal quality and properties are not fully understood. Therefore, studies on the oil droplets were carried out and will be discussed in this chapter.

The oil droplets are believed to contain the protein-rich phase (Muschol and Rosenberger, 1997; Haas and Drenth, 1998) and the sizes of oil droplets are of the interest to denote their role during crystallization. Experiments were carried out with Focused-Beam Reflectance Measurement (FBRM) and will be explained in the experimental section of this chapter. In addition, crystal size distribution and agglomeration were measured and observed using an optical cross-polarized light microscope. It is then followed by discussion on the experimental results that would provide some understanding in the characteristics of two phase formation and its effect on the crystallization behavior of Lysozyme system.

5.2 Experimental

5.2.1 Micro-batch Observations on Lysozyme Solutions with Different Concentrations

The experimental procedures of this system using a polarized light microscope (Olympus, BX-51) have been discussed in the experimental section of the previous two chapters. However, the solutions used in this experiment were prepared differently in the sense of the concentration used. Only two different Lysozyme concentrations were used.

In the first set of experiments, solutions with concentration of 119.9 mg/ml Lysozyme and 3.02 w/v% NaCl were prepared by mixing the stock solutions of each component at appropriate volume proportions. The mixed solution was then incubated at 25^{o}C for 2-3 minutes in a water bath. A drop (1.2-1.5 μl) of the final solution was then withdrawn and placed in a microscope quartz crucible (Linkam Scientific Instrument, model no. HSF-91). The sample was prepared in a crucible following the

procedures as explained previously. After preparing the sample droplet in a crucible (applying the double-oil layer method), the droplet was cooled from 25^{o}C to 8^{o}C at 15^{o}C/min. It is then followed by cooling at 0.5^{o}C/min to a temperature at which two phase formation was observable and the solution turned cloudy. Under these conditions, the solution was too opaque to be seen using the microscope. In order to observe the changes in the sample droplet, the system was reheated at step of 0.1^{o}C increment from the cloudy temperature until oil droplets were observable. The system was then kept at that final temperature, and the changes within the sample droplet were observed and recorded with imaging software (AnalySIS®) acquired at a regular time intervals.

In another set of experiments, the sample solution was prepared differently in order to obtain a solution with higher protein concentration. The sample solution was prepared via phase separation and centrifugation at low temperature. First, a 90 mg/ml Lysozyme solution was prepared by dissolving an appropriate amount of Lysozyme in sodium acetate buffer. The pH of the solution was adjusted to 4.5±0.05. NaCl was then added to it to form a final Lysozyme solution with 3 w/v% NaCl. The solution was filtered through a 0.22 μm Millipore Millex-GV filter into a clean vial. The vial was then inserted into a centrifuge tube containing crushed ice, and subjected to centrifugation at 3000 rpm at 0^{o}C for 20 minutes in a laboratory centrifuge (Sigma, Sartorius 3K30). The two distinct layers obtained were separated and the Lysozyme concentration in each layer was determined by a UV-Vis spectrophotometer (Shimadzu UV-2550) at 280 nm using an extinction coefficient of 2.64 absorbance units per 1mg/ml solution. Once the concentration was determined, a drop (1.2-1.5 μl) of the solution was withdrawn and placed in a crucible. The sample droplet, which was

sandwiched by two oil layers at room temperature initially, was first heated to 50^{o}C to dissolve any crystals formed in the solution. It was then followed by fast cooling at 15^{o}C/min to 8^{o}C. From 8^{o}C, the sample droplet was cooled at 0.5^{o}C/min to a temperature at which a cloudy state was observed. The subsequent procedures of observation and recording changes within the sample droplet were the same as mentioned in the previous paragraph.

5.2.2 Determination of Particle Size Distribution

Particle Size Distribution of Oil Droplets

The formation of the oil droplets in the phase separated Lysozyme solution has been characterized using Focused-Beam Reflectance Measurement method (FBRM, Lasentec). The measurement is based on the backscattering method where a laser beam is backscattered by the particles around the probe window to the detector and the data is collected by the FBRM optics and converted into an electronic signal. The uniqueness of this measurement is that the laser beam is focused and moved around the circumference of the probe window; chord length of a particle is then measured when its edges are intersected by the beam (as shown in Figure 5.1). A chord-length distribution from the measurement on each particle passing the probe window is obtained. This method had been used to monitor and control the droplet size of emulsions in situ (http://www.lasentec.com/M-2-004_abstract.html; Dowding et al., 2001; Hukkanen and Braatz, 2003) and in monitoring agglomeration in spherical crystallization of salicylic acid (http://www.lasentec.com/M-2-011_abstract.html). In addition, this measurement has been widely used in studying the kinetics of crystallization process (Fujiwara et al., 2002), monitoring the particle size distribution

(Ruf et al., 2000; Abbas et al., 2002), and studying the morphology and polymorphism of particles (Jeffers et al., 2003; Pearson et al., 2003; O'Sullivan et al., 2003).

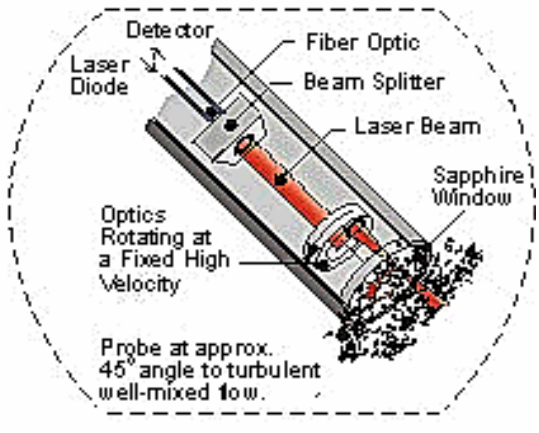

Figure 5.1 Focused-Beam Reflectance Measurement (FBRM) methods (This image is extracted without further modification from http://www.lasentec.com/method_of_measurement.html)

Lysozyme solution and NaCl solution were measured out separately in a 5ml vial and left to equilibrate at 25^{o}C in a water bath. The solutions were then mixed and stirred. The FBRM probe (S400 PI 8/91 probe) was placed in the final solution in such a way that the probe window was about 45^{o} to the flow. The measurement was started a few minutes after the solutions were mixed. A solution with the same composition was prepared with a temperature probe inserted in order to monitor the temperature change within the solution. The solution was then cooled at 0.5°C/min to a temperature where observable phase separation occurred. The temperature was then kept constant for two hours to monitor the subsequent changes in the solution.

Particle Size Distribution of Lysozyme Crystals

The effect of two phase formation on particle (crystal) size distribution of Lysozyme crystals has been studied. The Lysozyme crystals were obtained from two different sets of experiments. First, the Lysozyme crystals were obtained from a phase separated solution. The procedures in obtaining these crystals were explained in Chapter 4 (section 4.3.1) in a scaled up system. The solution was cooled at 5^{o}C and crystals were harvested after 2, 3 and 15 hours the solution being kept at that temperature. After filtering and drying the crystals, the shape of the crystals were observed using a polarized microscope and its size was measured with AnalySIS® program. In another set of experiment, crystals were grown under normal conditions. The sample solution with the same concentration as in the previous experimental set was used in this experiment. The solution was cooled and kept at 25^{o}C where the tetragonal crystals were expected to form in the solution. After cooling at 25^{o}C for 15 hours, the solution was filtered and the crystals were harvested and dried. The crystal size was then measured.

At least one thousand crystals were analyzed, in which the crystal size was characterized by the longest distance between two points of the crystal images, as shown in Figure 5.2. After measuring the crystal size for the required amount of crystals, the data were compiled and analyzed with Microsoft Excel program.

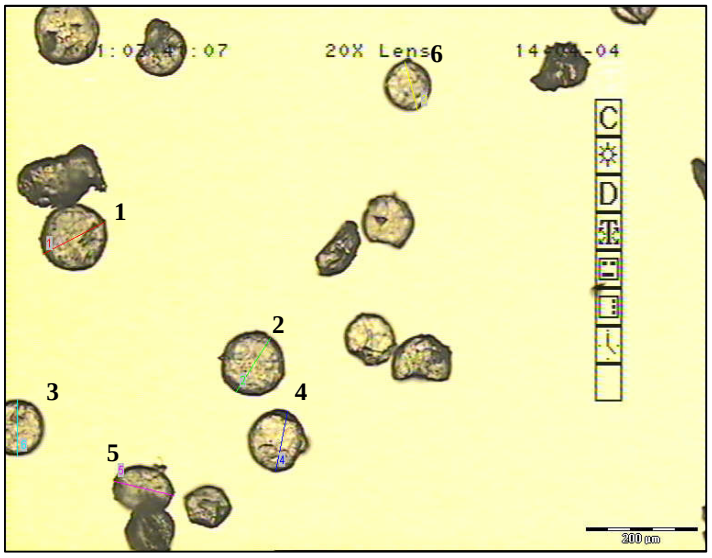

Crystal #	Size, µm
1.	123.35
2.	110.20
3.	86.83
4.	105.61
5.	109.52
6.	96.87

Figure 5.2 Crystal size was determined by measuring the longest distance between any two points of the crystals. The measurement was only done on those well-shaped crystals

5.3 Results and Discussion

5.3.1 Formation of Oil Droplets as the Dispersed Phase

Figure 5.3 shows the formation of oil droplets in two solutions with different initial protein concentrations. The solution in Figure 5.3(I) and 5.3(II) were cooled at 4^{o}C and 5.6^{o}C respectively. The oil droplets were first formed in the matrix of a dispersed phase. The volume of these oil droplets was different in both sets of solution (comparing Figure 5.3I (a) and Figure 5.3II (a)) with more droplets were formed in the solution with higher Lysozyme concentration. As the solution was further cooled at constant temperature, these oil droplets tend to coalesce. However, the volume of these droplets depleted with time in conjunction with the growth of spherical crystals. As the crystals grow, these oil droplets disappeared in the vicinity of crystals formed. These crystals were probably nucleated and grown within the oil droplets (ten Wolde and Frenkel, 1997 & 1999; Haas and Drenth, 1998; Anderson and Lekkerkerker, 2002),

and acquired the spherical shape of the oil droplets. The crystals were ultimately transformed into tetragonal shape, changing with time and temperature as detailed in Chapter 4.

The identity of the oil droplets in both series of Figure 5.3 can be deduced from a general phase diagram of Lysozyme (Figure 5.4) using the Lever rule. According to the Lever rule, the closer the overall composition to the liquid-liquid phase boundary, the more that particular liquid phase predominates in the two-phase region (Smith, 1993). For the solution in Figure 5.3(I) in which the solution was cooled at 4^{o}C, the ratio between the protein-rich phase and the protein-lean phase is proportional to AE/AF, referring to Figure 5.4. Therefore, the protein-lean phase predominates in that system as clearly seen in Figure 5.3(I). Hence, it can be concluded that the oil droplets exist as the protein-rich phase whereas the continuous phase is the protein-lean phase. Similarly for the solution in Figure 5.3(II) in accordance to the ratio of BC/BD in Figure 5.4, a large quantity of protein rich phase is expected to be formed in the solution. Thus, the oil droplets appeared in the solution that had been cooled at 5.6^{o}C are predominantly the protein-rich phase. In conclusion, protein-rich phase will always form as oil droplets dispersing in the matrix of the protein-lean phase (as continuous phase) regardless of the initial concentration in the protein solutions.

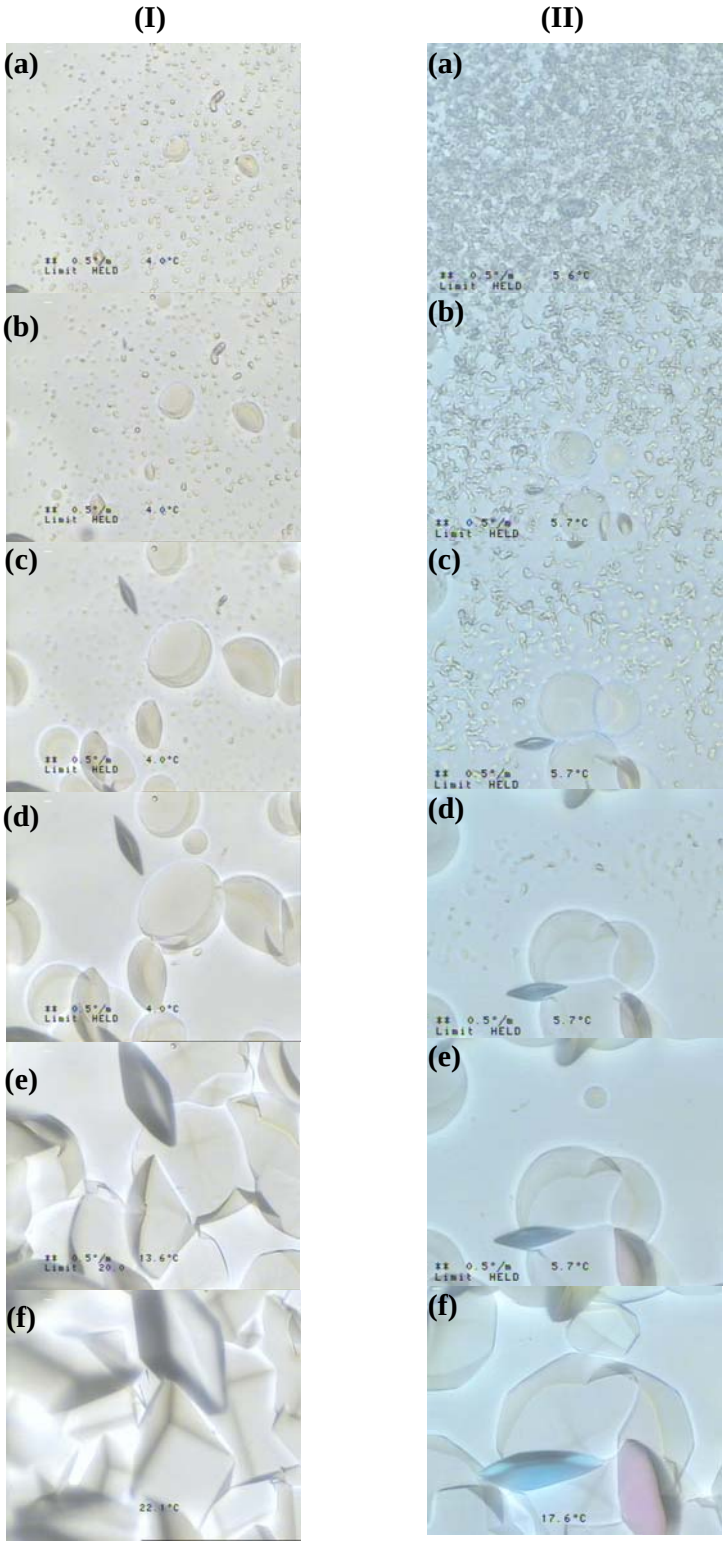

Figure 5.3 Time evolution of spherical crystals formed after the two phase formation in the solutions with different concentrations and temperatures, (I) protein solution (119.9 mg/ml Lysozyme and 3.02 w/v% NaCl) at 4°C and (II) protein solution (247.1 mg/ml Lysozyme and 3.01 w/v% NaCl) at 5.6°C. Transformation of the spherical crystals to the tetragonal crystals should be noted in the figures (e)-(f) in both series upon sitting at room temperature

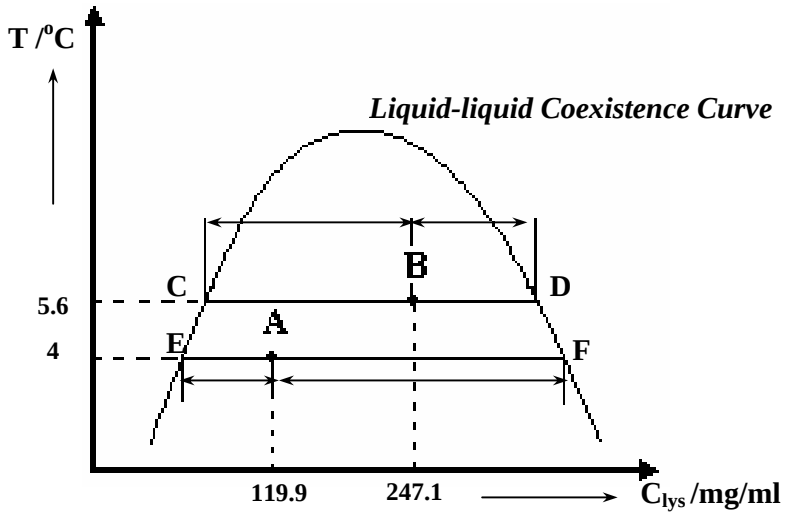

Figure 5.4 General phase diagram of the Lysozyme system which shows the final states of the solutions described in Figure 5.3. Points A and B are referring to the states for the solutions in Figure 5.3(I) and Figure 5.3(II) respectively

5.3.2 Particle Size Distribution of the Oil Droplets

Focused-Beam Reflectance Measurement (FBRM) was used to measure the sizes of oil droplets when liquid-liquid phase separation is taking place in Lysozyme solutions. Figure 5.5 shows the FBRM data for a Lysozyme solution (83.5 mg/ml Lysozyme and 3.02 w/v% NaCl) at 7°C (just at the onset of the cloudiness of sample solution) and at 3°C. 7°C was the temperature at which liquid-liquid phase separation first occurred and liquid droplets started to appear. The number of liquid droplets continued to increase with cooling and thus, there were more liquid droplets at 3 °C than at 7 °C. As the measurement principle of FBRM is based on random sampling of the droplets inside the solution, the larger the number of droplets present, the smaller will be the sampling error and fluctuations in the distribution. Therefore, the size distribution is more fluctuating at 7 °C than at 3 °C.

Sets of experiment with different solution concentrations have been carried out and the results confirmed with the size distribution as shown in Figure 5.5. After

reaching the final temperature (2.98 ± 0.1°C), the solution was then kept at that temperature for the subsequent 2 hours after the solution was cooled to that temperature. Changes in the size distribution of Lysozyme solution were monitored as a function of time is shown in Figure 5.6. The results showed that the shape of the size distribution curves remained unchanged, indicating that there is neither nucleation nor crystal growth taking place when the solution was further cooled at constant temperature. In addition, the experiment was repeated with the solutions at higher protein concentration and a similar size distribution was obtained.

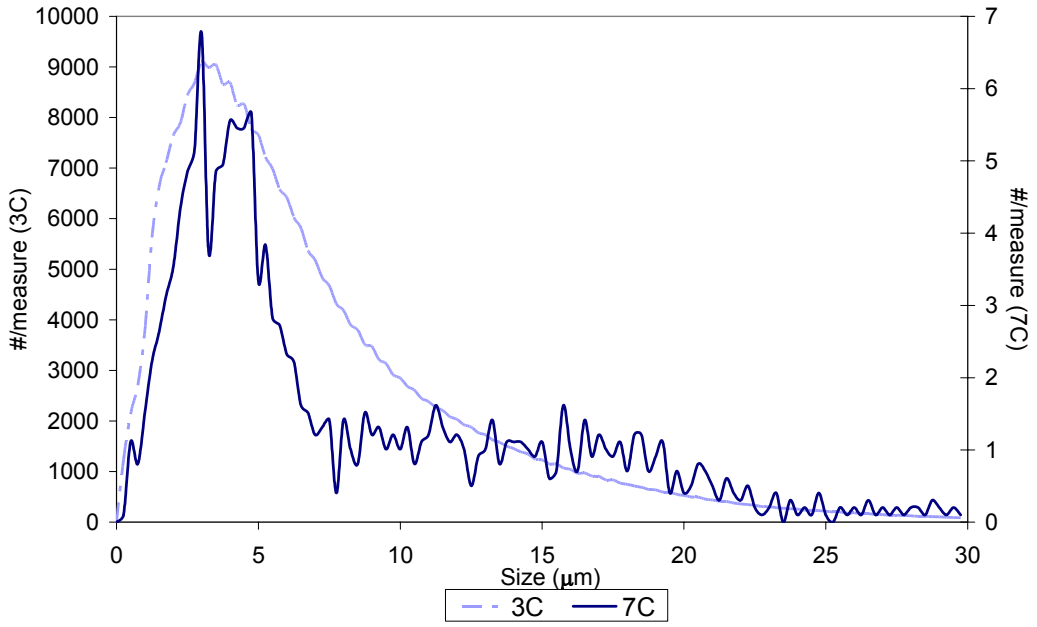

Figure 5.5 Particle size distribution of Lysozyme solution (83.5 mg/ml Lysozyme and 3.02 w/v% NaCl) at two different temperatures (the onset of cloudy solution at 7°C and the final experimental temperature, 3°C) exhibited the dominant size of oil droplets at 3-4µm

The predominant size of these oil droplets was about 3-5µm. This is consistent with the spherical crystals shown in Figure 4.5(a) and Figure 4.6(a) in which the crystals were obtained after cooling the crystallizing solutions at lower temperature for

at least 2 hours. These crystals were postulated to nucleate and grow within the oil droplets due to the supersaturation level in the confined environment.

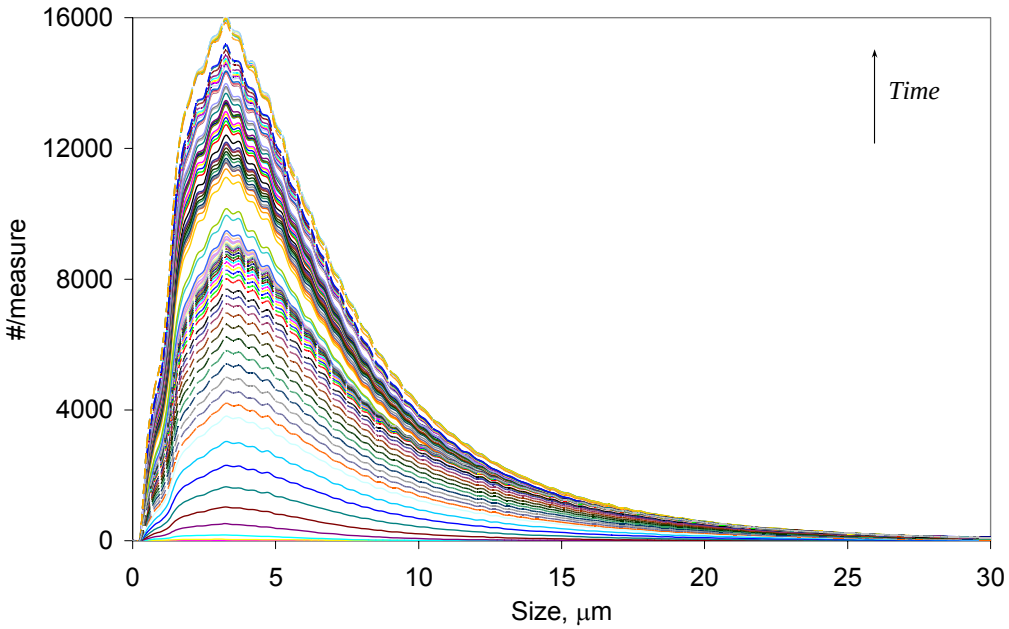

Figure 5.6 Consistency in particle size distribution of the crystallizing solution (83.5 mg/ml Lysozyme and 3.02 w/v% NaCl) throughout the experiment indicated the two phase formation was monitored instead of nucleation or crystal growth

5.3.3 Uniformity in Crystal Size

In addition to altering the crystal morphology (as described in Chapter 4), two phase formation can also give rise to a narrower crystal size distribution. This can be seen from the micrographs of crystals obtained at different time from the same solution that was kept at 5°C. When the crystals were harvested after 3 hours, mostly disc-like crystals with average size of about 100 μm were obtained (Figure 5.7(a)). After 15 hours, tetragonal crystals with average size of 140 μm were obtained (Figure 5.7(b)). In both Figure 5.7(a) and 5.7(b), the crystal size distributions are fairly uniform. On the other hand, Figure 5.7(c) shows the size distribution for the crystals obtained at 25°C after 17 hours. Table 5.1 shows the data for the distributions in Figure 5.7. It can be

clearly seen that a broader distribution is achieved if crystallization is carried out without passing through the liquid-liquid phase separation. As mentioned before, nucleation is believed to initiate within the oil droplets and possibly occurred simultaneously in the solute-rich phase. The oil droplets act as a 'core' for the crystal growth (ten Wolde and Frenkel, 1997; Anderson and Lekkerkerker, 2002) and thus play an important role in determining the final size distribution. On the other hand, variations in local concentration would give rise to the difference in nucleation and growth rate. Therefore rapidly growing, more-disordered and aggregated (Hass and Drenth, 2000; Anderson and Lekkerkerker, 2002) crystals can be observed in the solutions beyond the liquid-liquid metastable region. However, other factors such as growth rate and rate of transformation from spherical to tetragonal crystals (if they are different polymorphs) have to be further investigated.

Table 5. 1 Data for the particle size distributions in Figure 5.7

	Spherical crystals [Figure 5.7(a)]	Tetragonal crystals [Figure 5.7(b)]	Crystals at 25^{o}C [Figure 5.7(c)]
Mean Size, μm	99.42	138.22	205.11
Standard Deviation, μm	12.96	23.51	67.08
Coefficient of Variation (C.V), %	13.04	17.01	32.70

* C.V was tabulated in percentage of the ratio of standard deviation to mean size for each distribution (http://203.162.7.85/unescocourse/statistics/34.htm).

Crystallization of the solute-rich phase would be more controllable due to the uniformity in supersaturation level within the confined environment as compared to the crystallization under normal conditions (without passing through the liquid-liquid phase separation region). Thus, agglomeration of crystals, which poses a major problem in crystallization, could be reduced or diminished as shown in the images of Figure 5.7. Individual and well-shaped crystals were obtainable from the crystallizing

solutions after keeping the solutions at low temperature (where the two phases are formed) for 15 hours. Contrarily, agglomerated and irregularly shaped crystals were obtained when crystallized at temperatures beyond the cloud point temperature of solutions.

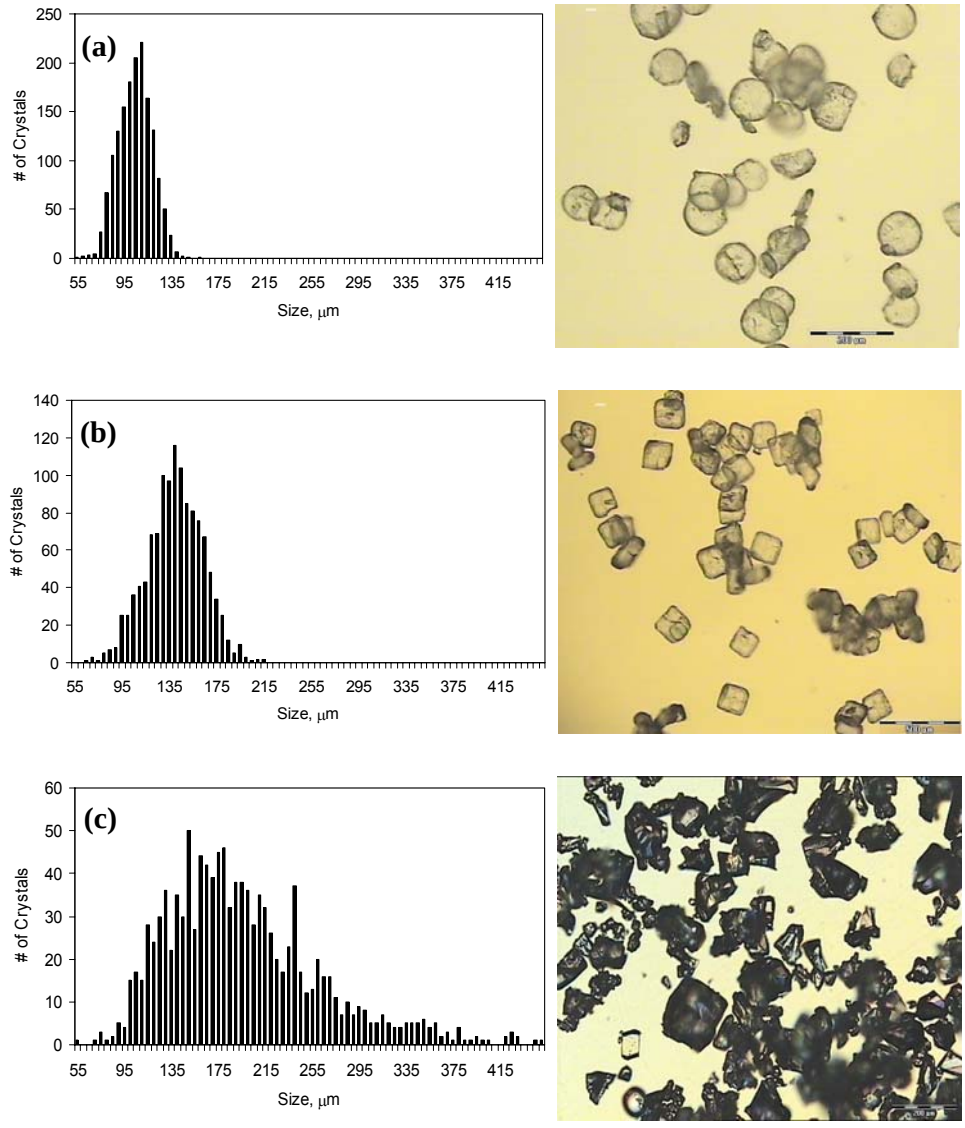

Figure 5. 7 Particle size distribution and optical micrograph of Lysozyme crystals, (a) spherical crystals obtained after 3 hours at 5°C, (b) tetragonal crystals obtained after 15 hours at 5°C (crystals in both (a) and (b) were obtained from the same solution under the conditions as in Figure 4.6), and (c) crystals obtained after 17 hours at 25^{o}C

Under normal crystallization conditions (Figure 5.7(c)), protein crystals formed in the solutions at a very high level of supersaturation. Once the crystals are nucleated, they subsequently grow at high supersaturation and would not approach the metastable zone where controlled and ordered growth could occur. Instead, protein molecules would deposit onto the surface of growing crystals vigorously and encourage the formation of disordered crystals and probably with defects. The deposition is not only due to molecular diffusion but also due to convective mixing driven by the density gradient in the crystallizing solutions (McPherson, 1999). Hence, rapid growth of crystals would produce a cascade result in agglomeration. These difficulties lead to the development of gravity control on crystal growth where a depletion zone is introduced as a hypothesis for improvements of crystal quality particularly on Lysozyme crystals (Otálora et al., 2002). Under microgravity conditions, convective mixing would be eliminated and crystal growth is controlled by molecular diffusion. However, molecular diffusion of protein system is extremely slow (Peng and Kim, 1994) due to its molecular size, a concentration gradient or depletion zone is established around the growing crystals (Dixit et al., 2001). Local supersaturation is reduced in the vicinity of these crystal and this create an environment that equivalent to the metastable zone which is suitable for growing good quality crystals as mentioned earlier. Though microgravity is not applied in this project, reduction in crystal agglomeration observed in Figure 5.7 could be due to the formation of depletion zone when crystals are formed within the oil droplets. Within the metastable liquid-liquid phase separation region (two phases are formed), after nucleated and grown in protein-rich phase (oil droplets), the crystals will subsequently grow in the protein-lean phase with a lower level of supersaturation. Convective mixing in the concentration depletion zone (surrounding the protein crystals) is possibly reduced due to the lower density gradient within the

protein-lean phase. Thus, the diffusion rate of protein molecules in this phase would be similar to the crystal growth rate. Individual and well-shaped Lysozyme crystals are obtainable. The influence of the depletion zone on crystal shape has been observed in other polymer crystallization systems (Wang et al., 2002; Rieter and Vidal, 2003). However the effect of two phase formation on crystal agglomeration is still not fully elucidated. Hence, further investigations to validate the hypothesis of reduction in agglomeration owing to oiling-out phenomenon during crystallization can be profitably pursued.

5.4 Conclusions

The characteristics of two phase formation and its effects on Lysozyme crystal properties were studied and presented in this chapter. It was found that the oil droplets, with dominant size of 3-4μm, had a pronounced influence on the size distribution and agglomeration of Lysozyme crystals. Narrower size distribution and less-agglomerated crystals were observed when crystallization followed by two phase formation was carried out in Lysozyme system. One possible reason could be that those crystals were formed under a controllable environment. Homogeneity in either protein-rich (oil droplets) or protein-lean phase (dispersed phase) would give rise to the possibility of similar growth rate in each crystals formed and thus prevent the vigorous deposition of Lysozyme molecules on the surfaces of these growing crystals. These findings may provide an advantage in controlling the crystal size distribution especially in the pharmaceutical industry. More detailed studies of molecular transport within the oil droplets and in the subsequent crystal growth should be carried out, to gain more understanding towards applying the technique to obtain homogeneous and well-shaped crystal populations.

CHAPTER 6

CONCLUSIONS AND RECOMMEDATIONS FOR FUTURE WORK

6.1 Conclusions

This project has been carried out to study the two phase formation (liquid-liquid phase separation) in protein crystallization. Understandings on the influence of variables in crystallization on two phase formation and the effect of that phenomenon on solution crystallization of Lysozyme have been gained.

In understanding the influence of process variables on two phase formation during crystallization, the effects of buffer solution, cooling rates and salt partitioning on the cloud point temperatures of Lysozyme solutions have been studied. It was found that buffer solution which was used to stabilize the pH of protein solutions increased the cloud point temperature of the solutions. Different cooling rates have been applied during crystallization of Lysozyme and the results showed that rate of cooling has an effect on the cloud point temperature determined for liquid-liquid phase separation of Lysozyme solutions; therefore the cloud point curve obtained experimentally depends on the kinetics of the experiments. These effects (buffer solution and cooling rates) would provide a means for tuning the crystallization process to avoid the formation of

solute-rich phase if it is undesirable. In addition, results on salt partitioning in phase separated solutions showed that the formation of oil droplets within Lysozyme system is independent to the salt added to the solutions. However, the cloud point temperature of the system is dependent to the salt concentration (Broide et al., 1996; Muschol and Rosenberger, 1997).

Oil droplets, with average size of less than 10μm, were dispersed in the matrix of another continuous liquid phase when liquid-liquid phase separation occurred during crystallization. These droplets existed as the protein-rich phase regardless of the initial concentration of protein in the solutions. Its formation has been shown to affect the crystal morphology of Lysozyme. When nucleation and crystallization occur within the oil droplets (ten Wolde and Frenkel, 1997; Anderson and Lekkerkerker, 2001), crystals with a new habit, spherically-shaped, that different from the known habits of Lysozyme (tetragonal (Cacioppo and Pusey, 1991a) and orthorhombic (Ewing et al., 1994)) were observed. Furthermore, XRPD pattern of these crystals showed that it poses a new potential polymorph of the Lysozyme system. These indicate the difficulties in controlling the crystal morphology and polymorphism of the final product in pharmaceutical and fine chemical industries when two phase formation occurs concurrently with crystallization. These crystals will gradually transform into the tetragonal shape when the conditions which favor the spherical crystals are no longer exist.

In addition to the effect of two phase formation on crystal morphology and polymorphism, the size distribution of the crystals obtained from the liquid-liquid phase separation was also affected. These crystals have a more uniform size and a

narrower size distribution. The crystal size distribution is profoundly influenced by the boundaries of oil droplets. These results may have practical implications as a possible means of controlling size distribution via the formation of an intermediate liquid-liquid state.

6.2 Recommendations for Future Work

The followings are the suggested areas to extend this study.

Further Studies on the Effect of Process Variables on the Two Phase Formation

1. Molecular interactions during cooling event should be studied in order to have an insight into the behavior of protein molecules especially when the solutions are cooled to a temperature below the solution cloud point temperature.
2. Characteristics of water (solvent) and salt (precipitant) to protein interactions under ambient temperature should be investigated to understand its influences on the two phase formation. The solubility of salt was reported by Davey and Garside (2000) where the solubility dropped drastically when the salt solutions were cooled to below 0^{o}C. As the solutions in this study were cooled to far below 0^{o}C, the effect of salt should not be excluded.
3. The effect of salt concentrations on the cloud point temperature has been studied by Broide et al. (1996) and Muschol and Rosenberger (1997). However, the salt partitioning in those studies was not fully investigated. Therefore, it may be useful to study the partition of salts when higher salt concentrations are employed, in order to further understand the role of salt during liquid-liquid phase separation.

4. Investigations on the two phase formation of a potential system of smaller molecules such as aspirin (http://www.chymist.com/aspirin.pdf) and benzoic acid (Ricci, 1951) can be carried out systematically.

Further Studies on the Effect of Two Phase Formation on Crystal Properties

1. Polymorphic change (if any) of Lysozyme crystals during two phase formation can possibly be further studied using FBRM. This method has been used to monitor the polymorphic change in D-mannitol (O'Sullivan et al., 2003) and the changes in particle dimensions, shape, solubility and crystal structure have been observed with in-line PVM (Particle Vision Microscopy) and Raman spectroscopy.
2. The experiment to obtain the spherical crystals should be scaled-up to a larger scale in order to obtain sufficient crystals for other analysis such as solubility, single crystals X-ray diffractometry, size distribution, etc.
3. Nucleation and crystal growth are thought to occur within the oil droplets as reported by ten Wolde and Frenkel (1997), Haas and Drenth (1998), and Anderson and Lekkerkerker (2002). However, they reported the results based on the theoretical modeling without any experimental support. Thus, crystallization kinetics within the oil droplets should be further investigated experimentally to support the hypothesis of nucleation and crystal growth within solute-rich droplets.
4. The size distribution of oil droplets has been shown remained constant when the solutions were cooled at low temperature (lower than its cloud point temperature) at a specific period of time. However, SEM images (Chapter 4) showed that there was a transformation in crystal size and shape beyond that period of time.

Therefore, the kinetic change in oil droplets should be monitored using FBRM for a longer period. The relationship between the growth kinetics and the crystal size distribution can then be further understood.

5. Crystal size distribution in this project was studied and measured using a image analysis software of the optical polarized-light microscope. The reliability of the result can be further established if the analyses are carried out using different techniques such as sieve analysis and particle size distribution by laser diffractometry (Malvern Mastersizer or Sympatec).

REFERENCES

Abbas, A. Nobbs, D. and Romagnoli, J.A. Investigation of On-line Optical Particle Characterization in Reaction and Cooling Crystallization Systems. Current State of the Art, Meas. Sci. Technol., *13*, pp. 349-356. 2002.

Alderton, G. and Fevold, H.L. Direct Crystallization of Lysozyme from Egg-White and Some Crystalline Salts of Lysozyme, J. Biol. Chem., *164*, pp. 1-5. 1946.

Alderton, G. Ward, W.H. and Fevold, H.L. Isolation of Lysozyme from Egg White, J. Biol. Chem, *157*, pp.43-58. 1945.

Allahyarov, E. Löwen, H. Hansen, J.P. and Louis, A.A. Nonmonotonic Variation with Salt Concentration of the Second Virial Coefficient in Protein Solutions, Phys. Rev. E, *67*, art. no. 051404. 2003.

Anderson, V. J. and Lekkerkerker, H. N. W. Insights into Phase Transition Kinetics from Colloid Science, Nature, *416*, pp.811-815. 2002.

Arkenbout, G.F. Melt Crystallization Technology, Technomic Publishing Company Inc., US, pg. 39. 1995.

Ataka M. and Asai, M. Systematic Studies on the Crystallization of Lysozyme – Determination and Use of Phase Diagrams, J. Cryst. Growth, *90*, pp. 86-93. 1988.

Aune, K.C. and Tanford, C. Thermodynamics of Denaturation of Lysozyme by Guanidine Hydrochloride II. Dependence on Denaturant Concentration at 25°C, Biochemistry, *14*, pp. 4953-4963. 1969.

Bauer, J. Spanton, S. Henry, R. Quick, J. Dziki, W. Porter, W. and Morris, J. Ritonavir: An Extraordinary Example of Conformational Polymorphism, Pharm. Res., *18(6)*, pp.859-866. 2001.

Berland, C.R. Thurston, G.M. Kondo, M. Broide, M.L. Pande, J. Ogun, O. and Benedek, G.B. Solid-Liquid Phase Boundaries of Lens Protein Solutions, Proc. Natl. Acad. Sci. U.S.A., *89*, pp. 1214-1218. 1992.

Berthou, J. and Jollès, P. A Phase Transition in a Protein Crystal: The Example of Hen Lysozyme, Biochim. Biophys. Acta, *336*, pp. 222-227. 1974.

Bester, B.H. and Lombard, S.H. Influence of Lysozyme on Selected Bacteria Associated with Gouda Cheese, J. Food Prot., *53*, pp. 306-311. 1990.

Bhamidi, V. Skrzypczak-Jankun, E. and Schall, C.A. Dependence of Nucleation Kinetics and Crystal Morphology of a Model Protein System on Ionic Strength, J. Cryst. Growth, *232*, pp. 77-85. 2001.

Bonnett, P.E. Carpenter, K.J. Dawson, S. and Davey, R.J. Solution Crystallization via a Submerged Liquid-liquid Phase boundary: Oiling Out, Chem. Commun., *6*, pp.698-699. 2003.

Broide, M.L. Berland, C.R. Pande, J. Ogun, O.O. and Benedek, G.B. Binary Liquid Phase Separation of Lens Protein Solutions, Proc. Natl. Acad. Sci. U.S.A., *88*, pp. 5660-5664. 1991.

Broide, M.L. Tominc, T.M. and Sazowsky, M.D. Using Phase Transitions to Investigate the Effect of Salts on Protein Interactions, Phys. Rev. E, *53*, pp. 5325-5335. 1996.

Cacioppo, E. and Pusey, M.L. The Solubility of the Tetragonal Form of Hen Egg White Lysozyme from pH 4.0 to 5.4, J. Cryst. Growth, *114*(3), pp.286-292. 1991a.

Cacioppo, E. Munson, S. and Pusey, M.L. Protein Solubilities Determined by a Rapid Technique and Modification of that Technique to a Macromethod, J. Cryst. Growth, *110*, pp. 66-71. 1991b.

Cahn, J.W. and Hilliard, J.E. Free Energy of a Nonuniform System. I. Interfacial Free Energy, J. Chem. Phys., *28*, pp. 258-267. 1958.

Canfield, R. The Amino Acid Sequence of Egg White Lysozyme, J. Biol. Chem., *238*, pp. 2698-2707. 1963.

Chayen, N.E. Crystallization with Oils: a New Dimension in Macromolecular Crystal Growth, J. Cryst. Growth, *196*, pp. 434-441. 1999.

Chayen, N.E. Stewart, P.D.S. and Blow, D.M. Microbatch Crystallization under Oil – A New Technique Allowing many Small-Volume Crystallization Trials, J. Cryst. Growth, *122*, pp. 176-180. 1992.

Chayen, N.E. Stewart, P.D.S. Maeder, D.L and Blow, D.M. An Automated-System for Microbatch Protein Crystallization and Screening, J. Applied Crystallogr., *23*, pp. 297-302. 1990.

Chayen, N.E. The Role of Oil in Macromolecular Crystallization, Structure, *5*, pp. 1269-1274. 1997.

Chow, P.S Zhang, J. Liu, X.Y. and Tan, R.B.H. Spherulitic Growth in Protein Solutions, Int. J. Mod. Phys. B, *16*, pp. 354-358. 2002.

Coates, J. Interpretation of Infrared Spectra, a Practical Approach. In Encyclopedia of Analytical Chemistry, ed by R.A. Meyers, pp.10815-10837. Chichester: John Wiley & Sons Ltd. 2000.

Cozzone, P.J. Opella, S.J. Jardetzky, O. Berthou, J. and Jollès, P. Detection of New Temeprature-Dependent Conformational Transition in Lysozyme by Carbon-13 Nuclear Magnectic Resonance Spectroscopy, Proc. Natl. Acad. Sci. U.S.A., *72*, pp. 2095-2098. 1975.

D'Arcy, A. Elmore, C. Stihle, M. and Johnston, J.E. Novel Approach to Crystallizing Proteins under Oil, J. Cryst. Growth, *168*, pp. 175-180. 1996.

Daanoun, A. Tejero, C.F. and Baus, M. Van-Der-Waals Theory for Solids, Phys. Rev. E, *50*, pp. 2913-2924. 1994.

Darcy, P. A. and Weincek, J. M. Identifying Nucleation Temperatures for Lysozyme via Differential Scanning Calorimetry, J. Cryst. Growth, *196*, pp. 243-249. 1999.

Davey, R. and Garside, J. From Molecules to Crystallizer: An introduction to Crystallization. pp. 8-20, Oxford: Oxford University Press, 1st edition, 2000.

Davies, A. Neuberger, A. and Wilson, B. The Dependence of Lysozyme Activity on pH and Ionic Strength, Biochim. Biophys. Acta, *178*, pp. 294-305. 1969.

Dijkstra, M. Phase Behavior of Hard Spheres with Short-Range Yukawa Attraction, Phys. Rev. E, *66*, art. no. 021402. 2002.

Dixit, N.M. and Zukoski, C.F. Crystal Nucleation Rates for Particles Experiencing Short-Range Attractions: Application to Proteins, J. Colloid and Interf. Sci., *228*, pp. 359-371. 2000.

Dixit, N.M. Kulkarni, A.M. and Zukoski, C.F. Comparison of Experimental Estimates and Model Predictions of Protein Crystal Nucleation Rates, Colloids Surf. A, *190*, pp. 47-60. 2001.

Dowding, P.J. Goodwin, J.W. and Vincent, B. Factors Governing Emulsion Droplet and Solid Particle Size Measurements Performed Using the Focused Beam Reflectance Technique, Colloids Surf. A, *192*, pp. 5-13. 2001.

Durbin, S.D. and Feher, G. Protein Crystallization, Annu. Rev. Phys. Chem., *47*, pp. 171-204. 1996.

Ewing, F. Forsythe, E. and Pusey, M. Orthorhombic Lysozyme Solubility, Acta Crystallogr. D, *50*, pp. 424-428. 1994.

Finnie, S.D. Ristic, R.I. Sherwood, J.N. and Zikic, A.M. Morphological and Growth Rate Distributions of Small Self-Nucleated Paracetamol Crystals Grown from Pure Aqueous Solutions, J. Cryst. Growth, *207*, pp. 308-318. 1999.

Forsythe, E.L. and Pusey, M.L. The Effects of Acetate Buffer Concentration on Lysozyme Solubility, J. Cryst. Growth, *168*, pp. 112-117. 1996.

Fujiwara, M. Chow, P.S. Ma, D.L. and Braatz, R. Paracetamol Crystallization Using Laser Backscattering and ATR-FTIR Spectroscopy : Metastability, Agglomeration and Control, Cryst. Growth & Design, *2*, pp. 365-370. 2002.

Galkin, O. and Vekilov, P.G. Are Nucleation Kinetics of Protein Crystals Similar to Those of liquid Droplets?, J. Am. Chem. Soc. *122*, pp. 156-163. 2000a.

Galkin, O. and Vekilov, P.G. Control of Protein Crystal Nucleation around the Metastable Liquid-Liquid Phase Boundary, Proc. Natl. Acad. Sci. U.S.A., *97*, pp. 6277-6281. 2000b.

Galkin, O. and Vekilov, P.G. Nucleation of Protein Crystals: Critical Nuclei, Phase Behavior, and Control Pathway, J. Cryst. Growth, *232*, pp. 63-76. 2001.

Georgalis, Y. Umbach, P. Soumpasis, D.M. and Saenger, W. Dynamics and Microstructure Formation during Nucleation of Lysozyme Solutions, J. Am. Chem. Soc., *120*, pp. 5539-5548. 1998.

George, A. and Wilson, W.W. Predicting Protein Crystallization from a Dilute-Solution Property, Acta Crystallogr. D, *50*, pp. 361-365. 1994.

George, A. Chiang, Y. Guo, B. Arabshahi, A. Cai, Z. and Wilson, W.W. Second Virial Coefficient as Predictor in Protein Crystal Growth, Methods Enzymol., *276*, pp. 100-110. 1997.

Giron, D. Monitoring of Polymorphism – From Detection to Quantification, Eng. Life Sci., *3*, pp. 103-112. 2003.

Giron, D. Thermal Analysis and Calorimetric Methods in the Characterization of Polymorphs and Solvates, Thermochim. Acta, *248*, pp. 1-59. 1995.

Goodman, H. Pollock, J.J. Katona, L.I. Iacono, V.J. Cho, M. and Thomas, E. Lysis of Streptococcus Mutans by Hen Egg White Lysozyme and Inorganic Sodium Salts, J. Bacteriol., *146*, pp. 764-774. 1981.

Grigsby, J.J. Blanch, H.W. and Prausnitz, J.M. Cloud-Point Temperature for Lysozyme in Electrolyte Solutions: Effect of Salt type, Salt Concentration and pH, Biophys. Chem., *91*, pp. 231-243. 2001.

Grimbergen, R.F.P. Bennema, P. and Meekas, H. On the Prediction of Crystal Morphology III. Equilibrium and Growth Behavior of Crystal Faces Containing Multiple Connected Nets, Acta Crystallogr. A, *55*, pp. 84-94. 1999a.

Grimbergen, R.F.P. Boek, E.S. Meekas, H. and Bennema, P. Explanation for the Supersaturation Dependence of the Morphology of Lysozyme Crystals, J. Cryst. Growth, *207*, pp. 112-121. 1999b.

Grossowicz, N. and Ariel, M. Methods for Determination of Lysozyme Activity, Methods Biochem. Anal., *29*, pp. 435-446. 1958.

Grouazel, S. Perez, J. Astier, J.-P. Bonneté, F. and Veesler, S. BPTI Liquid-Liquid Phase Separation Monitored by Light and Small-Angle X-Ray Scattering, Acta. Crystallogr. D, *58*, pp. 1560-1563. 2002.

Haas, C and Drenth, J. The Protein-Water Phase Diagram and the Growth of Protein Crystals from Aqueous Solution, J. Phys. Chem. B, *102*, pp. 4226-4232. 1998.

Haas, C. and Drenth, J. The Interface between a Protein Crystal and an Aqueous Solution and Its Effects on Nucleation and Crystal Growth, J. Phys. Chem. B, *104*, pp. 368-377. 2000.

Haas, C. and Drenth, J. Understanding Protein Crystallization on the Basis of the Phase Diagram, J. Cryst. Growth, *196*, pp. 388-394. 1999.

Hagen, M.J. and Frenkel, D. Determination of Phase Diagrams for the Hard-Core Attractive Yukawa System, J. Chem. Phys., *101*, pp. 4093-4097. 1994.

Hansen, J-P. and Pusey, P.N. Phase Behavior of Colloidal Systems, Europhys. News, *May/June*, pp. 81-83. 1999.

Harata, K. and Akiba, T. Phase Transition of Triclinic Hen Egg-White Lysozyme Crystal Associated with Sodium Binding, Acta Crystallogr. D, *60*, pp. 630-637. 2004.

Harata, K. X-ray Structure of a Monoclinic Form of Hen Egg-White Lysozyme Crystallized at 313K. Comparison of Two Independent Molecules, Acta Crystallogr. D, *50*, pp. 250-257. 1994.

Ho, J.X. Declercq, J-P. Myles, D.A.A. Wright, B.S. Ruble, J.R. and Carter, D.C. Neutron Structure of Monoclinic Lysozyme Crystals Produced in Microgravity, J. Cryst. Growth, *232*, pp. 317-325. 2001.

Hollander, F.F.A. Kaminski, D. Duret, D. van Enckevort, W.J.P. Meekes, H. and Bennema, P. Growth and Morphology of Thin Fat Crystals, Food Res. Int., *35*, pp. 909-918. 2002.

http://203.162.7.85/unescocourse/statistics/34.htm

http://spectra.galactic.com/SpectraOnline/

http://www.chymist.com/aspirin.pdf

http://www.cm.utexas.edu/CH210C/

http://www.ct.chemie.tu-darmstadt.de/ak_vogel/hetkat/drifts_en.html**;**

http://www.google.com/ with the searched page http://147.46.41.146/~1ii/DRIFT.htm

http://www.gsk.com/media/glaxo97.htm

http://www.lasentec.com/M-2-004_abstract.html

http://www.lasentec.com/M-2-011_abstract.html

http://www.lasentec.com/method_of_measurement.html

http://www.mt.com/mt/product/

http://www.scottlab.com/fodras.htm

http://www.seikagaku.com

http://www.uwgb.edu/dutchs/PETROLGY/

http://www.webster-online-dictionary.org

Hukkanen, E.J. and Braatz, R. Measurement of Particle Size Distribution in Suspension Polymerization using In Situ Laser Backscattering, Sens. Actuators B, *96*, pp. 451-459. 2003.

Ilett, S.M. Orrock, A. Poon, W.C.K. and Pusey, P.N. Phase Behavior of a Model Colloid-Polymer Mixture, Phys. Rev. E, *51*, pp. 1344-1352. 1995.

Ishimoto, C. and Tanaka, T. Critical Behavior of a Binary Mixture of Protein and Salt Water, Phys. Rev. Lett., *39(8)*, pp. 474-477. 1977.

Jeffers, P. Raposo, S. Lima-Costa, M-E. Connolly, P. Glennon, B. and Kieran, P.M. Focused Beam Reflectance Measurement (FBRM) Monitoring of Particle Size and Morphology in Suspension Cultures of Morinda Citrifolia and Centaurea Calcitrapa, Biotechnol. Lett., *25*, pp. 2023-2028. 2003.

Jollès, P. and Jollès, J. What's New in Lysozyme Research? Always a Model System, Today as Yesterday, Mol. Cell. Biochem., *63*, pp. 165-189. 1984.

Jollès, P. Introduction: From the Discovery of Lysozyme to the Characterization of Several Lysozyme Families. In Lysozymes- Model Enzymes in Biochemistry and Biology, ed by Jollès, P., pp. 3-8. Boston: Birkhauser Verlag. 1996.

Jones, R.B. and Pusey, P.N. Dynamics of Suspended Colloidal Spheres, Ann. Rev. Phys. Chem., *42*, pp. 137-169. 1991.

Jönsson, M. and Johansson, H-O. Protein Partitioning in Thermoseparating Systems of a Charged Hydrophobically Modified Ethylene Oxide Polymer, J. Chromatogr. A, *983*, pp. 133-144. 2003.

Kaplan, P.D. Rouke, J.L. and Yodh, A.G. Entropically Driven Surface Phase Separation in Binary Colloidal Mixtures, Phys. Rev. Lett., *72(4)*, pp. 582-585. 1994.

Kern, N. and Frenkel, D. Fluid-Fluid Coexistence in Colloidal Systems with Short-Ranged Strongly Directional Attraction, J. Chem. Phys., *118*, pp. 9882-9889. 2003.

Lafferrère, L. Hoff, C. and Veesler, S. Polymorphism and Liquid-Liquid Phase Separation of Pharmaceutical Compound. In Chemical Engineering Transactions, 15th International Symposium on Industrial Crystallization, 15-18 September 2002, Sorrento, Italy, pp. 819-824.

Legrand, L. Riès-Kautt, M. and Robert, M.C. Two Polymorphs of Lysozyme Nitrate: Temperature Dependence of Their Solubility, Acta Crystallogr. D, *58*, pp. 1564-1567. 2002.

Liu, W. Bratko, D. Prausnitz, J.M. and Blanch, H.W. Effect of Alcohols on Aqueous Lysozyme-Lysozyme Interactions from Light-Scattering Measurements, Biophys. Chem., *107*, pp. 289-298. 2004.

Lomakin, A. Asherie, N. and Benedek, G. Aeolotopic Interactions of globular Proteins, Proc. Natl. Acad. Sci. U.S.A., *96*, pp. 9465-9468. 1999.

Lorber, B. and Giegé, R. Containerless Protein Crystallization in Floating Drops: Application to Crystal Growth Monitoring under Reduced Nucleation Conditions, J. Cryst. Growth, *168*, pp. 204-215. 1996.

Lorber, B. Sauter, C. Robert, M.C. Capelle, B. and Giegé, R. Crystallization within Agarose Gel in Microgravity Improves the Quality of Thaumatin Crystals, Acta Crystallogr. D, *55*, pp. 1491-1494. 1999.

Louis, A.A. Allahyarov, E. Löwen, H. and Roth, R. Effective Forces in Colloidal Mixtures: from Depletion Attraction to Accumulation Repulsion, Phys. Rev. E, *65(6)*, art. no. 061407. 2002.

Lu, J. Carpenter, K. J. Li, R. Wang, X. and Ching, C-B. Cloud Point Temperature and Liquid-Liquid Phase Separation of Supersaturated Lysozyme Solution, Biophys. Chem., *109*, pp. 105-112. 2004.

Lu, J. Wang, X-J. and Ching, C-B, Effect of Additives on the Crystallization of Lysozyme and Chymotrypsinogen A, Cryst. Growth Des., *3*, pp. 83-87. 2003.

Manno, M. Xiao, C. Bulone, D. Martorana, V. and San Biago, P.L. Thermodynamic Stability in Supersaturated Lysozyme Solutions: Effect of Salt and Role of Concentration Fluctuations, Phys. Rev. E, *68*, art. no. 011904. 2003.

McPherson, A. Crystallization of Biological Macromolecules. pp. 435-472, New York: Cold Spring Harbor Lab. Press. 1999.

Mullin, J. W. Crystallization. pp. 181-288, London: Butterworth Heinemann. 2001.

Muschol, M. and Rosenberger, F. Liquid-Liquid Phase Separation in Supersaturated Lysozyme Solutions and Associated Precipitate Formation/Crystallization, J. Chem. Phys., *107*(6), pp. 1953-1962. 1997.

Myerson, A.S. Handbook of Industrial Crystallization. pp. 33-64, Boston: Butterworth-Heinemann. 1993.

Narayanan, J. and Deotare, V.W. Salt-Induced Liquid-Liquid Phase Separation of Protein-Surfactant Complexes, Phys. Rev. E, *60(4)*, pp. 4597-4603. 1999.

Nicolis, G. and Nicolis, C. Enhancement of the Nucleation of Protein Crystals by the Presence of an Intermediate Phase: A Kinetic Model, Physica A, *323*, pp. 139-154. 2003.

Ninomiya, K. Yamamoto, T. Oheda, T. Sato, K. Sazaki, G. and Matsuura, Y. Morphology and Solubility of Multiple Crystal Forms of Taka-Amylase A, J. Cryst. Growth, *222*, pp. 311-316. 2001.

O'Sullivan, B. Barrett, P. Hsiao, G. Carr, A. and Glennon, B. In Situ Monitoring of Polymorphic Transitions, Org. Process Res. Dev., *7(6)*, pp. 977-982. 2003.

Otálora, F. Garcia-Ruiz, J.M. Carotenuto, L. Castagnolo, D. Novella, M.L and Chernov, A.A. Lysozyme Crystal Growth Kinetics in Microgravity, Acta Crystallogr. D, *58*, pp. 1681-1689. 2002.

Pearson, A.P. Glennon, B. and Kieran, P.M. Comparison of Morphological Characteristics of Streptomyces Natalensis by Image Analysis and Focused Beam Reflectance Measurement, Biotechnol. Prog., *19*, pp. 1342-1347. 2003.

Pellicane, G. Costa, D. and Caccamo, C. Cloud and Solubility Temperatures Versus Ionic Strength in Model Lysozyme Solutions, J. Phys.: Condens. Matter, *15*, pp. S3485-S3489. 2003b.

Pellicane, G. Costa, D. and Caccamo, C. Phase Coexistence in a DLVO Model of Globular Protein Solutions, J. Phys.: Condens. Matter, *15*, pp. 375-384. 2003a.

Peng, Z.Y. and Kim, P.S. A Protein Dissection Study of a Molten Globule, Biochemistry, *33*, pp. 2136-2141. 1994.

Petsev, D.N. Wu, X.X. Galkin, O. and Vekilov, P.G. Thermodynamic Functions of Concentrated Protein Solutions from Phase Equilibria, J. Phys. Chem. B, *107*, pp. 3921-3926. 2003.

Piazza, R. Interactions in Protein Solutions near Crystallization: a Colloid Physics Approach, J. Cryst. Growth, *196*, pp. 415-423. 1999.

Poon, W.C.K, Crystallization of Globular Protein, Phys. Rev. E, *55*, pp. 3762-3764. 1997.

Poon, W.C.K. and Haw, M.D. Mesoscopic Structure Formation in Colloidal Aggregation and Gelation, Adv. Colloid Interface Sci., *73*, pp. 71-126. 1997.

Poon, W.C.K. Pirie, A.D. and Pusey, P.N. Gelation in Colloid-Polymer Mixture, Faraday Discuss., *101*, pp. 65-76. 1995.

Prager, E.M. and Jollès, P. Animal Lysozymes *c* and *g*: An Overview. In Lysozymes : Model in Biochemistry and Biology, ed by P. Jollès, pp. 9-31. Brikhäuser Verlag Basel, Switzerland. 1996.

Rascòn, C. Mederos, L and Navascues, G. Solid-to-Solid Isostructural Transition in the Hard-Sphere Attractive Yukawa System, J. Chem. Phys., *103*, pp. 9795-9799. 1995.

Ricci, J.E. The Phase Rule and Heterogeneous Equilibrium, pp. 174-177, New York: Van Nostrand. 1951.

Ries-Kautt, M.M. and Ducruix, A.F. Relative Effectiveness of Various Ions on the Solubility and Crystal Growth of Lysozyme, J. Biol. Chem., *264*, pp. 745-748. 1989.

Rieter, G. and Vidal, L. Crystal Growth Rates of Diblock Copolymers in Thin Film: Influence of Film Thickness, Eur. Phys. J. E, *12*, pp. 497-505. 2003.

Rosenbaum, D. and Zukoski, C.F. Protein Interactions and Crystallization, J. Cryst. Growth, *169*, pp. 752-758. 1996.

Rosenbaum, D. Zamora, P.C. and Zukoski, C.F. Phase Behavior of Small Attractive Colloidal Particles, Phys. Rev. Lett., *76*, pp. 150-153. 1996.

Rosenberger, F. Protein Crystallization, J. Cryst. Growth, *166*, pp. 40-54. 1996.

Ruf, A. Worlitschek, J. and Mazzotti, M. Modeling and Experimental Analysis of PSD Measurements through FBRM, Part. Part. Syst. Charact., *17*, pp. 167-179. 2000.

Sauter, C. Otalora, F. Gavira, J.A. Vidal, O.F. Giege, R. and Garcia-Ruiz, J.M. Structure of Tetragonal Hen Egg-White Lysozyme at 0.94 Angstrom from Crystals

Grown by the Counter-Diffusion Method, Acta Crystallogr. D, *57*, pp. 1119-1126. 2001.

Sava, G. Pharmacological Aspects and Therapeutic Applications of Lysozyme. In Lysozyme: Model Enzymes in Biochemistry and Biology, ed by P. Jollès, pp. 433-449. Basel: Birkhäuser Verlag. 1996.

Shang, M. Matsuyama, H. Maki, T. Teramoto, M. and Lioyd, D.R. Effect of Crystallization and Liquid-Liquid Phase Separation on Phase-Separation Kinetics in Poly (Ethylene-co-Vinyl Alcohol)/Glycerol Solution, J. Polym. Sci. B, *41*, pp. 194-201. 2003.

Sica F. Adinolfi, S. Vitagliano, L. Zagari, A. Capasso, S. and Mazzarella, L. Cosolute Effect on Crystallization of Two Dinucleotide Complexes of Bovine Seminal Ribonuclease from Concentrated Salt Solutions, J. Cryst. Growth, *168*, pp. 192-197. 1996.

Skouri, M. Lorber, B. Giegé, R. Munch, J.-P. and Candau, J.S. Effect of Macromolecular Impurities on Lysozyme Solubility and Crystallizability: Dynamic Light Scattering, Phase Diagram, and Crystal Growth Studies, J. Cryst. Growth, *152*, pp. 209-220, 1995.

Smith, W.F. Foundations of Materials Science and Engineering. pp. 380-382, New York: McGraw-Hill. 1993.

Soga, K.G. Melrose, J.R. and Ball, R.C. Metastable States and the Kinetics of Colloidal Phase Separation, J. Chem. Phys., *110*, pp. 2280-2288. 1999.

Sophiaopoulus, A.J. Rhodes, C.K. Holcomb, D.N. and Van Holde, K.E. Physical Studies of Lysozyme. I. Characterization, J. Biol. Chem., *237*, pp. 1107-1112. 1962.

Sorensen, T.J. Sontum, P.C. Thorsen, G. and Malthe-Sorenssen, D. Cluster Formation in Precrystalline Solutions, Chem. Eng. Technol., *26*, pp. 307-312. 2003.

Steiner, U. Meller, A. and Stavans, J. Entropy Driven Phase Separation in binary Emulsions, Phys. Rev. Lett., *74*, pp. 4750-4753. 1995.

Talanquer, V. and Oxtoby, D.W. Crystal Nucleation in the Presence of a Metastable Critical Point, J. Chem. Phys., *109*, pp. 223-227. 1998.

Tanaka, S. Ito, K. Hayakawa, R. and Ataka, M. Size and Number Density of Precrystalline Aggregates in Lysozyme Crystallization Process, J. Chem. Phys., *111(22)*, pp. 10330-10337. 1999.

Tanaka, S. Yamamoto, M. Kawashima, K. Ito, K. Hayakawa, R. and Ataka, M. Kinetic Study on the Early Stage of the Crystallization Process of Two Forms of Lysozyme Crystals by Photon Correlation Spectroscopy, J. Cryst. Growth, *168*, pp. 44-49. 1996.

Taratuta, V.G. Holschbach, A. Thurston, G.M. Blankschtein, D. and Benedek, G.B. Liquid-Liquid Phase Separation of Aqueous Lysozyme Solutions: Effects of pH and Salt Identity, J. Phys. Chem., *94*, pp. 2140-2144. 1990.

ten Wolde, P.R. and Frenkel, D. Enhancement of Protein Crystal Nucleation by Critical Density Fluctuations, Science, *277*, pp. 1975-1978. 1997.

ten Wolde, P.R. and Frenkel, D. Enhanced Protein Crystallization around the Metastable Critical Point, Theor. Chem. Acc., *101*, pp. 205-208. 1999.

Thomson, J.A. Schurtenberger, P. Thurston, G.M. and Benedek, G.B. Binary Liquid-Liquid Phase Separation and Critical Phenomena in a Protein/Water Solution, Proc. Natl. Acad. Sci. U.S.A., *84*, pp. 7079-7083. 1987.

Vekilov, P.G. Monaco, L.A. Thomas, B.R. Stojanoff, V. and Rosenberger, F. Repartitioning of NaCl and Protein Impurities in Lysozyme Crystallization, Acta Crystallogr. D, *52*, pp. 785-798. 1996.

Vliegenthart, G.A. Lodge, J.F.M. and Lekkerkerker, H.N.W. Strong Weak and Metastable Liquids Structural and Dynamical Aspects of the Liquid State, Physica A, *263*, pp. 378-388. 1999.

Wang, H. Shimizu, Kim, H. Hobbie, E.K. Wang, Z. and Han, C.C. Competing Growth Kinetics in Simultaneously Crystallizing and Phase-Separating Polymer Blends, J. Chem. Phys., 116, pp. 7311-7315. 2002.

Weiss, M.S. Palm, G.J. and Hilgenfeld, R. Crystallization, Structure Solution and Refinement of Hen Egg-White Lysozyme at pH 8.0 in the Presence of MPD, Acta Crystallogr. D, *56*, pp. 952-958. 2000.

Wiltzius, P. and Cumming, A. Domain Growth and Wetting in Polymer Mixtures, Phys. Rev. Lett., *66*, pp. 3000-3003. 1991.

Wood, W.M.L. Crystal Science Techniques in the Manufacture of Chiral Compound. In Chirality in Industry II, ed by Collins, A.N. Sheldrake, G.N. and Crosby, J., pp. 119-156. Chichester: John Wiley & Sons. 1997.

Yonezawa, Y. Tanaka, S. Kubota, T. Wakabayashi, K. Yutani, K. and Fujiwara, S. An Insight into the Pathway of the Amyloid Fibril Formation of Hen Egg White Lysozyme Obtained from a Small-angle X-ray and Neutron Scattering Study, J. Mol. Biol., *323*, pp. 237-251. 2002.

Yu, L. X. Furness, M.S. Raw, A. Outlaw, K.P. Nashed, N.E. Ramos, E. Miller, S.P. Adams, R.C. Fang, F. Patel, R.M. Holcombe, F.O. Jr. Chiu, Y.Y. and Hussain, A.S. Scientific Considerations of Pharmaceutical Solid Polymorphism in Abbreviated New Drug Applications, Pharmaceutical Research, *20(4)*, pp. 531-536. 2003.

Zhang, J. and Liu, X. Y. Effect of Protein-Protein Interactions on Protein Aggregation Kinetics, J. Chem. Phys., *119(20)*, pp. 10972-10976. 2003.